

TUM-HEP-349/99

May 1999

CP Violation and Rare Decays of K and B Mesons

Andrzej J. Buras

Technische Universität München

Physik Department

D-85748 Garching, Germany

Abstract

These lectures describe CP violation and rare decays of K and B mesons and consist of ten chapters: i) Grand view of the field including CKM matrix and the unitarity triangle, ii) General aspects of the theoretical framework, iii) Particle-antiparticle mixing and CP violation, iv) Standard analysis of the unitarity triangle, v) The ratio ε'/ε including most recent developments, vi) Rare decays $K^+ \rightarrow \pi^+ \nu \bar{\nu}$ and $K_L \rightarrow \pi^0 \nu \bar{\nu}$, vii) Express review of other rare decays, viii) Express review of CP violation in B decays, ix) A brief look beyond the Standard Model including connections between ε'/ε and CP violating rare K decays, x) Final messages.

Lectures given at the 14th

Lake Louise Winter Institute

February 14-20, 1999

Contents

1	Grand View	1
1.1	Preface	1
1.2	Some Facts about the Standard Model	1
1.3	CKM Matrix	2
1.3.1	General Remarks	2
1.3.2	Standard Parametrization	2
1.3.3	Wolfenstein Parameterization	3
1.3.4	Wolfenstein Parametrization beyond LO	4
1.3.5	Unitarity Triangle	5
1.4	Grand Picture	7
2	Theoretical Framework	9
2.1	OPE and Renormalization Group	9
2.2	Inclusive Decays	12
2.3	Status of NLO Calculations	13
2.4	Penguin–Box Expansion	13
3	Particle-Antiparticle Mixing and CP Violation	16
3.1	Preliminaries	16
3.2	Express Review of $K^0 - \bar{K}^0$ Mixing	16
3.3	The First Look at ε and ε'	19
3.4	Basic Formula for ε	20
3.5	Basic Formula for $B^0 - \bar{B}^0$ Mixing	22
4	Standard Analysis of the Unitarity Triangle	24
4.1	Basic Procedure	24
4.2	Numerical Results	26
4.2.1	Input Parameters	26
4.2.2	Output of the Standard Analysis	26
4.3	Final Remarks	28
5	ε'/ε in the Standard Model	28
5.1	Preliminaries	28
5.2	Basic Formulae	30
5.3	Hadronic Matrix Elements	32
5.4	An Analytic Formula for ε'/ε	33

5.5	The Status of m_s , $B_6^{(1/2)}$, $B_8^{(3/2)}$, $\Omega_{\eta+\eta'}$ and $\Lambda_{\overline{\text{MS}}}^{(4)}$	34
5.5.1	m_s	34
5.5.2	$B_6^{(1/2)}$ and $B_8^{(3/2)}$	35
5.5.3	$\Omega_{\eta+\eta'}$ and $\Lambda_{\overline{\text{MS}}}^{(4)}$	36
5.6	Numerical Results for ε'/ε	37
5.7	Summary	39
6	The Decays $K^+ \rightarrow \pi^+ \nu \bar{\nu}$ and $K_L \rightarrow \pi^0 \nu \bar{\nu}$	41
6.1	General Remarks	41
6.2	The Decay $K^+ \rightarrow \pi^+ \nu \bar{\nu}$	42
6.2.1	The effective Hamiltonian	42
6.2.2	Deriving the Branching Ratio	43
6.2.3	Basic Phenomenology	43
6.2.4	Numerical Analysis of $K^+ \rightarrow \pi^+ \nu \bar{\nu}$	44
6.2.5	$ V_{td} $ from $K^+ \rightarrow \pi^+ \nu \bar{\nu}$	45
6.2.6	Summary and Outlook	45
6.3	The Decay $K_L \rightarrow \pi^0 \nu \bar{\nu}$	46
6.3.1	The effective Hamiltonian	46
6.3.2	Deriving the Branching Ratio	47
6.3.3	Master Formulae for $Br(K_L \rightarrow \pi^0 \nu \bar{\nu})$	48
6.3.4	Numerical Analysis of $K_L \rightarrow \pi^0 \nu \bar{\nu}$	48
6.3.5	Summary and Outlook	49
6.4	Unitarity Triangle and $\sin 2\beta$ from $K \rightarrow \pi \nu \bar{\nu}$	50
7	Express Review of Rare K and B Decays	51
7.1	The Decays $B \rightarrow X_{s,d} \nu \bar{\nu}$	51
7.2	The Decays $B_{s,d} \rightarrow l^+ l^-$	52
7.3	$B \rightarrow X_s \gamma$ and $B \rightarrow X_s l^+ l^-$	54
7.4	$K_L \rightarrow \pi^0 e^+ e^-$	55
7.5	$K_L \rightarrow \mu^+ \mu^-$	55
8	Express Review of CP Violation in B Decays	56
8.1	CP-Asymmetries in B-Decays: General Picture	56
8.2	B^0 -Decays to CP Eigenstates	57
8.3	Recent Developments	59
8.4	CP-Asymmetries in B-Decays versus $K \rightarrow \pi \nu \bar{\nu}$	60

9	A Brief Look Beyond the Standard Model	61
9.1	General Remarks	61
9.2	Classification of New Physics	62
9.3	Upper Bounds on $K \rightarrow \pi\nu\bar{\nu}$ and $K_L \rightarrow \pi^0 e^+ e^-$ from ε'/ε and $K_L \rightarrow \mu^+ \mu^-$.	63
10	Summary and Outlook	66

1 Grand View

1.1 Preface

CP violation and rare decays of K and B mesons play an important role in the tests of the Standard Model and of its extensions. The prime examples, already observed experimentally, are $K^0 - \bar{K}^0$ and $B_d^0 - \bar{B}_d^0$ mixings, CP violation in $K_L \rightarrow \pi\pi$ and the rare decays $B \rightarrow X\gamma$, $K_L \rightarrow \mu\bar{\mu}$ and $K^+ \rightarrow \pi^+\nu\bar{\nu}$. In the coming years CP violation in B decays, $B_s^0 - \bar{B}_s^0$ mixing and rare decays $K_L \rightarrow \pi^0\nu\bar{\nu}$, $K_L \rightarrow \pi^0 e^+ e^-$, $B \rightarrow X_{s,d} l^+ l^-$, $B_{d,s} \rightarrow l^+ l^-$ and $B \rightarrow X_{s,d} \nu\bar{\nu}$ will hopefully be included in this list.

These lectures provide a non-technical description of this fascinating field. There is unavoidably an overlap with my Les Houches lectures [1] and with the reviews [2] and [3]. On the other hand new developments are included and all numerical results updated.

1.2 Some Facts about the Standard Model

Throughout these lectures we will dominantly work in the context of the Standard Model with three generations of quarks and leptons and the interactions described by the gauge group $SU(3)_C \otimes SU(2)_L \otimes U(1)_Y$ spontaneously broken to $SU(3)_C \otimes U(1)_Q$. There are excellent text books on the dynamics of the Standard Model. Let us therefore collect here only those ingredients of this model which are fundamental for the subject of weak decays.

- The strong interactions are mediated by eight gluons G_a , the electroweak interactions by W^\pm , Z^0 and γ .
- Concerning *Electroweak Interactions*, the left-handed leptons and quarks are put into $SU(2)_L$ doublets:

$$\begin{pmatrix} \nu_e \\ e^- \end{pmatrix}_L \quad \begin{pmatrix} \nu_\mu \\ \mu^- \end{pmatrix}_L \quad \begin{pmatrix} \nu_\tau \\ \tau^- \end{pmatrix}_L \quad (1.1)$$

$$\begin{pmatrix} u \\ d' \end{pmatrix}_L \quad \begin{pmatrix} c \\ s' \end{pmatrix}_L \quad \begin{pmatrix} t \\ b' \end{pmatrix}_L \quad (1.2)$$

with the corresponding right-handed fields transforming as singlets under $SU(2)_L$. The primes in (1.2) will be discussed in a moment.

- The charged current processes mediated by W^\pm are flavour violating with the strength of violation given by the gauge coupling g_2 and effectively at low energies by the Fermi constant

$$\frac{G_F}{\sqrt{2}} = \frac{g_2^2}{8M_W^2} \quad (1.3)$$

and a *unitary* 3×3 CKM matrix.

- The CKM matrix [4, 5] connects the *weak eigenstates* (d', s', b') and the corresponding *mass eigenstates* d, s, b through

$$\begin{pmatrix} d' \\ s' \\ b' \end{pmatrix} = \begin{pmatrix} V_{ud} & V_{us} & V_{ub} \\ V_{cd} & V_{cs} & V_{cb} \\ V_{td} & V_{ts} & V_{tb} \end{pmatrix} \begin{pmatrix} d \\ s \\ b \end{pmatrix} = \hat{V}_{\text{CKM}} \begin{pmatrix} d \\ s \\ b \end{pmatrix}. \quad (1.4)$$

In the leptonic sector the analogous mixing matrix is a unit matrix due to the masslessness of neutrinos in the Standard Model.

- The unitarity of the CKM matrix assures the absence of flavour changing neutral current transitions at the tree level. This means that the elementary vertices involving neutral gauge bosons (G_a, Z^0, γ) are flavour conserving. This property is known under the name of GIM mechanism [6].
- The fact that the V_{ij} 's can a priori be complex numbers allows CP violation in the Standard Model [5].

1.3 CKM Matrix

1.3.1 General Remarks

We know from the text books that the CKM matrix can be parametrized by three angles and a single complex phase. This phase leading to an imaginary part of the CKM matrix is a necessary ingredient to describe CP violation within the framework of the Standard Model.

Many parametrizations of the CKM matrix have been proposed in the literature. We will use two parametrizations in these lectures: the standard parametrization [7] recommended by the Particle Data Group [8] and the Wolfenstein parametrization [9].

1.3.2 Standard Parametrization

With $c_{ij} = \cos \theta_{ij}$ and $s_{ij} = \sin \theta_{ij}$ ($i, j = 1, 2, 3$), the standard parametrization is given by:

$$\hat{V}_{CKM} = \begin{pmatrix} c_{12}c_{13} & s_{12}c_{13} & s_{13}e^{-i\delta} \\ -s_{12}c_{23} - c_{12}s_{23}s_{13}e^{i\delta} & c_{12}c_{23} - s_{12}s_{23}s_{13}e^{i\delta} & s_{23}c_{13} \\ s_{12}s_{23} - c_{12}c_{23}s_{13}e^{i\delta} & -s_{23}c_{12} - s_{12}c_{23}s_{13}e^{i\delta} & c_{23}c_{13} \end{pmatrix}, \quad (1.5)$$

where δ is the phase necessary for CP violation. c_{ij} and s_{ij} can all be chosen to be positive and δ may vary in the range $0 \leq \delta \leq 2\pi$. However, the measurements of CP violation in K decays force δ to be in the range $0 < \delta < \pi$.

From phenomenological applications we know that s_{13} and s_{23} are small numbers: $\mathcal{O}(10^{-3})$ and $\mathcal{O}(10^{-2})$, respectively. Consequently to an excellent accuracy $c_{13} = c_{23} = 1$ and the four independent parameters are given as

$$s_{12} = |V_{us}|, \quad s_{13} = |V_{ub}|, \quad s_{23} = |V_{cb}|, \quad \delta. \quad (1.6)$$

The first three can be extracted from tree level decays mediated by the transitions $s \rightarrow u$, $b \rightarrow u$ and $b \rightarrow c$ respectively. The phase δ can be extracted from CP violating transitions or loop processes sensitive to $|V_{td}|$. The latter fact is based on the observation that for $0 \leq \delta \leq \pi$, as required by the analysis of CP violation in the K system, there is a one-to-one correspondence between δ and $|V_{td}|$ given by

$$|V_{td}| = \sqrt{a^2 + b^2 - 2ab \cos \delta}, \quad a = |V_{cd}V_{cb}|, \quad b = |V_{ud}V_{ub}|. \quad (1.7)$$

The main phenomenological advantages of (1.5) over other parametrizations proposed in the literature are basically these two:

- s_{12} , s_{13} and s_{23} being related in a very simple way to $|V_{us}|$, $|V_{ub}|$ and $|V_{cb}|$ respectively, can be measured independently in three decays.
- The CP violating phase is always multiplied by the very small s_{13} . This shows clearly the suppression of CP violation independently of the actual size of δ .

For numerical evaluations the use of the standard parametrization is strongly recommended. However once the four parameters in (1.6) have been determined it is often useful to make a change of basic parameters in order to see the structure of the result more transparently. This brings us to the Wolfenstein parametrization [9] and its generalization given in [10].

1.3.3 Wolfenstein Parameterization

The Wolfenstein parametrization is an approximate parametrization of the CKM matrix in which each element is expanded as a power series in the small parameter $\lambda = |V_{us}| = 0.22$,

$$\hat{V} = \begin{pmatrix} 1 - \frac{\lambda^2}{2} & \lambda & A\lambda^3(\varrho - i\eta) \\ -\lambda & 1 - \frac{\lambda^2}{2} & A\lambda^2 \\ A\lambda^3(1 - \varrho - i\eta) & -A\lambda^2 & 1 \end{pmatrix} + \mathcal{O}(\lambda^4), \quad (1.8)$$

and the set (1.6) is replaced by

$$\lambda, \quad A, \quad \varrho, \quad \eta. \quad (1.9)$$

Because of the smallness of λ and the fact that for each element the expansion parameter is actually λ^2 , it is sufficient to keep only the first few terms in this expansion.

The Wolfenstein parametrization is certainly more transparent than the standard parametrization. However, if one requires sufficient level of accuracy, the higher order terms in λ have to be included in phenomenological applications. This can be done in many ways. The point is that since (1.8) is only an approximation the *exact* definition of the parameters in (1.9) is not unique by terms of the neglected order $\mathcal{O}(\lambda^4)$. This situation is familiar from any perturbative expansion, where different definitions of expansion parameters (coupling constants) are possible. This is also the reason why in different papers in the literature different $\mathcal{O}(\lambda^4)$ terms in (1.8) can be found. They simply correspond to different definitions of the parameters in (1.9). Since the physics does not depend on a particular definition, it is useful to make a choice for which the transparency of the original Wolfenstein parametrization is not lost. Here we present one way of achieving this.

1.3.4 Wolfenstein Parametrization beyond LO

An efficient and systematic way of finding higher order terms in λ is to go back to the standard parametrization (1.5) and to *define* the parameters $(\lambda, A, \varrho, \eta)$ through [10, 11]

$$s_{12} = \lambda, \quad s_{23} = A\lambda^2, \quad s_{13}e^{-i\delta} = A\lambda^3(\varrho - i\eta) \quad (1.10)$$

to *all orders* in λ . It follows that

$$\varrho = \frac{s_{13}}{s_{12}s_{23}} \cos \delta, \quad \eta = \frac{s_{13}}{s_{12}s_{23}} \sin \delta. \quad (1.11)$$

(1.10) and (1.11) represent simply the change of variables from (1.6) to (1.9). Making this change of variables in the standard parametrization (1.5) we find the CKM matrix as a function of $(\lambda, A, \varrho, \eta)$ which satisfies unitarity exactly. Expanding next each element in powers of λ we recover the matrix in (1.8) and in addition find explicit corrections of $\mathcal{O}(\lambda^4)$ and higher order terms:

$$V_{ud} = 1 - \frac{1}{2}\lambda^2 - \frac{1}{8}\lambda^4 + \mathcal{O}(\lambda^6) \quad (1.12)$$

$$V_{us} = \lambda + \mathcal{O}(\lambda^7), \quad V_{ub} = A\lambda^3(\varrho - i\eta) \quad (1.13)$$

$$V_{cd} = -\lambda + \frac{1}{2}A^2\lambda^5[1 - 2(\varrho + i\eta)] + \mathcal{O}(\lambda^7) \quad (1.14)$$

$$V_{cs} = 1 - \frac{1}{2}\lambda^2 - \frac{1}{8}\lambda^4(1 + 4A^2) + \mathcal{O}(\lambda^6) \quad (1.15)$$

$$V_{cb} = A\lambda^2 + \mathcal{O}(\lambda^8), \quad V_{tb} = 1 - \frac{1}{2}A^2\lambda^4 + \mathcal{O}(\lambda^6) \quad (1.16)$$

$$V_{td} = A\lambda^3 \left[1 - (\varrho + i\eta)(1 - \frac{1}{2}\lambda^2) \right] + \mathcal{O}(\lambda^7) \quad (1.17)$$

$$V_{ts} = -A\lambda^2 + \frac{1}{2}A(1 - 2\varrho)\lambda^4 - i\eta A\lambda^4 + \mathcal{O}(\lambda^6) \quad (1.18)$$

We note that by definition V_{ub} remains unchanged and the corrections to V_{us} and V_{cb} appear only at $\mathcal{O}(\lambda^7)$ and $\mathcal{O}(\lambda^8)$, respectively. Consequently to an excellent accuracy we have:

$$V_{us} = \lambda, \quad V_{cb} = A\lambda^2, \quad (1.19)$$

$$V_{ub} = A\lambda^3(\varrho - i\eta), \quad V_{td} = A\lambda^3(1 - \bar{\varrho} - i\bar{\eta}) \quad (1.20)$$

with

$$\bar{\varrho} = \varrho(1 - \frac{\lambda^2}{2}), \quad \bar{\eta} = \eta(1 - \frac{\lambda^2}{2}). \quad (1.21)$$

The advantage of this generalization of the Wolfenstein parametrization over other generalizations found in the literature is the absence of relevant corrections to V_{us} , V_{cb} and V_{ub} and an elegant change in V_{td} which allows a simple generalization of the so-called unitarity triangle beyond LO.

Finally let us collect useful approximate analytic expressions for $\lambda_i = V_{id}V_{is}^*$ with $i = c, t$:

$$\text{Im}\lambda_t = -\text{Im}\lambda_c = \eta A^2 \lambda^5 = |V_{ub}| |V_{cb}| \sin \delta \quad (1.22)$$

$$\text{Re}\lambda_c = -\lambda(1 - \frac{\lambda^2}{2}) \quad (1.23)$$

$$\text{Re}\lambda_t = -(1 - \frac{\lambda^2}{2})A^2\lambda^5(1 - \bar{\varrho}). \quad (1.24)$$

Expressions (1.22) and (1.23) represent to an accuracy of 0.2% the exact formulae obtained using (1.5). The expression (1.24) deviates by at most 2% from the exact formula in the full range of parameters considered. For ϱ close to zero this deviation is below 1%. After inserting the expressions (1.22)–(1.24) in the exact formulae for quantities of interest, a further expansion in λ should not be made.

1.3.5 Unitarity Triangle

The unitarity of the CKM-matrix implies various relations between its elements. In particular, we have

$$V_{ud}V_{ub}^* + V_{cd}V_{cb}^* + V_{td}V_{tb}^* = 0. \quad (1.25)$$

Phenomenologically this relation is very interesting as it involves simultaneously the elements V_{ub} , V_{cb} and V_{td} which are under extensive discussion at present.

The relation (1.25) can be represented as a “unitarity” triangle in the complex $(\bar{\varrho}, \bar{\eta})$ plane. The invariance of (1.25) under any phase-transformations implies that the corresponding

triangle is rotated in the $(\bar{\varrho}, \bar{\eta})$ plane under such transformations. Since the angles and the sides (given by the moduli of the elements of the mixing matrix) in these triangles remain unchanged, they are phase convention independent and are physical observables. Consequently they can be measured directly in suitable experiments. The area of the unitarity triangle is related to the measure of CP violation J_{CP} [12, 13]:

$$|J_{\text{CP}}| = 2 \cdot A_{\Delta}, \quad (1.26)$$

where A_{Δ} denotes the area of the unitarity triangle.

The construction of the unitarity triangle proceeds as follows:

- We note first that

$$V_{cd}V_{cb}^* = -A\lambda^3 + \mathcal{O}(\lambda^7). \quad (1.27)$$

Thus to an excellent accuracy $V_{cd}V_{cb}^*$ is real with $|V_{cd}V_{cb}^*| = A\lambda^3$.

- Keeping $\mathcal{O}(\lambda^5)$ corrections and rescaling all terms in (1.25) by $A\lambda^3$ we find

$$\frac{1}{A\lambda^3}V_{ud}V_{ub}^* = \bar{\varrho} + i\bar{\eta}, \quad \frac{1}{A\lambda^3}V_{td}V_{tb}^* = 1 - (\bar{\varrho} + i\bar{\eta}) \quad (1.28)$$

with $\bar{\varrho}$ and $\bar{\eta}$ defined in (1.21).

- Thus we can represent (1.25) as the unitarity triangle in the complex $(\bar{\varrho}, \bar{\eta})$ plane as shown in fig. 1.

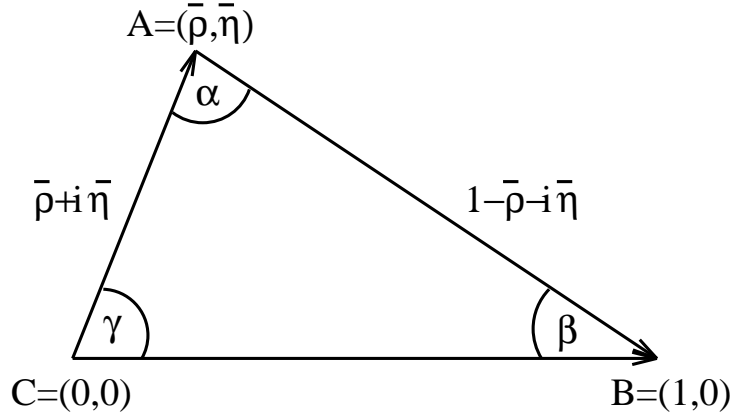


Figure 1: Unitarity Triangle.

Let us collect useful formulae related to this triangle:

- Using simple trigonometry one can express $\sin(2\phi_i)$, $\phi_i = \alpha, \beta, \gamma$, in terms of $(\bar{\varrho}, \bar{\eta})$ as follows:

$$\sin(2\alpha) = \frac{2\bar{\eta}(\bar{\eta}^2 + \bar{\varrho}^2 - \bar{\varrho})}{(\bar{\varrho}^2 + \bar{\eta}^2)((1 - \bar{\varrho})^2 + \bar{\eta}^2)} \quad (1.29)$$

$$\sin(2\beta) = \frac{2\bar{\eta}(1 - \bar{\varrho})}{(1 - \bar{\varrho})^2 + \bar{\eta}^2} \quad (1.30)$$

$$\sin(2\gamma) = \frac{2\bar{\varrho}\bar{\eta}}{\bar{\varrho}^2 + \bar{\eta}^2} = \frac{2\varrho\eta}{\varrho^2 + \eta^2}. \quad (1.31)$$

- The lengths CA and BA in the rescaled triangle to be denoted by R_b and R_t , respectively, are given by

$$R_b \equiv \frac{|V_{ud}V_{ub}^*|}{|V_{cd}V_{cb}^*|} = \sqrt{\bar{\varrho}^2 + \bar{\eta}^2} = (1 - \frac{\lambda^2}{2}) \frac{1}{\lambda} \left| \frac{V_{ub}}{V_{cb}} \right| \quad (1.32)$$

$$R_t \equiv \frac{|V_{td}V_{tb}^*|}{|V_{cd}V_{cb}^*|} = \sqrt{(1 - \bar{\varrho})^2 + \bar{\eta}^2} = \frac{1}{\lambda} \left| \frac{V_{td}}{V_{cb}} \right|. \quad (1.33)$$

- The angles β and γ of the unitarity triangle are related directly to the complex phases of the CKM-elements V_{td} and V_{ub} , respectively, through

$$V_{td} = |V_{td}|e^{-i\beta}, \quad V_{ub} = |V_{ub}|e^{-i\gamma}. \quad (1.34)$$

- The angle α can be obtained through the relation

$$\alpha + \beta + \gamma = 180^\circ \quad (1.35)$$

expressing the unitarity of the CKM-matrix.

The triangle depicted in fig. 1 together with $|V_{us}|$ and $|V_{cb}|$ gives a full description of the CKM matrix. Looking at the expressions for R_b and R_t , we observe that within the Standard Model the measurements of four CP *conserving* decays sensitive to $|V_{us}|$, $|V_{ub}|$, $|V_{cb}|$ and $|V_{td}|$ can tell us whether CP violation ($\eta \neq 0$) is predicted in the Standard Model. This is a very remarkable property of the Kobayashi-Maskawa picture of CP violation: quark mixing and CP violation are closely related to each other.

1.4 Grand Picture

What do we know about the CKM matrix and the unitarity triangle on the basis of *tree level* decays? A detailed answer to this question can be found in the reports of the Particle Data Group [8] as well as other reviews [14, 15], where references to the relevant experiments and related theoretical work can be found. In particular we have

$$|V_{us}| = \lambda = 0.2205 \pm 0.0018 \quad |V_{cb}| = 0.040 \pm 0.002, \quad (1.36)$$

$$\frac{|V_{ub}|}{|V_{cb}|} = 0.089 \pm 0.016, \quad |V_{ub}| = (3.56 \pm 0.56) \cdot 10^{-3}. \quad (1.37)$$

Using (1.19 and (1.32) we find then

$$A = 0.826 \pm 0.041, \quad R_b = 0.39 \pm 0.07. \quad (1.38)$$

This tells us only that the apex A of the unitarity triangle lies in the band shown in fig. 2. In order to answer the question where the apex A lies on this "unitarity clock" we have to look at different decays. Most promising in this respect are the so-called "loop induced" decays and transitions which are the subject of several sections in these lectures and CP asymmetries in B-decays which will be briefly discussed in Section 8. These two different

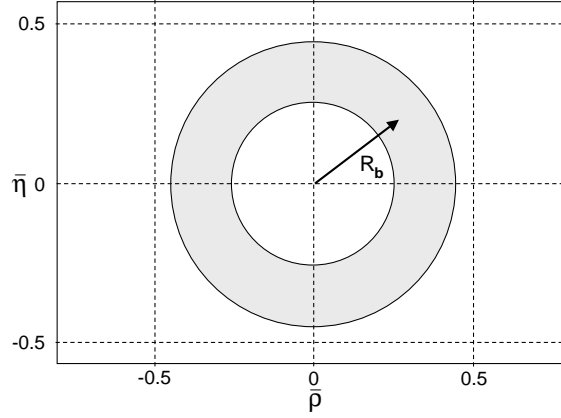


Figure 2: "Unitarity Clock".

routes for explorations of the CKM matrix and of the related unitarity triangle may answer the important question, whether the Kobayashi-Maskawa picture of CP violation is correct and more generally whether the Standard Model offers a correct description of weak decays of hadrons. Indeed, in order to answer these important questions it is essential to calculate as many branching ratios as possible, measure them experimentally and check if they all can be described by the same set of the parameters $(\lambda, A, \varrho, \eta)$. In the language of the unitarity triangle this means that the various curves in the $(\bar{\varrho}, \bar{\eta})$ plane extracted from different decays should cross each other at a single point as shown in fig. 3. Moreover the angles (α, β, γ) in the resulting triangle should agree with those extracted one day from CP-asymmetries in B-decays. For artistic reasons the value of $\bar{\eta}$ in fig. 3 has been chosen to be higher than the fitted central value $\bar{\eta} \approx 0.35$.

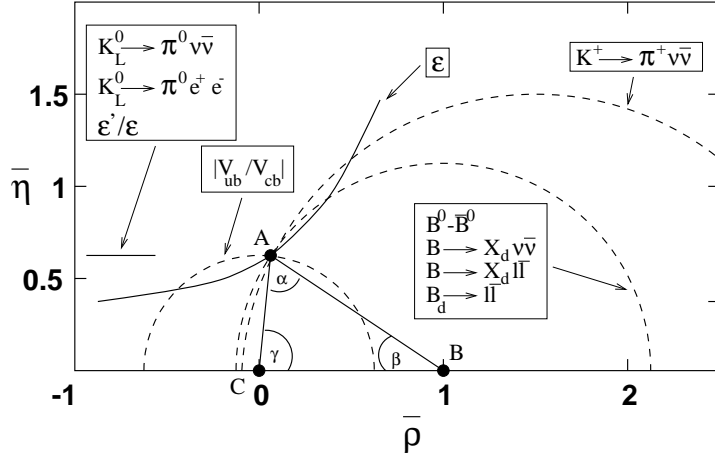


Figure 3: The ideal Unitarity Triangle.

On the other hand if new physics contributes to weak decays the different curves based on the Standard Model expressions, will not cross each other at a single point and the angles (α, β, γ) extracted one day from CP-asymmetries in B-decays will disagree with the ones determined from rare K and B decays. Clearly the plot in fig. 3 is highly idealized because in order to extract such nice curves from various decays one needs perfect experiments and perfect theory. One of the goals of these lectures is to identify those decays for which at least the theory is under control. For such decays, if they can be measured with a sufficient precision, the curves in fig. 3 are not fully unrealistic. Let us then briefly discuss the theoretical framework for weak decays.

2 Theoretical Framework

2.1 OPE and Renormalization Group

The basis for any serious phenomenology of weak decays of hadrons is the *Operator Product Expansion* (OPE) [16, 17], which allows to write the effective weak Hamiltonian simply as follows

$$\mathcal{H}_{eff} = \frac{G_F}{\sqrt{2}} \sum_i V_{CKM}^i C_i(\mu) Q_i . \quad (2.1)$$

Here G_F is the Fermi constant and Q_i are the relevant local operators which govern the decays in question. They are built out of quark and lepton fields. The Cabibbo-Kobayashi-Maskawa factors V_{CKM}^i [4, 5] and the Wilson coefficients C_i [16] describe the strength with which a given operator enters the Hamiltonian. An amplitude for a decay of a given meson

$M = K, B, \dots$ into a final state $F = \pi\nu\bar{\nu}, \pi\pi, DK$ is then simply given by

$$A(M \rightarrow F) = \langle F | \mathcal{H}_{eff} | M \rangle = \frac{G_F}{\sqrt{2}} \sum_i V_{CKM}^i C_i(\mu) \langle F | Q_i(\mu) | M \rangle, \quad (2.2)$$

where $\langle F | Q_i(\mu) | M \rangle$ are the hadronic matrix elements of Q_i between M and F .

The essential virtue of OPE is this one. It allows to separate the problem of calculating the amplitude $A(M \rightarrow F)$ into two distinct parts: the *short distance* (perturbative) calculation of the coefficients $C_i(\mu)$ and the *long-distance* (generally non-perturbative) calculation of the matrix elements $\langle Q_i(\mu) \rangle$. The scale μ separates the physics contributions into short distance contributions contained in $C_i(\mu)$ and the long distance contributions contained in $\langle Q_i(\mu) \rangle$. Thus C_i include the top quark contributions and contributions from other heavy particles such as W, Z -bosons and charged Higgs particles or supersymmetric particles in the supersymmetric extensions of the Standard Model. Consequently $C_i(\mu)$ depend generally on m_t and also on the masses of new particles if extensions of the Standard Model are considered. This dependence can be found by evaluating so-called *box* and *penguin* diagrams with full W -, Z -, top- and new particles exchanges and *properly* including short distance QCD effects. The latter govern the μ -dependence of $C_i(\mu)$.

The value of μ can be chosen arbitrarily but the final result must be μ -independent. Therefore the μ -dependence of $C_i(\mu)$ has to cancel the μ -dependence of $\langle Q_i(\mu) \rangle$. In other words it is a matter of choice what exactly belongs to $C_i(\mu)$ and what to $\langle Q_i(\mu) \rangle$. This cancellation of μ -dependence involves generally several terms in the expansion in (2.2). The coefficients $C_i(\mu)$ depend also on the renormalization scheme. This scheme dependence must also be cancelled by the one of $\langle Q_i(\mu) \rangle$ so that the physical amplitudes are renormalization scheme independent. Again, as in the case of the μ -dependence, the cancellation of the renormalization scheme dependence involves generally several terms in the expansion (2.2).

Although μ is in principle arbitrary, it is customary to choose μ to be of the order of the mass of the decaying hadron. This is $\mathcal{O}(m_b)$ and $\mathcal{O}(m_c)$ for B -decays and D -decays respectively. In the case of K -decays the typical choice is $\mu = \mathcal{O}(1-2 \text{ GeV})$ instead of $\mathcal{O}(m_K)$, which is much too low for any perturbative calculation of the couplings C_i . Now due to the fact that $\mu \ll M_{W,Z}, m_t$, large logarithms $\ln M_W/\mu$ compensate in the evaluation of $C_i(\mu)$ the smallness of the QCD coupling constant α_s and terms $\alpha_s^n (\ln M_W/\mu)^n, \alpha_s^n (\ln M_W/\mu)^{n-1}$ etc. have to be resummed to all orders in α_s before a reliable result for C_i can be obtained. This can be done very efficiently by means of the renormalization group methods. The resulting *renormalization group improved* perturbative expansion for $C_i(\mu)$ in terms of the effective coupling constant $\alpha_s(\mu)$ does not involve large logarithms and is more reliable.

All this looks rather formal but in fact should be familiar. Indeed, in the simplest case of

the β -decay, \mathcal{H}_{eff} takes the familiar form

$$\mathcal{H}_{eff}^{(\beta)} = \frac{G_F}{\sqrt{2}} \cos \theta_c [\bar{u} \gamma_\mu (1 - \gamma_5) d \otimes \bar{e} \gamma^\mu (1 - \gamma_5) \nu_e] , \quad (2.3)$$

where V_{ud} has been expressed in terms of the Cabibbo angle. In this particular case the Wilson coefficient is equal unity and the local operator, the object between the square brackets, is given by a product of two $V - A$ currents. Equation (2.3) represents the Fermi theory for β -decays as formulated by Sudarshan and Marshak [18] and Feynman and Gell-Mann [19] forty years ago, except that in (2.3) the quark language has been used and following Cabibbo a small departure of V_{ud} from unity has been incorporated. In this context the basic formula (2.1) can be regarded as a generalization of the Fermi Theory to include all known quarks and leptons as well as their strong and electroweak interactions as summarized by the Standard Model.

Due to the interplay of electroweak and strong interactions the structure of the local operators is much richer than in the case of the β -decay. They can be classified with respect to the Dirac structure, colour structure and the type of quarks and leptons relevant for a given decay. Of particular interest are the operators involving quarks only. In the case of the $\Delta S = 1$ transitions the relevant set of operators is given as follows:

Current–Current :

$$Q_1 = (\bar{s}_\alpha u_\beta)_{V-A} (\bar{u}_\beta d_\alpha)_{V-A} \quad Q_2 = (\bar{s}u)_{V-A} (\bar{u}d)_{V-A} \quad (2.4)$$

QCD–Penguins :

$$Q_3 = (\bar{s}d)_{V-A} \sum_{q=u,d,s} (\bar{q}q)_{V-A} \quad Q_4 = (\bar{s}_\alpha d_\beta)_{V-A} \sum_{q=u,d,s} (\bar{q}_\beta q_\alpha)_{V-A} \quad (2.5)$$

$$Q_5 = (\bar{s}d)_{V-A} \sum_{q=u,d,s} (\bar{q}q)_{V+A} \quad Q_6 = (\bar{s}_\alpha d_\beta)_{V-A} \sum_{q=u,d,s} (\bar{q}_\beta q_\alpha)_{V+A} \quad (2.6)$$

Electroweak–Penguins :

$$Q_7 = \frac{3}{2} (\bar{s}d)_{V-A} \sum_{q=u,d,s} e_q (\bar{q}q)_{V+A} \quad Q_8 = \frac{3}{2} (\bar{s}_\alpha d_\beta)_{V-A} \sum_{q=u,d,s} e_q (\bar{q}_\beta q_\alpha)_{V+A} \quad (2.7)$$

$$Q_9 = \frac{3}{2} (\bar{s}d)_{V-A} \sum_{q=u,d,s} e_q (\bar{q}q)_{V-A} \quad Q_{10} = \frac{3}{2} (\bar{s}_\alpha d_\beta)_{V-A} \sum_{q=u,d,s} e_q (\bar{q}_\beta q_\alpha)_{V-A} . \quad (2.8)$$

Here, e_q denotes the electric quark charges reflecting the electroweak origin of Q_7, \dots, Q_{10} .

Clearly, in order to calculate the amplitude $A(M \rightarrow F)$, the matrix elements $\langle Q_i(\mu) \rangle$ have to be evaluated. Since they involve long distance contributions one is forced in this case to use non-perturbative methods such as lattice calculations, the $1/N$ expansion (N is the number of colours), QCD sum rules, hadronic sum rules, chiral perturbation theory and so

on. In the case of certain B-meson decays, the *Heavy Quark Effective Theory* (HQET) also turns out to be a useful tool. Needless to say, all these non-perturbative methods have some limitations. Consequently the dominant theoretical uncertainties in the decay amplitudes reside in the matrix elements $\langle Q_i(\mu) \rangle$.

The fact that in most cases the matrix elements $\langle Q_i(\mu) \rangle$ cannot be reliably calculated at present, is very unfortunate. One of the main goals of the experimental studies of weak decays is the determination of the CKM factors V_{CKM} and the search for the physics beyond the Standard Model. Without a reliable estimate of $\langle Q_i(\mu) \rangle$ this goal cannot be achieved unless these matrix elements can be determined experimentally or removed from the final measurable quantities by taking the ratios or suitable combinations of amplitudes or branching ratios. However, this can be achieved only in a handful of decays and generally one has to face directly the calculation of $\langle Q_i(\mu) \rangle$. We will discuss these issues later on.

2.2 Inclusive Decays

So far I have discussed only *exclusive* decays. It turns out that in the case of *inclusive* decays of heavy mesons, like B-mesons, things turn out to be easier. In an inclusive decay one sums over all (or over a special class) of accessible final states so that the amplitude for an inclusive decay takes the form:

$$A(B \rightarrow X) = \frac{G_F}{\sqrt{2}} \sum_{f \in X} V_{\text{CKM}}^i C_i(\mu) \langle f | Q_i(\mu) | B \rangle . \quad (2.9)$$

At first sight things look as complicated as in the case of exclusive decays. It turns out, however, that the resulting branching ratio can be calculated in the expansion in inverse powers of m_b with the leading term described by the spectator model in which the B-meson decay is modelled by the decay of the b -quark:

$$\text{Br}(B \rightarrow X) = \text{Br}(b \rightarrow q) + \mathcal{O}\left(\frac{1}{m_b^2}\right) . \quad (2.10)$$

This formula is known under the name of the Heavy Quark Expansion (HQE) [20]. Since the leading term in this expansion represents the decay of the quark, it can be calculated in perturbation theory or more correctly in the renormalization group improved perturbation theory. It should be realized that also here the basic starting point is the effective Hamiltonian (2.1) and that the knowledge of $C_i(\mu)$ is essential for the evaluation of the leading term in (2.10). But there is an important difference relative to the exclusive case: the matrix elements of the operators Q_i can be "effectively" evaluated in perturbation theory. This means, in particular, that their μ and renormalization scheme dependences can be evaluated and the cancellation of these dependences by those present in $C_i(\mu)$ can be investigated.

Clearly in order to complete the evaluation of $Br(B \rightarrow X)$ also the remaining terms in (2.10) have to be considered. These terms are of a non-perturbative origin, but fortunately they are suppressed by at least two powers of m_b . They have been studied by several authors in the literature with the result that they affect various branching ratios by less than 10% and often by only a few percent. Consequently the inclusive decays give generally more precise theoretical predictions at present than the exclusive decays. On the other hand their measurements are harder. There are of course some important theoretical issues related to the validity of HQE in (2.10) which appear in the literature under the name of quark-hadron duality. Since these matters are rather involved I will not discuss them here.

2.3 Status of NLO Calculations

In order to achieve sufficient precision for the theoretical predictions it is desirable to have accurate values of $C_i(\mu)$. Indeed it has been realized at the end of the eighties that the leading term (LO) in the renormalization group improved perturbation theory, in which the terms $\alpha_s^n (\ln M_W/\mu)^n$ are summed, is generally insufficient and the inclusion of next-to-leading corrections (NLO) which correspond to summing the terms $\alpha_s^n (\ln M_W/\mu)^{n-1}$ is necessary. In particular, unphysical left-over μ -dependences in the decay amplitudes and branching ratios resulting from the truncation of the perturbative series are considerably reduced by including NLO corrections. These corrections are known by now for the most important and interesting decays and will be taken into account in these lectures. The review of all existing NLO calculations can be found in [2, 21].

2.4 Penguin–Box Expansion

The rare and CP violating decays of K and B mesons are governed by various penguin and box diagrams with internal top quark and charm quark exchanges. Some examples are shown in fig. 4. Evaluating these diagrams one finds a set of basic universal (process independent) m_t -dependent functions $F_r(x_t)$ [22] where $x_t = m_t^2/M_W^2$. Explicit expressions for these functions will be given below.

It is useful to express the OPE formula (2.2) directly in terms of the functions $F_r(x_t)$ [23]:

$$A(M \rightarrow F) = P_0(M \rightarrow F) + \sum_r P_r(M \rightarrow F) F_r(x_t), \quad (2.11)$$

where the sum runs over all possible functions contributing to a given amplitude. P_0 summarizes contributions stemming from internal quarks other than the top, in particular the charm quark. The coefficients P_0 and P_r are process dependent and include QCD corrections. They depend also on hadronic matrix elements of local operators and the relevant CKM factors. I

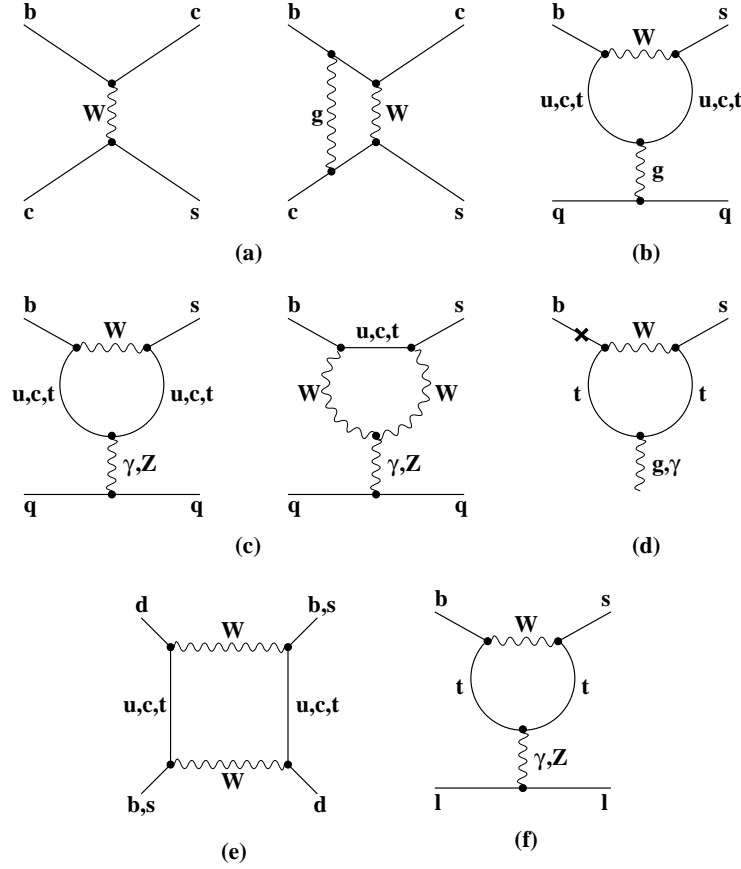


Figure 4: Typical Penguin and Box Diagrams.

would like to call (2.11) *Penguin-Box Expansion* (PBE). We will encounter many examples of PBE in the course of these lectures.

Originally PBE was designed to expose the m_t -dependence of FCNC processes [23]. After the top quark mass has been measured precisely this role of PBE is less important. On the other hand, PBE is very well suited for the study of the extensions of the Standard Model in which new particles are exchanged in the loops. If there are no new local operators the mere change is to modify the functions $F_r(x_t)$ which now acquire the dependence on the masses of new particles such as charged Higgs particles and supersymmetric particles. The process dependent coefficients P_0 and P_r remain unchanged. The effects of new physics can be then transparently seen. However, if new effective operators with different Dirac and colour structures are present the values of P_0 and P_r are modified.

Let us denote by B_0 , C_0 and D_0 the functions $F_r(x_t)$ resulting from $\Delta F = 1$ (F stands for flavour) box diagram, Z^0 -penguin and γ -penguin diagram respectively. These diagrams

are gauge dependent and it is useful to introduce gauge independent combinations [23]

$$X_0 = C_0 - 4B_0, \quad Y_0 = C_0 - B_0, \quad Z_0 = C_0 + \frac{1}{4}D_0 \quad (2.12)$$

Then the set of gauge independent basic functions which govern the FCNC processes in the Standard Model is given to a very good approximation as follows:

$$S_0(x_t) = 2.46 \left(\frac{m_t}{170 \text{ GeV}} \right)^{1.52}, \quad S_0(x_c) = x_c \quad (2.13)$$

$$S_0(x_c, x_t) = x_c \left[\ln \frac{x_t}{x_c} - \frac{3x_t}{4(1-x_t)} - \frac{3x_t^2 \ln x_t}{4(1-x_t)^2} \right]. \quad (2.14)$$

$$X_0(x_t) = 1.57 \left(\frac{m_t}{170 \text{ GeV}} \right)^{1.15}, \quad Y_0(x_t) = 1.02 \left(\frac{m_t}{170 \text{ GeV}} \right)^{1.56}, \quad (2.15)$$

$$Z_0(x_t) = 0.71 \left(\frac{m_t}{170 \text{ GeV}} \right)^{1.86}, \quad E_0(x_t) = 0.26 \left(\frac{m_t}{170 \text{ GeV}} \right)^{-1.02}, \quad (2.16)$$

$$D'_0(x_t) = 0.38 \left(\frac{m_t}{170 \text{ GeV}} \right)^{0.60}, \quad E'_0(x_t) = 0.19 \left(\frac{m_t}{170 \text{ GeV}} \right)^{0.38}. \quad (2.17)$$

The first three functions correspond to $\Delta F = 2$ box diagrams with (t, t) , (c, c) and (t, c) exchanges. E_0 results from QCD penguin diagram with off-shell gluon, D'_0 and E'_0 from γ and QCD penguins with on-shell photons and gluons respectively. The subscript “0” indicates that these functions do not include QCD corrections to the relevant penguin and box diagrams.

In the range $150 \text{ GeV} \leq m_t \leq 200 \text{ GeV}$ these approximations reproduce the exact expressions to an accuracy better than 1%. These formulae will allow us to exhibit elegantly the m_t dependence of various branching ratios in the phenomenological sections of these lectures. Exact expressions for all functions can be found in [1].

Generally, several basic functions contribute to a given decay, although decays exist which depend only on a single function. We have the following correspondence between the most interesting FCNC processes and the basic functions:

$K^0 - \bar{K}^0$ -mixing	$S_0(x_t), S_0(x_c, x_t), S_0(x_c)$
$B^0 - \bar{B}^0$ -mixing	$S_0(x_t)$
$K \rightarrow \pi \nu \bar{\nu}, B \rightarrow X_{d,s} \nu \bar{\nu}$	$X_0(x_t)$
$K_L \rightarrow \mu \bar{\mu}, B \rightarrow l \bar{l}$	$Y_0(x_t)$
$K_L \rightarrow \pi^0 e^+ e^-$	$Y_0(x_t), Z_0(x_t), E_0(x_t)$
ε'	$X_0(x_t), Y_0(x_t), Z_0(x_t), E_0(x_t)$
$B \rightarrow X_s \gamma$	$D'_0(x_t), E'_0(x_t)$
$B \rightarrow X_s \mu^+ \mu^-$	$Y_0(x_t), Z_0(x_t), E_0(x_t), D'_0(x_t), E'_0(x_t)$

3 Particle-Antiparticle Mixing and CP Violation

3.1 Preliminaries

Let us next discuss particle–antiparticle mixing which in the past has been of fundamental importance in testing the Standard Model and often has proven to be an undefeatable challenge for suggested extensions of this model. Let us just recall that from the calculation of the $K_L - K_S$ mass difference, Gaillard and Lee [24] were able to estimate the value of the charm quark mass before charm discovery. On the other hand $B_d^0 - \bar{B}_d^0$ mixing [25] gave the first indication of a large top quark mass. Finally, particle–antiparticle mixing in the $K^0 - \bar{K}^0$ system offers within the Standard Model a plausible description of CP violation in $K_L \rightarrow \pi\pi$ discovered in 1964 [26].

In this section we will predominantly discuss the parameter ε describing the *indirect* CP violation in the K system and the mass differences $\Delta M_{d,s}$ which describe the size of $B_{d,s}^0 - \bar{B}_{d,s}^0$ mixings. In the Standard Model these phenomena appear first at the one-loop level and as such they are sensitive measures of the top quark couplings $V_{ti}(i = d, s, b)$ and in particular of the phase $\delta = \gamma$. They allow then to construct the unitarity triangle.

Let us next enter some details. The following subsection borrows a lot from [27, 28]. A nice review of CP violation can also be found in [29].

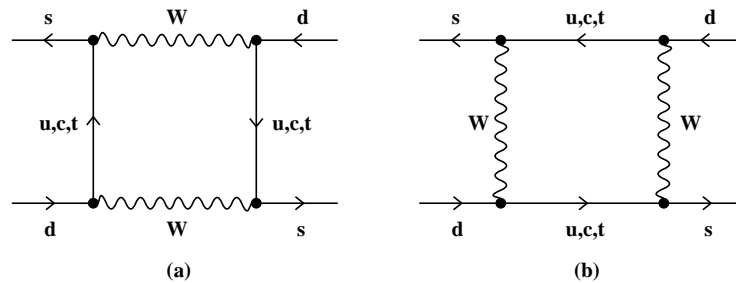


Figure 5: Box diagrams contributing to $K^0 - \bar{K}^0$ mixing in the Standard Model.

3.2 Express Review of $K^0 - \bar{K}^0$ Mixing

$K^0 = (\bar{s}d)$ and $\bar{K}^0 = (s\bar{d})$ are flavour eigenstates which in the Standard Model may mix via weak interactions through the box diagrams in fig. 5. We will choose the phase conventions so that

$$CP|K^0\rangle = -|\bar{K}^0\rangle, \quad CP|\bar{K}^0\rangle = -|K^0\rangle. \quad (3.1)$$

In the absence of mixing the time evolution of $|K^0(t)\rangle$ is given by

$$|K^0(t)\rangle = |K^0(0)\rangle \exp(-iHt) , \quad H = M - i\frac{\Gamma}{2} , \quad (3.2)$$

where M is the mass and Γ the width of K^0 . Similar formula for \bar{K}^0 exists.

On the other hand, in the presence of flavour mixing the time evolution of the $K^0 - \bar{K}^0$ system is described by

$$i\frac{d\psi(t)}{dt} = \hat{H}\psi(t) \quad \psi(t) = \begin{pmatrix} |K^0(t)\rangle \\ |\bar{K}^0(t)\rangle \end{pmatrix} \quad (3.3)$$

where

$$\hat{H} = \hat{M} - i\frac{\hat{\Gamma}}{2} = \begin{pmatrix} M_{11} - i\frac{\Gamma_{11}}{2} & M_{12} - i\frac{\Gamma_{12}}{2} \\ M_{21} - i\frac{\Gamma_{21}}{2} & M_{22} - i\frac{\Gamma_{22}}{2} \end{pmatrix} \quad (3.4)$$

with \hat{M} and $\hat{\Gamma}$ being hermitian matrices having positive (real) eigenvalues in analogy with M and Γ . M_{ij} and Γ_{ij} are the transition matrix elements from virtual and physical intermediate states respectively. Using

$$M_{21} = M_{12}^* , \quad \Gamma_{21} = \Gamma_{12}^* , \quad (\text{hermiticity}) \quad (3.5)$$

$$M_{11} = M_{22} \equiv M , \quad \Gamma_{11} = \Gamma_{22} \equiv \Gamma , \quad (\text{CPT}) \quad (3.6)$$

we have

$$\hat{H} = \begin{pmatrix} M - i\frac{\Gamma}{2} & M_{12} - i\frac{\Gamma_{12}}{2} \\ M_{12}^* - i\frac{\Gamma_{12}^*}{2} & M - i\frac{\Gamma}{2} \end{pmatrix} . \quad (3.7)$$

We can next diagonalize the system to find:

Eigenstates:

$$K_{L,S} = \frac{(1 + \bar{\varepsilon})K^0 \pm (1 - \bar{\varepsilon})\bar{K}^0}{\sqrt{2(1 + |\bar{\varepsilon}|^2)}} \quad (3.8)$$

where $\bar{\varepsilon}$ is a small complex parameter given by

$$\frac{1 - \bar{\varepsilon}}{1 + \bar{\varepsilon}} = \sqrt{\frac{M_{12}^* - i\frac{1}{2}\Gamma_{12}^*}{M_{12} - i\frac{1}{2}\Gamma_{12}}} = \frac{\Delta M - i\frac{1}{2}\Delta\Gamma}{2M_{12} - i\Gamma_{12}} \equiv r \exp(i\kappa) . \quad (3.9)$$

with $\Delta\Gamma$ and ΔM given below.

Eigenvalues:

$$M_{L,S} = M \pm \text{Re}Q \quad \Gamma_{L,S} = \Gamma \mp 2\text{Im}Q \quad (3.10)$$

where

$$Q = \sqrt{(M_{12} - i\frac{1}{2}\Gamma_{12})(M_{12}^* - i\frac{1}{2}\Gamma_{12}^*)} . \quad (3.11)$$

Consequently we have

$$\Delta M = M_L - M_S = 2\text{Re}Q \quad \Delta\Gamma = \Gamma_L - \Gamma_S = -4\text{Im}Q . \quad (3.12)$$

It should be noted that the mass eigenstates K_S and K_L differ from CP eigenstates

$$K_1 = \frac{1}{\sqrt{2}}(K^0 - \bar{K}^0), \quad CP|K_1\rangle = |K_1\rangle, \quad (3.13)$$

$$K_2 = \frac{1}{\sqrt{2}}(K^0 + \bar{K}^0), \quad CP|K_2\rangle = -|K_2\rangle, \quad (3.14)$$

by a small admixture of the other CP eigenstate:

$$K_S = \frac{K_1 + \bar{\varepsilon}K_2}{\sqrt{1 + |\bar{\varepsilon}|^2}}, \quad K_L = \frac{K_2 + \bar{\varepsilon}K_1}{\sqrt{1 + |\bar{\varepsilon}|^2}}. \quad (3.15)$$

It should be stressed that the small parameter $\bar{\varepsilon}$ depends on the phase convention chosen for K^0 and \bar{K}^0 . Therefore it may not be taken as a physical measure of CP violation. On the other hand $\text{Re}\bar{\varepsilon}$ and r are independent of phase conventions. In particular the departure of r from 1 measures CP violation in the $K^0 - \bar{K}^0$ mixing:

$$r = 1 + \frac{2|\Gamma_{12}|^2}{4|M_{12}|^2 + |\Gamma_{12}|^2} \text{Im} \left(\frac{M_{12}}{\Gamma_{12}} \right). \quad (3.16)$$

Since $\bar{\varepsilon}$ is $\mathcal{O}(10^{-3})$, one has to a very good approximation:

$$\Delta M_K = 2\text{Re}M_{12}, \quad \Delta\Gamma_K = 2\text{Re}\Gamma_{12}, \quad (3.17)$$

where we have introduced the subscript K to stress that these formulae apply only to the $K^0 - \bar{K}^0$ system.

The $K_L - K_S$ mass difference is experimentally measured to be [8]

$$\Delta M_K = M(K_L) - M(K_S) = (3.489 \pm 0.009) \cdot 10^{-15} \text{ GeV}. \quad (3.18)$$

In the Standard Model roughly 70% of the measured ΔM_K is described by the real parts of the box diagrams with charm quark and top quark exchanges, whereby the contribution of the charm exchanges is by far dominant. This is related to the smallness of the real parts of the CKM top quark couplings compared with the corresponding charm quark couplings. Some non-negligible contribution comes from the box diagrams with simultaneous charm and top exchanges. The remaining 20% of the measured ΔM_K is attributed to long distance contributions which are difficult to estimate [30]. Further information with the relevant references can be found in [31].

The situation with $\Delta\Gamma_K$ is rather different. It is fully dominated by long distance effects. Experimentally one has $\Delta\Gamma_K \approx -2\Delta M_K$.

3.3 The First Look at ε and ε'

Since a two pion final state is CP even while a three pion final state is CP odd, K_S and K_L preferably decay to 2π and 3π , respectively via the following CP conserving decay modes:

$$K_L \rightarrow 3\pi \quad (\text{via } K_2), \quad K_S \rightarrow 2\pi \quad (\text{via } K_1). \quad (3.19)$$

This difference is responsible for the large disparity in their life-times. A factor of 579. However, K_L and K_S are not CP eigenstates and may decay with small branching fractions as follows:

$$K_L \rightarrow 2\pi \quad (\text{via } K_1), \quad K_S \rightarrow 3\pi \quad (\text{via } K_2). \quad (3.20)$$

This violation of CP is called *indirect* as it proceeds not via explicit breaking of the CP symmetry in the decay itself but via the admixture of the CP state with opposite CP parity to the dominant one. The measure for this indirect CP violation is defined as

$$\varepsilon = \frac{A(K_L \rightarrow (\pi\pi)_{I=0})}{A(K_S \rightarrow (\pi\pi)_{I=0})}. \quad (3.21)$$

Following the derivation in [27] one finds

$$\varepsilon = \frac{\exp(i\pi/4)}{\sqrt{2}\Delta M_K} (\text{Im}M_{12} + 2\xi\text{Re}M_{12}), \quad \xi = \frac{\text{Im}A_0}{\text{Re}A_0}. \quad (3.22)$$

where the term involving $\text{Im}M_{12}$ represents $\bar{\varepsilon}$ defined in (3.9). The phase convention dependence of the term involving ξ cancels the convention dependence of $\bar{\varepsilon}$ so that ε is free from this dependence.

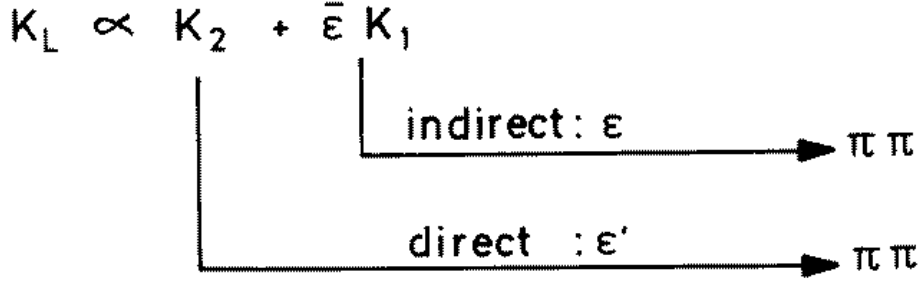


Figure 6: Indirect versus direct CP violation in $K_L \rightarrow \pi\pi$.

While *indirect* CP violation reflects the fact that the mass eigenstates are not CP eigenstates, so-called *direct* CP violation is realized via a direct transition of a CP odd to a CP even state or vice versa (see fig. 6). A measure of such a direct CP violation in $K_L \rightarrow \pi\pi$ is characterized by a complex parameter ε' defined as

$$\varepsilon' = \frac{1}{\sqrt{2}} \text{Im} \left(\frac{A_2}{A_0} \right) \exp(i\Phi_{\varepsilon'}), \quad \Phi_{\varepsilon'} = \frac{\pi}{2} + \delta_2 - \delta_0, \quad (3.23)$$

where the isospin amplitudes A_I in $K \rightarrow \pi\pi$ decays are introduced through

$$A(K^+ \rightarrow \pi^+\pi^0) = \sqrt{\frac{3}{2}}A_2e^{i\delta_2} \quad (3.24)$$

$$A(K^0 \rightarrow \pi^+\pi^-) = \sqrt{\frac{2}{3}}A_0e^{i\delta_0} + \sqrt{\frac{1}{3}}A_2e^{i\delta_2} \quad (3.25)$$

$$A(K^0 \rightarrow \pi^0\pi^0) = \sqrt{\frac{2}{3}}A_0e^{i\delta_0} - 2\sqrt{\frac{1}{3}}A_2e^{i\delta_2}. \quad (3.26)$$

Here the subscript $I = 0, 2$ denotes states with isospin 0, 2 equivalent to $\Delta I = 1/2$ and $\Delta I = 3/2$ transitions, respectively, and $\delta_{0,2}$ are the corresponding strong phases. The weak CKM phases are contained in A_0 and A_2 . The isospin amplitudes A_I are complex quantities which depend on phase conventions. On the other hand, ε' measures the difference between the phases of A_2 and A_0 and is a physical quantity. The strong phases $\delta_{0,2}$ can be extracted from $\pi\pi$ scattering. Then $\Phi_{\varepsilon'} \approx \pi/4$.

Experimentally ε and ε' can be found by measuring the ratios

$$\eta_{00} = \frac{A(K_L \rightarrow \pi^0\pi^0)}{A(K_S \rightarrow \pi^0\pi^0)}, \quad \eta_{+-} = \frac{A(K_L \rightarrow \pi^+\pi^-)}{A(K_S \rightarrow \pi^+\pi^-)}. \quad (3.27)$$

Indeed, assuming ε and ε' to be small numbers one finds

$$\eta_{00} = \varepsilon - \frac{2\varepsilon'}{1 - \sqrt{\omega}} \simeq \varepsilon - 2\varepsilon', \quad \eta_{+-} = \varepsilon + \frac{\varepsilon'}{1 + \omega/\sqrt{2}} \simeq \varepsilon + \varepsilon' \quad (3.28)$$

where experimentally $\omega = \text{Re}A_2/\text{Re}A_0 = 0.045$.

In the absence of direct CP violation $\eta_{00} = \eta_{+-}$. The ratio ε'/ε can then be measured through

$$\left| \frac{\eta_{00}}{\eta_{+-}} \right|^2 \simeq 1 - 6 \text{Re}\left(\frac{\varepsilon'}{\varepsilon}\right). \quad (3.29)$$

3.4 Basic Formula for ε

With all this information at hand let us derive a formula for ε which can be efficiently used in phenomenological applications. The off-diagonal element M_{12} in the neutral K -meson mass matrix representing K^0 - \bar{K}^0 mixing is given by

$$2m_K M_{12}^* = \langle \bar{K}^0 | \mathcal{H}_{\text{eff}}(\Delta S = 2) | K^0 \rangle, \quad (3.30)$$

where $\mathcal{H}_{\text{eff}}(\Delta S = 2)$ is the effective Hamiltonian for the $\Delta S = 2$ transitions. That M_{12}^* and not M_{12} stands on the l.h.s of this formula, is evident from (3.7). The factor $2m_K$ reflects our normalization of external states.

To lowest order in electroweak interactions $\Delta S = 2$ transitions are induced through the box diagrams of fig. 5. Including QCD corrections one has

$$\begin{aligned} \mathcal{H}_{\text{eff}}^{\Delta S=2} &= \frac{G_F^2}{16\pi^2} M_W^2 \left[\lambda_c^2 \eta_1 S_0(x_c) + \lambda_t^2 \eta_2 S_0(x_t) + 2\lambda_c \lambda_t \eta_3 S_0(x_c, x_t) \right] \times \\ &\times \left[\alpha_s^{(3)}(\mu) \right]^{-2/9} \left[1 + \frac{\alpha_s^{(3)}(\mu)}{4\pi} J_3 \right] Q(\Delta S = 2) + h.c. \end{aligned} \quad (3.31)$$

where $\lambda_i = V_{is}^* V_{id}$, $\mu < \mu_c = \mathcal{O}(m_c)$ and $\alpha_s^{(3)}$ is the strong coupling constant in an effective three flavour theory. In (3.31), the relevant operator

$$Q(\Delta S = 2) = (\bar{s}d)_{V-A}(\bar{s}d)_{V-A}, \quad (3.32)$$

is multiplied by the corresponding coefficient function. This function is decomposed into a charm-, a top- and a mixed charm-top contribution. The functions S_0 are given in (2.13) and (2.14).

Short-distance QCD effects are described through the correction factors η_1, η_2, η_3 and the explicitly α_s -dependent terms in (3.31). The NLO values of η_i are given as follows [31, 32, 33]:

$$\eta_1 = 1.38 \pm 0.20, \quad \eta_2 = 0.57 \pm 0.01, \quad \eta_3 = 0.47 \pm 0.04. \quad (3.33)$$

The quoted errors reflect the remaining theoretical uncertainties due to leftover μ -dependences at $\mathcal{O}(\alpha_s^2)$ and $\Lambda_{\overline{MS}}$, the scale in the QCD running coupling.

Defining the renormalization group invariant parameter \hat{B}_K by

$$\hat{B}_K = B_K(\mu) \left[\alpha_s^{(3)}(\mu) \right]^{-2/9} \left[1 + \frac{\alpha_s^{(3)}(\mu)}{4\pi} J_3 \right] \quad (3.34)$$

$$\langle \bar{K}^0 | (\bar{s}d)_{V-A} (\bar{s}d)_{V-A} | K^0 \rangle \equiv \frac{8}{3} B_K(\mu) F_K^2 m_K^2 \quad (3.35)$$

and using (3.31) one finds

$$M_{12} = \frac{G_F^2}{12\pi^2} F_K^2 \hat{B}_K m_K M_W^2 \left[\lambda_c^{*2} \eta_1 S_0(x_c) + \lambda_t^{*2} \eta_2 S_0(x_t) + 2\lambda_c^* \lambda_t^* \eta_3 S_0(x_c, x_t) \right], \quad (3.36)$$

where F_K is the K -meson decay constant and m_K the K -meson mass.

To proceed further we neglect the last term in (3.22) as it constitutes at most a 2% correction to ε . This is justified in view of other uncertainties, in particular those connected with \hat{B}_K . Inserting (3.36) into (3.22) we find

$$\varepsilon = C_\varepsilon \hat{B}_K \text{Im} \lambda_t \{ \text{Re} \lambda_c [\eta_1 S_0(x_c) - \eta_3 S_0(x_c, x_t)] - \text{Re} \lambda_t \eta_2 S_0(x_t) \} \exp(i\pi/4), \quad (3.37)$$

where we have used the unitarity relation $\text{Im} \lambda_c^* = \text{Im} \lambda_t$ and have neglected $\text{Re} \lambda_t / \text{Re} \lambda_c = \mathcal{O}(\lambda^4)$ in evaluating $\text{Im}(\lambda_c^* \lambda_t^*)$. The numerical constant C_ε is given by

$$C_\varepsilon = \frac{G_F^2 F_K^2 m_K M_W^2}{6\sqrt{2}\pi^2 \Delta M_K} = 3.84 \cdot 10^4. \quad (3.38)$$

To this end we have used the experimental value of ΔM_K in (3.18).

Using the standard parametrization of (1.5) to evaluate $\text{Im}\lambda_i$ and $\text{Re}\lambda_i$, setting the values for s_{12} , s_{13} , s_{23} and m_t in accordance with experiment and taking a value for \hat{B}_K (see below), one can determine the phase δ by comparing (3.37) with the experimental value for ε

$$\varepsilon_{exp} = (2.280 \pm 0.013) \cdot 10^{-3} \exp i\Phi_\varepsilon, \quad \Phi_\varepsilon = \frac{\pi}{4}. \quad (3.39)$$

Once δ has been determined in this manner one can find the apex $(\bar{\varrho}, \bar{\eta})$ of the unitarity triangle in fig. 1 by using

$$\varrho = \frac{s_{13}}{s_{12}s_{23}} \cos \delta, \quad \eta = \frac{s_{13}}{s_{12}s_{23}} \sin \delta \quad (3.40)$$

and

$$\bar{\varrho} = \varrho(1 - \frac{\lambda^2}{2}), \quad \bar{\eta} = \eta(1 - \frac{\lambda^2}{2}). \quad (3.41)$$

For a given set $(s_{12}, s_{13}, s_{23}, m_t, \hat{B}_K)$ there are two solutions for δ and consequently two solutions for $(\bar{\varrho}, \bar{\eta})$. This will be evident from the analysis of the unitarity triangle discussed in detail below.

Finally we have to say a few words about the non-perturbative parameter \hat{B}_K , the main uncertainty in this analysis. Reviews are given in [34, 35]. Here we only collect in table 1 values for \hat{B}_K obtained in various non-perturbative approaches. In our numerical analysis presented below we will use

$$\hat{B}_K = 0.80 \pm 0.15 \quad (3.42)$$

which is in the ball park of various lattice and large-N estimates.

3.5 Basic Formula for B^0 - \bar{B}^0 Mixing

The strength of the $B_{d,s}^0 - \bar{B}_{d,s}^0$ mixings is described by the mass differences

$$\Delta M_{d,s} = M_H^{d,s} - M_L^{d,s} \quad (3.43)$$

with ‘‘H’’ and ‘‘L’’ denoting *Heavy* and *Light* respectively. In contrast to ΔM_K , in this case the long distance contributions are estimated to be very small and $\Delta M_{d,s}$ is very well approximated by the relevant box diagrams. Moreover, due $m_{u,c} \ll m_t$ only the top sector can contribute significantly to $B_{d,s}^0 - \bar{B}_{d,s}^0$ mixings. The charm sector and the mixed top-charm contributions are entirely negligible.

$\Delta M_{d,s}$ can be expressed in terms of the off-diagonal element in the neutral B-meson mass matrix by using the formulae developed previously for the K-meson system. One finds

$$\Delta M_q = 2|M_{12}^{(q)}|, \quad q = d, s. \quad (3.44)$$

Table 1: \hat{B}_K obtained using various methods. WA stands for recent world average.

Method	\hat{B}_K	Reference
Chiral QM	1.1 ± 0.2	[36]
Lattice (APE)	0.93 ± 0.16	[37]
Lattice (JLQCD)	0.86 ± 0.06	[38]
Lattice (GKS)	0.85 ± 0.05	[39]
Lattice (WA)	0.89 ± 0.13	[40]
Large-N	0.70 ± 0.10	[41, 42]
Large-N	$0.4 - 0.7$	[43]
QCDS	$0.5 - 0.6$	[44]
CHPTH	0.42 ± 0.06	[45]
QCD HD	0.39 ± 0.10	[46]
SU(3)+PCAC	0.33	[47]

This formula differs from $\Delta M_K = 2\text{Re}M_{12}$ because in the B-system $\Gamma_{12} \ll M_{12}$.

The off-diagonal term M_{12} in the neutral B -meson mass matrix is then given by a formula analogous to (3.30)

$$2m_{B_q}|M_{12}^{(q)}| = |\langle \bar{B}_q^0 | \mathcal{H}_{\text{eff}}(\Delta B = 2) | B_q^0 \rangle|, \quad (3.45)$$

where in the case of $B_d^0 - \bar{B}_d^0$ mixing

$$\begin{aligned} \mathcal{H}_{\text{eff}}^{\Delta B=2} &= \frac{G_F^2}{16\pi^2} M_W^2 (V_{tb}^* V_{td})^2 \eta_B S_0(x_t) \times \\ &\times [\alpha_s^{(5)}(\mu_b)]^{-6/23} \left[1 + \frac{\alpha_s^{(5)}(\mu_b)}{4\pi} J_5 \right] Q(\Delta B = 2) + h.c. \end{aligned} \quad (3.46)$$

Here $\mu_b = \mathcal{O}(m_b)$,

$$Q(\Delta B = 2) = (\bar{b}d)_{V-A}(\bar{b}d)_{V-A} \quad (3.47)$$

and [32]

$$\eta_B = 0.55 \pm 0.01. \quad (3.48)$$

In the case of $B_s^0 - \bar{B}_s^0$ mixing one should simply replace $d \rightarrow s$ in (3.46) and (3.47) with all other quantities unchanged.

Defining the renormalization group invariant parameters \hat{B}_q in analogy to (3.34) and (3.35) one finds using (3.46)

$$\Delta M_q = \frac{G_F^2}{6\pi^2} \eta_B m_{B_q} (\hat{B}_{B_q} F_{B_q}^2) M_W^2 S_0(x_t) |V_{tq}|^2, \quad (3.49)$$

where F_{B_q} is the B_q -meson decay constant. This implies two useful formulae

$$\Delta M_d = 0.50/\text{ps} \cdot \left[\frac{\sqrt{\hat{B}_{B_d}} F_{B_d}}{200 \text{ MeV}} \right]^2 \left[\frac{\overline{m}_t(m_t)}{170 \text{ GeV}} \right]^{1.52} \left[\frac{|V_{td}|}{8.8 \cdot 10^{-3}} \right]^2 \left[\frac{\eta_B}{0.55} \right] \quad (3.50)$$

and

$$\Delta M_s = 15.1/\text{ps} \cdot \left[\frac{\sqrt{\hat{B}_{B_s}} F_{B_s}}{240 \text{ MeV}} \right]^2 \left[\frac{\overline{m}_t(m_t)}{170 \text{ GeV}} \right]^{1.52} \left[\frac{|V_{ts}|}{0.040} \right]^2 \left[\frac{\eta_B}{0.55} \right]. \quad (3.51)$$

There is a vast literature on the calculations of F_{B_d} and \hat{B}_d . The most recent lattice results are summarized in [48]. They are compatible with the results obtained with the help of QCD sum rules [49]. In our numerical analysis we will use the value for $F_{B_d} \sqrt{\hat{B}_{B_d}}$ given in table 2. The experimental situation on $\Delta M_{d,s}$ is also given there.

4 Standard Analysis of the Unitarity Triangle

4.1 Basic Procedure

With all these formulae at hand we can now summarize the standard analysis of the unitarity triangle in fig. 1. It proceeds in five steps.

Step 1:

From $b \rightarrow c$ transition in inclusive and exclusive leading B meson decays one finds $|V_{cb}|$ and consequently the scale of the unitarity triangle:

$$|V_{cb}| \implies \lambda |V_{cb}| = \lambda^3 A \quad (4.52)$$

Step 2:

From $b \rightarrow u$ transition in inclusive and exclusive B meson decays one finds $|V_{ub}/V_{cb}|$ and consequently the side $CA = R_b$ of the unitarity triangle:

$$\left| \frac{V_{ub}}{V_{cb}} \right| \implies R_b = \sqrt{\bar{\varrho}^2 + \bar{\eta}^2} = 4.44 \cdot \left| \frac{V_{ub}}{V_{cb}} \right| \quad (4.53)$$

Step 3:

From the experimental value of ε (3.39) and the formula (3.37) one derives, using the approximations (1.22)–(1.24), the constraint

$$\bar{\eta} \left[(1 - \bar{\varrho}) A^2 \eta_2 S_0(x_t) + P_0(\varepsilon) \right] A^2 \hat{B}_K = 0.224, \quad (4.54)$$

where

$$P_0(\varepsilon) = [\eta_3 S_0(x_c, x_t) - \eta_1 x_c] \frac{1}{\lambda^4}, \quad x_t = \frac{m_t^2}{M_W^2}. \quad (4.55)$$

$P_0(\varepsilon) = 0.31 \pm 0.05$ summarizes the contributions of box diagrams with two charm quark exchanges and the mixed charm-top exchanges. The main uncertainties in the constraint (4.54) reside in \hat{B}_K and to some extent in A^4 which multiplies the leading term. Equation (4.54) specifies a hyperbola in the $(\bar{\varrho}, \bar{\eta})$ plane. This hyperbola intersects the circle found in step 2 in two points which correspond to the two solutions for δ mentioned earlier. This is illustrated in fig. 7. The position of the hyperbola (4.54) in the $(\bar{\varrho}, \bar{\eta})$ plane depends on m_t , $|V_{cb}| = A\lambda^2$ and \hat{B}_K . With decreasing m_t , $|V_{cb}|$ and \hat{B}_K the ε -hyperbola moves away from the origin of the $(\bar{\varrho}, \bar{\eta})$ plane.

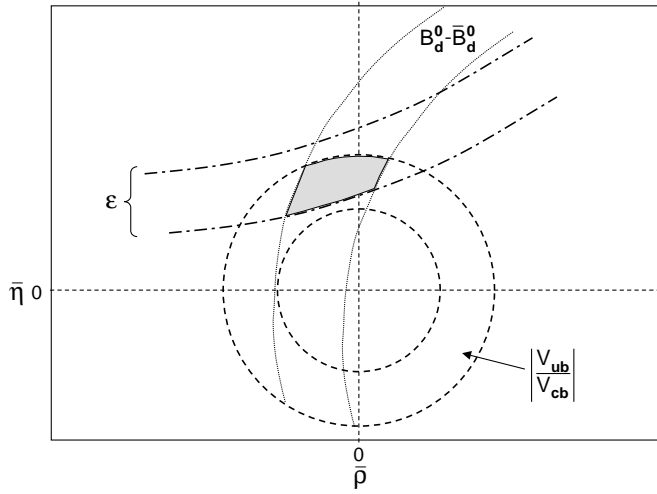


Figure 7: Schematic determination of the Unitarity Triangle.

Step 4: From the observed $B_d^0 - \bar{B}_d^0$ mixing parametrized by ΔM_d the side $BA = R_t$ of the unitarity triangle can be determined:

$$R_t = \frac{1}{\lambda} \frac{|V_{td}|}{|V_{cb}|} = 1.0 \cdot \left[\frac{|V_{td}|}{8.8 \cdot 10^{-3}} \right] \left[\frac{0.040}{|V_{cb}|} \right] \quad (4.56)$$

with

$$|V_{td}| = 8.8 \cdot 10^{-3} \left[\frac{200 \text{ MeV}}{\sqrt{B_{B_d}} F_{B_d}} \right] \left[\frac{170 \text{ GeV}}{\bar{m}_t(m_t)} \right]^{0.76} \left[\frac{\Delta M_d}{0.50/\text{ps}} \right]^{0.5} \sqrt{\frac{0.55}{\eta_B}}. \quad (4.57)$$

Since m_t , ΔM_d and η_B are already rather precisely known, the main uncertainty in the determination of $|V_{td}|$ from $B_d^0 - \bar{B}_d^0$ mixing comes from $F_{B_d} \sqrt{B_{B_d}}$. Note that R_t suffers from additional uncertainty in $|V_{cb}|$, which is absent in the determination of $|V_{td}|$ this way. The constraint in the $(\bar{\varrho}, \bar{\eta})$ plane coming from this step is illustrated in fig. 7.

Step 5:

Table 2: Collection of input parameters.

Quantity	Central	Error	Reference
$ V_{cb} $	0.040	± 0.002	[8]
$ V_{ub} $	$3.56 \cdot 10^{-3}$	$\pm 0.56 \cdot 10^{-3}$	[15]
\hat{B}_K	0.80	± 0.15	See Text
$\sqrt{B_d} F_{B_d}$	200 MeV	± 40 MeV	[48]
m_t	165 GeV	± 5 GeV	[50]
ΔM_d	0.471 ps^{-1}	$\pm 0.016 \text{ ps}^{-1}$	[51]
ΔM_s	$> 12.4 \text{ ps}^{-1}$	95% C.L.	[51]
ξ	1.14	± 0.08	[48, 52]

The measurement of $B_s^0 - \bar{B}_s^0$ mixing parametrized by ΔM_s together with ΔM_d allows to determine R_t in a different way. Using (3.49) one finds

$$\frac{|V_{td}|}{|V_{ts}|} = \xi \sqrt{\frac{m_{B_s}}{m_{B_d}}} \sqrt{\frac{\Delta M_d}{\Delta M_s}}, \quad \xi = \frac{F_{B_s} \sqrt{B_{B_s}}}{F_{B_d} \sqrt{B_{B_d}}}. \quad (4.58)$$

Using next $\Delta M_d^{\max} = 0.487/\text{ps}$ and $|V_{ts}/V_{cb}|^{\max} = 0.991$ one finds a useful approximate formula

$$(R_t)_{\max} = 1.0 \cdot \xi \sqrt{\frac{10.2/\text{ps}}{(\Delta M_s)_{\min}}}, \quad (4.59)$$

One should note that m_t and $|V_{cb}|$ dependences have been eliminated this way and that ξ should in principle contain much smaller theoretical uncertainties than the hadronic matrix elements in ΔM_d and ΔM_s separately. The most recent values relevant for (4.59) are summarized in table 2.

4.2 Numerical Results

4.2.1 Input Parameters

The input parameters needed to perform the standard analysis of the unitarity triangle are given in table 2, where m_t refers to the running current top quark mass defined at $\mu = m_t^{\text{Pole}}$. It corresponds to $m_t^{\text{Pole}} = 174.3 \pm 5.1 \text{ GeV}$ measured by CDF and D0 [50].

4.2.2 Output of the Standard Analysis

In what follows we will present two types of numerical analyses [35, 53]:

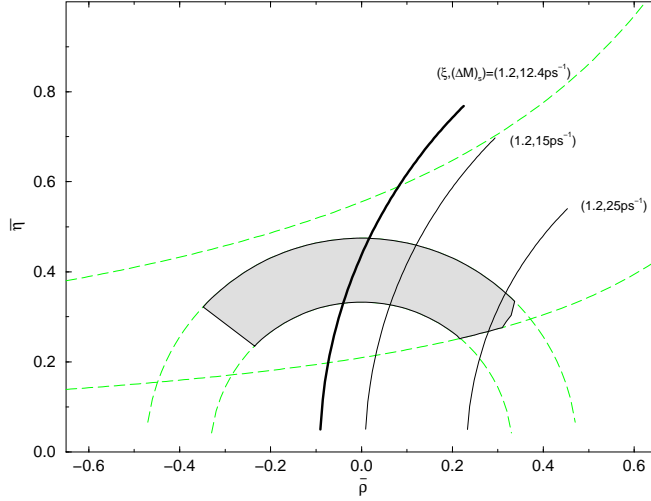


Figure 8: Unitarity Triangle 1999.

- Method 1: The experimentally measured numbers are used with Gaussian errors and for the theoretical input parameters we take a flat distribution in the ranges given in table 2.
- Method 2: Both the experimentally measured numbers and the theoretical input parameters are scanned independently within the ranges given in table 2.

The results are shown in table 3. The allowed region for $(\bar{\rho}, \bar{\eta})$ is presented in fig. 8. It is the shaded area on the right hand side of the solid circle which represents the upper bound for $(\Delta M)_d/(\Delta M)_s$. The hyperbolas give the constraint from ϵ and the two circles centered at $(0,0)$ the constraint from $|V_{ub}/V_{cb}|$. The white areas between the lower ϵ -hyperbola and the shaded region are excluded by $B_d^0 - \bar{B}_d^0$ mixing. We observe that the region $\bar{\rho} < 0$ is practically excluded. The results in fig. 8 correspond to a simple independent scanning of all parameters within one standard deviation. We find that whereas the angle β is rather constrained, the uncertainties in α and γ are substantially larger:

$$66^\circ \leq \alpha \leq 113^\circ, \quad 17^\circ \leq \beta \leq 29^\circ, \quad 44^\circ \leq \gamma \leq 97^\circ. \quad (4.60)$$

The result for $\sin 2\beta$ is consistent with the recent measurement of CP asymmetry in $B \rightarrow \psi K_S$ by CDF [54], although the large experimental error precludes any definite conclusion.

Other studies of the unitarity triangle can be found in [14, 15, 55, 56].

Table 3: Output of the Standard Analysis. $\lambda_t = V_{ts}^* V_{td}$.

Quantity	Scanning	Gaussian
$ V_{td} /10^{-3}$	7.0 – 9.8	8.1 ± 0.6
$ V_{ts}/V_{cb} $	0.975 – 0.991	0.984 ± 0.004
$ V_{td}/V_{ts} $	0.17 – 0.24	0.201 ± 0.017
$\sin(2\beta)$	0.57 – 0.84	0.73 ± 0.09
$\sin(2\alpha)$	−0.72 – 1.0	$−0.03 \pm 0.36$
$\sin(\gamma)$	0.69 – 1.0	0.89 ± 0.08
$\text{Im}\lambda_t/10^{-4}$	1.04 – 1.63	1.33 ± 0.14

4.3 Final Remarks

In this section we have completed the determination of the CKM matrix. It is given by the values of $|V_{us}|$, $|V_{cb}|$ and $|V_{ub}|$ in (1.36) and (1.37), the results in table 3 and the unitarity triangle shown in fig. 8. Clearly the accuracy of this determination is not yet impressive. We should stress, however, that in a few years from now the standard analysis may give much more accurate results. In particular a single precise measurement of ΔM_s will have a very important impact on the allowed area in the $(\bar{\varrho}, \bar{\eta})$ plane. Such a measurement should come from SLD and later from LHC.

Having the values of CKM parameters at hand, we can use them to predict various branching ratios for rare and CP-violating decays. This we will do in the subsequent sections.

5 ε'/ε in the Standard Model

5.1 Preliminaries

Direct CP violation remains one of the important targets of contemporary particle physics. In the case of $K \rightarrow \pi\pi$, a non-vanishing value of the ratio $\text{Re}(\varepsilon'/\varepsilon)$ defined in (3.23) would give the first signal for direct CP violation ruling out superweak models [57]. Until recently the experimental situation on ε'/ε was rather unclear:

$$\text{Re}(\varepsilon'/\varepsilon) = \begin{cases} (23 \pm 7) \cdot 10^{-4} & \text{(NA31) [58]} \\ (7.4 \pm 5.9) \cdot 10^{-4} & \text{(E731) [59]}. \end{cases} \quad (5.1)$$

While the result of the NA31 collaboration at CERN [58] clearly indicated direct CP violation, the value of E731 at Fermilab [59], was compatible with superweak theories [57] in which

$\varepsilon'/\varepsilon = 0$. This controversy is now settled with the very recent measurement by KTeV at Fermilab [60]

$$\text{Re}(\varepsilon'/\varepsilon) = (28.0 \pm 4.1) \cdot 10^{-4} \quad (\text{KTeV}) \quad (5.2)$$

which together with the NA31 result confidently establishes direct CP violation in nature. The grand average including NA31, E731 and KTeV results reads [60]

$$\text{Re}(\varepsilon'/\varepsilon) = (21.8 \pm 3.0) \cdot 10^{-4} \quad (5.3)$$

very close to the NA31 result but with a smaller error. The error should be further reduced once the first data from NA48 collaboration at CERN are available and complete data from both collaborations have been analyzed. It is also of great interest to see what value for ε'/ε will be measured by KLOE at Frascati, which uses a different experimental technique than KTeV and NA48.

There is a long history of calculations of ε'/ε in the Standard Model. The first calculation of ε'/ε for $m_t \ll M_W$ without the inclusion of renormalization group effects can be found in [61]. Renormalization group effects in the leading logarithmic approximation have been first presented in [62]. For $m_t \ll M_W$ only QCD penguins play a substantial role. First extensive phenomenological analyses in this approximation can be found in [63]. Over the eighties these calculations were refined through the inclusion of QED penguin effects for $m_t \ll M_W$ [64, 65, 66], the inclusion of isospin breaking in the quark masses [65, 66, 67], and through improved estimates of hadronic matrix elements in the framework of the $1/N$ approach [68]. This era of ε'/ε culminated in the analyses in [69, 70], where QCD penguins, electroweak penguins (γ and Z^0 penguins) and the relevant box diagrams were included for arbitrary top quark masses. The strong cancellation between QCD penguins and electroweak penguins for $m_t > 150 \text{ GeV}$ found in these papers was confirmed by other authors [71].

During the nineties considerable progress has been made by calculating complete NLO corrections to ε' [72]–[76]. Together with the NLO corrections to ε and $B^0 - \bar{B}^0$ mixing [31, 32, 33], this allowed a complete NLO analysis of ε'/ε including constraints from the observed indirect CP violation (ε) and $B_{d,s}^0 - \bar{B}_{d,s}^0$ mixings ($\Delta M_{d,s}$). The improved determination of the V_{ub} and V_{cb} elements of the CKM matrix, the improved estimates of hadronic matrix elements using the lattice approach as well as other non-perturbative approaches and in particular the determination of the top quark mass m_t had of course also an important impact on ε'/ε .

Now, ε'/ε is given by (5.5) where in a crude approximation (not to be used for any serious analysis)

$$F_{\varepsilon'} \approx 13 \cdot \left[\frac{110 \text{ MeV}}{m_s(2 \text{ GeV})} \right]^2 \left[B_6^{(1/2)} (1 - \Omega_{\eta+\eta'}) - 0.4 \cdot B_8^{(3/2)} \left(\frac{m_t}{165 \text{ GeV}} \right)^{2.5} \right] \left(\frac{\Lambda_{\overline{\text{MS}}}^{(4)}}{340 \text{ MeV}} \right). \quad (5.4)$$

Here $\Omega_{\eta+\eta'} \approx 0.25$ represents isospin breaking corrections and B_i are hadronic parameters which we will define later on. This formula exhibits very clearly the dominant uncertainties in $F_{\varepsilon'}$ which reside in the values of m_s , $B_6^{(1/2)}$, $B_8^{(3/2)}$, $\Lambda_{\overline{\text{MS}}}^{(4)}$ and $\Omega_{\eta+\eta'}$. Moreover, the partial cancellation between QCD penguin ($B_6^{(1/2)}$) and electroweak penguin ($B_8^{(3/2)}$) contributions requires accurate values of $B_6^{(1/2)}$ and $B_8^{(3/2)}$ for an acceptable estimate of ε'/ε . Because of the accurate value $m_t(m_t) = 165 \pm 5$ GeV, the uncertainty in ε'/ε due to the top quark mass amounts only to a few percent. A more accurate formula for $F_{\varepsilon'}$ will be given below.

Now, it has been known for some time that for central values of the input parameters the size of ε'/ε in the Standard Model is well below the NA31 value of $(23.0 \pm 6.5) \cdot 10^{-4}$. Indeed, extensive NLO analyses with lattice and large-N estimates of $B_6^{(1/2)} \approx 1$ and $B_8^{(3/2)} \approx 1$ performed first in [74, 75] and after the top discovery in [77, 78, 79] have found ε'/ε in the ballpark of $(3-7) \cdot 10^{-4}$ for $m_s(2 \text{ GeV}) \approx 130$ MeV. On the other hand it has been stressed repeatedly in [1, 78] that for extreme values of $B_6^{(1/2)}$, $B_8^{(3/2)}$ and m_s still consistent with lattice, QCD sum rules and large-N estimates as well as sufficiently high values of $\text{Im}\lambda_t$ and $\Lambda_{\overline{\text{MS}}}^{(4)}$, a ratio ε'/ε as high as $(2-3) \cdot 10^{-3}$ could be obtained within the Standard Model. Yet, it has also been admitted that such simultaneously extreme values of all input parameters and consequently values of ε'/ε close to the NA31 result are rather improbable in the Standard Model. Different conclusions have been reached in [80], where values $(1-2) \cdot 10^{-3}$ for ε'/ε can be found. Also the Trieste group [81], which calculated the parameters $B_6^{(1/2)}$ and $B_8^{(3/2)}$ in the chiral quark model, found $\varepsilon'/\varepsilon = (1.7 \pm 1.4) \cdot 10^{-3}$. On the other hand using an effective chiral lagrangian approach, the authors in [83] found ε'/ε consistent with zero.

After these general remarks let us discuss ε'/ε in explicit terms. Other reviews of ε'/ε can be found in [82, 81].

5.2 Basic Formulae

The parameter ε' is given in terms of the isospin amplitudes A_I in (3.23). Applying OPE to these amplitudes one finds

$$\frac{\varepsilon'}{\varepsilon} = \text{Im}\lambda_t \cdot F_{\varepsilon'}, \quad (5.5)$$

where

$$F_{\varepsilon'} = \left[P^{(1/2)} - P^{(3/2)} \right] \exp(i\Phi), \quad (5.6)$$

with

$$P^{(1/2)} = r \sum y_i \langle Q_i \rangle_0 (1 - \Omega_{\eta+\eta'}) , \quad (5.7)$$

$$P^{(3/2)} = \frac{r}{\omega} \sum y_i \langle Q_i \rangle_2 . \quad (5.8)$$

Here

$$r = \frac{G_F \omega}{2|\varepsilon| \text{Re} A_0} , \quad \langle Q_i \rangle_I \equiv \langle (\pi\pi)_I | Q_i | K \rangle , \quad \omega = \frac{\text{Re} A_2}{\text{Re} A_0}. \quad (5.9)$$

Since

$$\Phi = \Phi_{\varepsilon'} - \Phi_{\varepsilon} \approx 0, \quad (5.10)$$

$F_{\varepsilon'}$ and ε'/ε are real to an excellent approximation. The operators Q_i have been given already in (2.4)-(2.8). The Wilson coefficient functions $y_i(\mu)$ were calculated including the complete next-to-leading order (NLO) corrections in [72]–[76]. The details of these calculations can be found there and in the review [2]. Their numerical values for $\Lambda_{\overline{\text{MS}}}^{(4)}$ corresponding to $\alpha_{\overline{\text{MS}}}^{(5)}(M_Z) = 0.119 \pm 0.003$ and two renormalization schemes (NDR and HV) are given in table 4 [35].

Table 4: $\Delta S = 1$ Wilson coefficients at $\mu = m_c = 1.3 \text{ GeV}$ for $m_t = 165 \text{ GeV}$ and $f = 3$ effective flavours. $y_1 = y_2 \equiv 0$.

	$\Lambda_{\overline{\text{MS}}}^{(4)} = 290 \text{ MeV}$		$\Lambda_{\overline{\text{MS}}}^{(4)} = 340 \text{ MeV}$		$\Lambda_{\overline{\text{MS}}}^{(4)} = 390 \text{ MeV}$	
Scheme	NDR	HV	NDR	HV	NDR	HV
y_3	0.027	0.030	0.030	0.034	0.033	0.038
y_4	−0.054	−0.056	−0.059	−0.061	−0.064	−0.067
y_5	0.006	0.015	0.005	0.016	0.003	0.017
y_6	−0.082	−0.074	−0.092	−0.083	−0.105	−0.093
y_7/α	−0.038	−0.037	−0.037	−0.036	−0.037	−0.034
y_8/α	0.118	0.127	0.134	0.143	0.152	0.161
y_9/α	−1.410	−1.410	−1.437	−1.437	−1.466	−1.466
y_{10}/α	0.496	0.502	0.539	0.546	0.585	0.593

It is customary in phenomenological applications to take $\text{Re} A_0$ and ω from experiment, i.e.

$$\text{Re} A_0 = 3.33 \cdot 10^{-7} \text{ GeV}, \quad \omega = 0.045, \quad (5.11)$$

where the last relation reflects the so-called $\Delta I = 1/2$ rule. This strategy avoids to a large extent the hadronic uncertainties in the real parts of the isospin amplitudes A_I .

The sum in (5.7) and (5.8) runs over all contributing operators. $P^{(3/2)}$ is fully dominated by electroweak penguin contributions. $P^{(1/2)}$ on the other hand is governed by QCD penguin contributions which are suppressed by isospin breaking in the quark masses ($m_u \neq m_d$). The latter effect is described by

$$\Omega_{\eta+\eta'} = \frac{1}{\omega} \frac{(\text{Im}A_2)_{\text{I.B.}}}{\text{Im}A_0}. \quad (5.12)$$

For $\Omega_{\eta+\eta'}$ we will first set

$$\Omega_{\eta+\eta'} = 0.25, \quad (5.13)$$

which is in the ball park of the values obtained in the $1/N$ approach [66] and in chiral perturbation theory [65, 67]. $\Omega_{\eta+\eta'}$ is independent of m_t . We will investigate the sensitivity of ε'/ε to $\Omega_{\eta+\eta'}$ later on.

5.3 Hadronic Matrix Elements

The main source of uncertainty in the calculation of ε'/ε are the hadronic matrix elements $\langle Q_i \rangle_I$. They generally depend on the renormalization scale μ and on the scheme used to renormalize the operators Q_i . These two dependences are canceled by those present in the Wilson coefficients $y_i(\mu)$ so that the resulting physical ε'/ε does not (in principle) depend on μ and on the renormalization scheme of the operators. Unfortunately, the accuracy of the present non-perturbative methods used to evaluate $\langle Q_i \rangle_I$ is not sufficient to have the μ and scheme dependences of $\langle Q_i \rangle_I$ fully under control. We believe that this situation will change once the lattice calculations and QCD sum rule calculations improve. A brief review of the existing methods including most recent developments will be given below.

In view of this situation it has been suggested in [74] to determine as many matrix elements $\langle Q_i \rangle_I$ as possible from the leading CP conserving $K \rightarrow \pi\pi$ decays, for which the experimental data is summarized in (5.11). To this end it turned out to be very convenient to determine $\langle Q_i \rangle_I$ in the three-flavour effective theory at a scale $\mu \approx m_c$. The details of this approach will not be discussed here. It suffices to say that this method allows to determine only the matrix elements of the $(V - A) \otimes (V - A)$ operators. For the central value of $\text{Im}\lambda_t$ these operators give a negative contribution to ε'/ε of about $-2.5 \cdot 10^{-4}$. This shows that these operators are only relevant if ε'/ε is below $1 \cdot 10^{-3}$. Unfortunately the matrix elements of the dominant $(V - A) \otimes (V + A)$ operators cannot be determined by the CP conserving data and one has to use non-perturbative methods to estimate them.

Concerning the $(V - A) \otimes (V + A)$ operators $Q_5 - Q_8$, it is customary to express their matrix elements $\langle Q_i \rangle_I$ in terms of non-perturbative parameters $B_i^{(1/2)}$ and $B_i^{(3/2)}$ as follows:

$$\langle Q_i \rangle_0 \equiv B_i^{(1/2)} \langle Q_i \rangle_0^{(\text{vac})}, \quad \langle Q_i \rangle_2 \equiv B_i^{(3/2)} \langle Q_i \rangle_2^{(\text{vac})}. \quad (5.14)$$

The label “vac” stands for the vacuum insertion estimate of the hadronic matrix elements in question for which $B_i^{(1/2)} = B_i^{(3/2)} = 1$.

As the numerical analysis in [74] shows ε'/ε is only weakly sensitive to the values of the parameters $B_3^{(1/2)}$, $B_5^{(1/2)}$, $B_7^{(1/2)}$, $B_8^{(1/2)}$ and $B_7^{(3/2)}$ as long as their absolute values are not substantially larger than 1. As in [74] our strategy is to set

$$B_{3,7,8}^{(1/2)}(m_c) = 1, \quad B_5^{(1/2)}(m_c) = B_6^{(1/2)}(m_c), \quad B_7^{(3/2)}(m_c) = B_8^{(3/2)}(m_c) \quad (5.15)$$

and to treat $B_6^{(1/2)}(m_c)$ and $B_8^{(3/2)}(m_c)$ as free parameters.

The approach in [74] allows then in a good approximation to express ε'/ε or equivalently $F_{\varepsilon'}$ in terms of $\Lambda_{\overline{\text{MS}}}^{(4)}$, m_t , m_s and the two non-perturbative parameters $B_6^{(1/2)} \equiv B_6^{(1/2)}(m_c)$ and $B_8^{(3/2)} \equiv B_8^{(3/2)}(m_c)$ which cannot be fixed by the CP conserving data.

5.4 An Analytic Formula for ε'/ε

As shown in [84], it is possible to cast the formal expressions for ε'/ε in (5.5)–(5.8) into an analytic formula which exhibits the m_t dependence together with the dependence on m_s , $\Lambda_{\overline{\text{MS}}}^{(4)}$, $B_6^{(1/2)}$ and $B_8^{(3/2)}$. To this end the approach for hadronic matrix elements presented above is used and $\Omega_{\eta+\eta'}$ is set to 0.25. The analytic formula given below, while being rather accurate, exhibits various features which are not transparent in a pure numerical analysis. It can be used in phenomenological applications if one is satisfied with a few percent accuracy. Needless to say, in the numerical analysis [35] presented below we have used exact expressions.

In this formulation the function $F_{\varepsilon'}$ is given simply as follows ($x_t = m_t^2/M_W^2$):

$$F_{\varepsilon'} = P_0 + P_X X_0(x_t) + P_Y Y_0(x_t) + P_Z Z_0(x_t) + P_E E_0(x_t). \quad (5.16)$$

with the m_t -dependent functions given in subsection 2.4.

The coefficients P_i are given in terms of $B_6^{(1/2)} \equiv B_6^{(1/2)}(m_c)$, $B_8^{(3/2)} \equiv B_8^{(3/2)}(m_c)$ and $m_s(m_c)$ as follows:

$$P_i = r_i^{(0)} + r_i^{(6)} R_6 + r_i^{(8)} R_8. \quad (5.17)$$

where

$$R_6 \equiv B_6^{(1/2)} \left[\frac{137 \text{ MeV}}{m_s(m_c) + m_d(m_c)} \right]^2, \quad R_8 \equiv B_8^{(3/2)} \left[\frac{137 \text{ MeV}}{m_s(m_c) + m_d(m_c)} \right]^2. \quad (5.18)$$

The P_i are renormalization scale and scheme independent. They depend, however, on $\Lambda_{\overline{\text{MS}}}^{(4)}$. In table 5 we give the numerical values of $r_i^{(0)}$, $r_i^{(6)}$ and $r_i^{(8)}$ for different values of $\Lambda_{\overline{\text{MS}}}^{(4)}$ at $\mu = m_c$ in the NDR renormalization scheme [35]. Actually at NLO only r_0 coefficients are renormalization scheme dependent. The last row gives them in the HV scheme. The inspection of table 5 shows that the terms involving $r_0^{(6)}$ and $r_Z^{(8)}$ dominate the ratio ε'/ε . Moreover, the function $Z_0(x_t)$ representing a gauge invariant combination of Z^0 - and γ -penguins grows rapidly with m_t and due to $r_Z^{(8)} < 0$ these contributions suppress ε'/ε strongly for large m_t [69, 70].

Table 5: Coefficients in the formula (5.17) for various $\Lambda_{\overline{\text{MS}}}^{(4)}$ in the NDR scheme. The last row gives the r_0 coefficients in the HV scheme.

	$\Lambda_{\overline{\text{MS}}}^{(4)} = 290 \text{ MeV}$			$\Lambda_{\overline{\text{MS}}}^{(4)} = 340 \text{ MeV}$			$\Lambda_{\overline{\text{MS}}}^{(4)} = 390 \text{ MeV}$		
i	$r_i^{(0)}$	$r_i^{(6)}$	$r_i^{(8)}$	$r_i^{(0)}$	$r_i^{(6)}$	$r_i^{(8)}$	$r_i^{(0)}$	$r_i^{(6)}$	$r_i^{(8)}$
0	-2.771	9.779	1.429	-2.811	11.127	1.267	-2.849	12.691	1.081
X_0	0.532	0.017	0	0.518	0.021	0	0.506	0.024	0
Y_0	0.396	0.072	0	0.381	0.079	0	0.367	0.087	0
Z_0	0.354	-0.013	-9.404	0.409	-0.015	-10.230	0.470	-0.017	-11.164
E_0	0.182	-1.144	0.411	0.167	-1.254	0.461	0.153	-1.375	0.517
0	-2.749	8.596	1.050	-2.788	9.638	0.871	-2.825	10.813	0.669

5.5 The Status of m_s , $B_6^{(1/2)}$, $B_8^{(3/2)}$, $\Omega_{\eta+\eta'}$ and $\Lambda_{\overline{\text{MS}}}^{(4)}$

The present status of these parameters has been recently reviewed in details in [35]. Therefore our presentation will be very brief.

5.5.1 m_s

The present values for $m_s(2 \text{ GeV})$ extracted from lattice calculations and QCD sum rules are

$$m_s(2 \text{ GeV}) = \begin{cases} (110 \pm 20) \text{ MeV} & \text{(Lattice) [34, 85]} \\ (124 \pm 22) \text{ MeV} & \text{(QCDS) [86]} \end{cases} \quad (5.19)$$

The value for QCD sum rules is an average over the results given in [86]. QCD sum rules also allow to derive lower bounds on the strange quark mass. It was found that generally $m_s(2 \text{ GeV}) \gtrsim 100 \text{ MeV}$ [87]. If these bounds hold, they would rule out the very low strange mass values found in unquenched lattice QCD simulations given above.

Finally, one should also mention the very recent determination of the strange mass from the hadronic τ -spectral function [88, 89]: $m_s(2 \text{ GeV}) = (170_{-55}^{+44}) \text{ MeV}$. We observe that the central value is much larger than the corresponding results given above although the error is still large. In the future, however, improved experimental statistics and a better understanding of perturbative QCD corrections should make the determination of m_s from the τ -spectral function competitive to the other methods. On the other hand a very recent estimate using new τ -like ϕ -meson sum rules gives $m_s(2 \text{ GeV}) = (136 \pm 16) \text{ MeV}$ [90].

We conclude that the error on m_s is still rather large. In our numerical analysis of ε'/ε , where m_s is evaluated at the scale m_c , we will set

$$m_s(m_c) = (130 \pm 25) \text{ MeV}, \quad (5.20)$$

roughly corresponding to $m_s(2 \text{ GeV})$ obtained in the lattice approach.

5.5.2 $B_6^{(1/2)}$ and $B_8^{(3/2)}$

The values for $B_6^{(1/2)}$ and $B_8^{(3/2)}$ obtained in various approaches are collected in table 6. The lattice results have been obtained at $\mu = 2 \text{ GeV}$. The results in the large- N approach and the chiral quark model correspond to scales below 1 GeV . However, as a detailed numerical analysis in [74] showed, $B_6^{(1/2)}$ and $B_8^{(3/2)}$ are only weakly dependent on μ . Consequently the comparison of these parameters obtained in different approaches at different μ is meaningful.

Next, the values coming from lattice and chiral quark model are given in the NDR renormalization scheme. The corresponding values in the HV scheme can be found using approximate relations [35]

$$(B_6^{(1/2)})_{\text{HV}} \approx 1.2(B_6^{(1/2)})_{\text{NDR}}, \quad (B_8^{(3/2)})_{\text{HV}} \approx 1.2(B_8^{(3/2)})_{\text{NDR}}. \quad (5.21)$$

The results in the large- N approach are unfortunately not sensitive to the renormalization scheme.

Concerning the lattice results for $B_6^{(1/2)}$, the old results read $B_{5,6}^{(1/2)}(2 \text{ GeV}) = 1.0 \pm 0.2$ [93, 94]. More accurate estimates for $B_6^{(1/2)}$ have been given in [95]: $B_6^{(1/2)}(2 \text{ GeV}) = 0.67 \pm 0.04 \pm 0.05$ (quenched) and $B_6^{(1/2)}(2 \text{ GeV}) = 0.76 \pm 0.03 \pm 0.05$ ($f = 2$). However, a recent work in [96] shows that lattice calculations of $B_6^{(1/2)}$ are very uncertain and one has to conclude that there are no solid predictions for $B_6^{(1/2)}$ from the lattice at present.

Table 6: Results for $B_6^{(1/2)}$ and $B_8^{(3/2)}$ obtained in various approaches.

Method	$B_6^{(1/2)}$	$B_8^{(3/2)}$
Lattice[39, 91, 37]	—	0.69 – 1.06
Large- N [92, 43]	0.72 – 1.10	0.42 – 0.64
ChQM[81]	1.07 – 1.58	0.75 – 0.79

We observe that most non-perturbative approaches discussed above found $B_8^{(3/2)}$ below unity. The suppression of $B_8^{(3/2)}$ below unity is rather modest (at most 20%) in the lattice approaches and in the chiral quark model. In the $1/N$ approach $B_8^{(3/2)}$ is rather strongly suppressed and can be as low as 0.5.

Concerning $B_6^{(1/2)}$ the situation is worse. As we stated above there is no solid prediction for this parameter in the lattice approach. On the other hand while the average value of $B_6^{(1/2)}$ in the $1/N$ approach is close to 1.0, the chiral quark model gives in the NDR scheme

the value for $B_6^{(1/2)}$ as high as 1.33 ± 0.25 . Interestingly both approaches give the ratio $B_6^{(1/2)}/B_8^{(3/2)}$ in the ball park of 1.7.

Guided by the results presented above and biased to some extent by the results from the large-N approach and lattice calculations, we will use in our numerical analysis below $B_6^{(1/2)}$ and $B_8^{(3/2)}$ in the ranges:

$$B_6^{(1/2)} = 1.0 \pm 0.3, \quad B_8^{(3/2)} = 0.8 \pm 0.2 \quad (5.22)$$

keeping always $B_6^{(1/2)} \geq B_8^{(3/2)}$.

5.5.3 $\Omega_{\eta+\eta'}$ and $\Lambda_{\overline{\text{MS}}}^{(4)}$

The dependence of ε'/ε on $\Omega_{\eta+\eta'}$ can be studied numerically by using the formula (5.7) or incorporated approximately into the analytic formula (5.16) by simply replacing $B_6^{(1/2)}$ with an effective parameter

$$(B_6^{(1/2)})_{\text{eff}} = B_6^{(1/2)} \frac{(1 - 0.9 \Omega_{\eta+\eta'})}{0.775} \quad (5.23)$$

A numerical analysis shows that using $(1 - \Omega_{\eta+\eta'})$ overestimates the role of $\Omega_{\eta+\eta'}$. In our numerical analysis we have incorporated the uncertainty in $\Omega_{\eta+\eta'}$ by increasing the error in $B_6^{(1/2)}$ from ± 0.2 to ± 0.3 .

The last estimates of $\Omega_{\eta+\eta'}$ have been done more than ten years ago [65]-[67] and it is desirable to update these analyses which can be summarized by

$$\Omega_{\eta+\eta'} = 0.25 \pm 0.08 . \quad (5.24)$$

In table 7 we summarize the input parameters used in the numerical analysis of ε'/ε below. The range for $\Lambda_{\overline{\text{MS}}}^{(4)}$ in table 7 corresponds roughly to $\alpha_s(M_Z) = 0.119 \pm 0.003$.

Table 7: Collection of input parameters. We impose $B_6^{(1/2)} \geq B_8^{(3/2)}$.

Quantity	Central	Error	Reference
$\Lambda_{\overline{\text{MS}}}^{(4)}$	340 MeV	± 50 MeV	[8, 97]
$m_s(m_c)$	130 MeV	± 25 MeV	See Text
$B_6^{(1/2)}$	1.0	± 0.3	See Text
$B_8^{(3/2)}$	0.8	± 0.2	See Text

5.6 Numerical Results for ε'/ε

In order to make predictions for ε'/ε we need the value of $\text{Im}\lambda_t$. This can be obtained from the standard analysis of the unitarity triangle as discussed in section 4.

In what follows we will present two types of numerical analyses of ε'/ε which use the methods 1 and 2 discussed already in section 4. This analysis is based on [35].

Using the first method we find the probability density distributions for ε'/ε in fig. 9. From this distribution we deduce the following results:

$$\varepsilon'/\varepsilon = \begin{cases} (7.7^{+6.0}_{-3.5}) \cdot 10^{-4} & (\text{NDR}) \\ (5.2^{+4.6}_{-2.7}) \cdot 10^{-4} & (\text{HV}) \end{cases} \quad (5.25)$$

The difference between these two results indicates the left over renormalization scheme dependence. Since, the resulting probability density distributions for ε'/ε are very asymmetric with very long tails towards large values we quote the medians and the 68%(95%) confidence level intervals. This means that 68%(95%) of our data can be found inside the corresponding error interval and that 50% of our data has smaller ε'/ε than our median.

We observe that negative values of ε'/ε can be excluded at 95% C.L. For completeness we quote the mean and the standard deviation for ε'/ε :

$$\varepsilon'/\varepsilon = \begin{cases} (9.1 \pm 6.2) \cdot 10^{-4} & (\text{NDR}) \\ (6.3 \pm 4.8) \cdot 10^{-4} & (\text{HV}) \end{cases} \quad (5.26)$$

Using the second method and the parameters in table 2 we find :

$$1.05 \cdot 10^{-4} \leq \varepsilon'/\varepsilon \leq 28.8 \cdot 10^{-4} \quad (\text{NDR}). \quad (5.27)$$

and

$$0.26 \cdot 10^{-4} \leq \varepsilon'/\varepsilon \leq 22.0 \cdot 10^{-4} \quad (\text{HV}). \quad (5.28)$$

We observe that ε'/ε is generally lower in the HV scheme if the same values for $B_6^{(1/2)}$ and $B_8^{(3/2)}$ are used in both schemes. Since the present non-perturbative methods do not have renormalization scheme dependence fully under control we think that such treatment of $B_6^{(1/2)}$ and $B_8^{(3/2)}$ is the proper way of estimating scheme dependences at present. Assuming, on the other hand, that the values in (5.22) correspond to the NDR scheme and using the relation (5.21), we find for the HV scheme the range $0.58 \cdot 10^{-4} \leq \varepsilon'/\varepsilon \leq 26.9 \cdot 10^{-4}$ which is much closer to the NDR result in (5.27). This exercise shows that it is very desirable to have the scheme dependence under control.

We observe that the most probable values for ε'/ε in the NDR scheme are in the ballpark of $1 \cdot 10^{-3}$. They are lower by roughly 30% in the HV scheme if the same values for $(B_6^{(1/2)}, B_8^{(3/2)})$ are used. On the other hand the ranges in (5.27) and (5.28) show that for

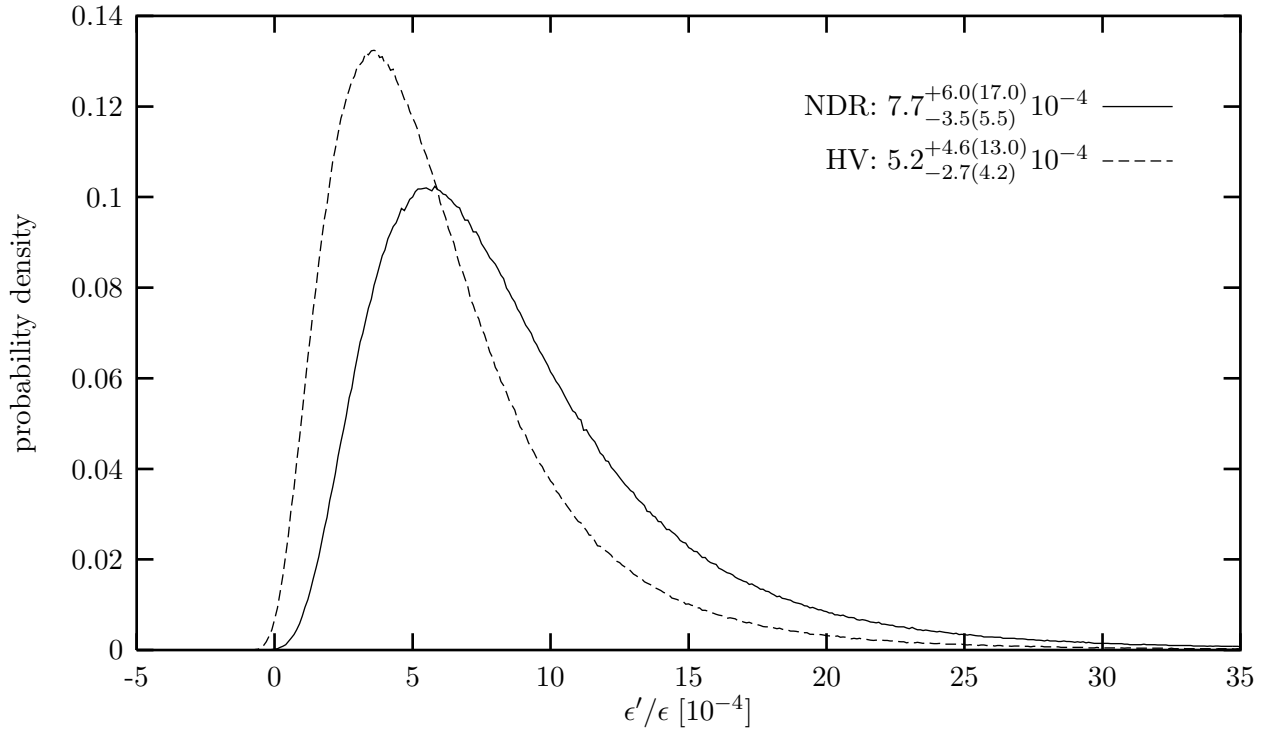


Figure 9: Probability density distributions for ϵ'/ϵ in NDR and HV schemes.

particular choices of the input parameters, values for ε'/ε as high as $(2-3) \cdot 10^{-3}$ cannot be excluded at present. Let us study this in more detail.

In table 8, taken from [35], we show the values of ε'/ε in units of 10^{-4} for specific values of $B_6^{(1/2)}$, $B_8^{(3/2)}$ and $m_s(m_c)$ as calculated in the NDR scheme. The corresponding values in the HV scheme are lower as discussed above. The fourth column shows the results for central values of all remaining parameters. The comparison of the the fourth and the fifth column demonstrates how ε'/ε is increased when $\Lambda_{\overline{\text{MS}}}^{(4)}$ is raised from 340 MeV to 390 MeV. As stated in (5.4) ε'/ε is roughly proportional to $\Lambda_{\overline{\text{MS}}}^{(4)}$. Finally, in the last column maximal values of ε'/ε are given. To this end we have scanned all parameters relevant for the analysis of $\text{Im}\lambda_t$ within one standard deviation and have chosen the highest value of $\Lambda_{\overline{\text{MS}}}^{(4)} = 390$ MeV. Comparison of the last two columns demonstrates the impact of the increase of $\text{Im}\lambda_t$ from its central to its maximal value and of the variation of m_t .

Table 8 gives a good insight in the dependence of ε'/ε on various parameters which is roughly described by (5.4). We observe the following hierarchies:

- The largest uncertainties reside in m_s , $B_6^{(1/2)}$ and $B_8^{(3/2)}$. ε'/ε increases universally by roughly a factor of 2.3 when $m_s(m_c)$ is changed from 155 MeV to 105 MeV. The increase of $B_6^{(1/2)}$ from 1.0 to 1.3 increases ε'/ε by $(55 \pm 10)\%$, depending on m_s and $B_8^{(3/2)}$. The corresponding changes due to $B_8^{(3/2)}$ are approximately $(40 \pm 15)\%$.
- The combined uncertainty due to $\text{Im}\lambda_t$ and m_t , present both in $\text{Im}\lambda_t$ and $F_{\varepsilon'}$, is approximately $\pm 25\%$. The uncertainty due to m_t alone is only $\pm 5\%$.
- The uncertainty due to $\Lambda_{\overline{\text{MS}}}^{(4)}$ is approximately $\pm 16\%$.
- The uncertainty due to $\Omega_{\eta+\eta'}$ is approximately $\pm 12\%$.

The large sensitivity of ε'/ε to m_s has been known since the analyses in the eighties. In the context of the KTeV result this issue has been analyzed in [98]. It has been found that provided $2B_6^{(1/2)} - B_8^{(3/2)} \leq 2$ the consistency of the Standard Model with the KTeV result requires the 2σ bound $m_s(2 \text{ GeV}) \leq 110$ MeV. Our analysis is compatible with these findings.

5.7 Summary

As we have seen, the estimates of ε'/ε in the Standard Model are typically below the experimental data. However, as our scanning analysis shows, for suitably chosen parameters, ε'/ε in the Standard Model can be made consistent with data. However, this happens only if all relevant parameters are simultaneously close to their extreme values. This is clearly seen in table 8. Moreover, the probability density distributions for ε'/ε in fig. 9 indicates that values of ε'/ε in the ball park of NA31 and KTeV results are rather improbable.

Table 8: Values of ε'/ε in units of 10^{-4} for specific values of $B_6^{(1/2)}$, $B_8^{(3/2)}$ and $m_s(m_c)$ and other parameters as explained in the text.

$B_6^{(1/2)}$	$B_8^{(3/2)}$	$m_s(m_c)[\text{MeV}]$	Central	$\Lambda_{\overline{\text{MS}}}^{(4)} = 390 \text{ MeV}$	Maximal
1.3	0.6	105	20.2	23.3	28.8
		130	12.8	14.8	18.3
		155	8.5	9.9	12.3
1.3	0.8	105	18.1	20.8	26.0
		130	11.3	13.1	16.4
		155	7.5	8.7	10.9
1.3	1.0	105	15.9	18.3	23.2
		130	9.9	11.5	14.5
		155	6.5	7.6	9.6
1.0	0.6	105	13.7	15.8	19.7
		130	8.4	9.8	12.2
		155	5.4	6.4	7.9
1.0	0.8	105	11.5	13.3	16.9
		130	7.0	8.1	10.4
		155	4.4	5.2	6.6
1.0	1.0	105	9.4	10.9	14.1
		130	5.5	6.5	8.5
		155	3.3	4.0	5.2

Unfortunately, in view of very large hadronic and substantial parametric uncertainties, it is impossible to conclude at present whether new physics contributions are indeed required to fit the data. Similarly it is difficult to conclude what is precisely the impact of the ε'/ε -data on the CKM matrix. However, as analyzed in [35] there are indications that the lower limit on $\text{Im}\lambda_t$ is improved. The same applies to the lower limits for the branching ratios for $K_L \rightarrow \pi^0 \nu \bar{\nu}$ and $K_L \rightarrow \pi^0 e^+ e^-$ decays discussed in the following sections.

It is also clear that the ε'/ε data puts models in which there are new positive contributions to ε and negative contributions to ε' in serious difficulties. In particular as analyzed in [35] the two Higgs Doublet Model II [99] can either be ruled out with improved hadronic matrix elements or a powerful lower bound on $\tan\beta$ can be obtained from ε'/ε . In the Minimal Supersymmetric Standard Model, in addition to charged Higgs exchanges in loop diagrams, also charginos contribute. For suitable choice of the supersymmetric parameters, the chargino

contribution can enhance ε'/ε with respect to the Standard Model expectations [100]. Yet, generally the most conspicuous effect of minimal supersymmetry is a depletion of ε'/ε . The situation can be different in more general models in which there are more parameters than in the two Higgs doublet model II and in the MSSM, in particular new CP violating phases. As an example, in more general supersymmetric models ε'/ε can be made consistent with experimental findings [101, 102]. Unfortunately, in view of the large number of free parameters such models are not very predictive.

The future of ε'/ε in the Standard Model and in its extensions depends on the progress in the reduction of parametric and hadronic uncertainties. In any case ε'/ε already played a decisive role in establishing direct CP violation in nature and its rather large value gives additional strong motivation for searching for this phenomenon in cleaner K decays like $K_L \rightarrow \pi^0 \nu \bar{\nu}$ and $K_L \rightarrow \pi^0 e^+ e^-$, in B decays, in D decays and elsewhere. We now turn to discuss some of these topics.

6 The Decays $K^+ \rightarrow \pi^+ \nu \bar{\nu}$ and $K_L \rightarrow \pi^0 \nu \bar{\nu}$

6.1 General Remarks

We will now move to discuss the semileptonic rare FCNC transitions $K^+ \rightarrow \pi^+ \nu \bar{\nu}$ and $K_L \rightarrow \pi^0 \nu \bar{\nu}$. Within the Standard Model these decays are loop-induced semileptonic FCNC processes determined only by Z^0 -penguin and box diagrams and are governed by the single function $X_0(x_t)$ given in (2.15).

A particular and very important virtue of $K \rightarrow \pi \nu \bar{\nu}$ is their clean theoretical character. This is related to the fact that the low energy hadronic matrix elements required are just the matrix elements of quark currents between hadron states, which can be extracted from the leading (non-rare) semileptonic decays. Other long-distance contributions are negligibly small [103, 104]. As a consequence of these features, the scale ambiguities, inherent to perturbative QCD, essentially constitute the only theoretical uncertainties present in the analysis of these decays. These theoretical uncertainties have been considerably reduced through the inclusion of the next-to-leading QCD corrections [105]–[109].

The investigation of these low energy rare decay processes in conjunction with their theoretical cleanliness, allows to probe, albeit indirectly, high energy scales of the theory and in particular to measure V_{td} and $\text{Im}\lambda_t = \text{Im}V_{ts}^* V_{td}$ from $K^+ \rightarrow \pi^+ \nu \bar{\nu}$ and $K_L \rightarrow \pi^0 \nu \bar{\nu}$ respectively. However, the very fact that these processes are based on higher order electroweak effects implies that their branching ratios are expected to be very small and not easy to access experimentally.

6.2 The Decay $K^+ \rightarrow \pi^+ \nu \bar{\nu}$

6.2.1 The effective Hamiltonian

The effective Hamiltonian for $K^+ \rightarrow \pi^+ \nu \bar{\nu}$ can be written as

$$\mathcal{H}_{\text{eff}} = \frac{G_F}{\sqrt{2}} \frac{\alpha}{2\pi \sin^2 \Theta_W} \sum_{l=e,\mu,\tau} \left(V_{cs}^* V_{cd} X_{\text{NL}}^l + V_{ts}^* V_{td} X(x_t) \right) (\bar{s}d)_{V-A} (\bar{\nu}_l \nu_l)_{V-A}. \quad (6.1)$$

The index $l=e, \mu, \tau$ denotes the lepton flavour. The dependence on the charged lepton mass resulting from the box-graph is negligible for the top contribution. In the charm sector this is the case only for the electron and the muon but not for the τ -lepton.

The function $X(x_t)$ relevant for the top part is given by

$$X(x_t) = X_0(x_t) + \frac{\alpha_s}{4\pi} X_1(x_t) = \eta_X \cdot X_0(x_t), \quad \eta_X = 0.994, \quad (6.2)$$

with the QCD correction [106, 108, 109]

$$X_1(x_t) = \tilde{X}_1(x_t) + 8x_t \frac{\partial X_0(x_t)}{\partial x_t} \ln x_\mu. \quad (6.3)$$

Here $x_\mu = \mu_t^2/M_W^2$ with $\mu_t = \mathcal{O}(m_t)$ and $\tilde{X}_1(x_t)$ is a complicated function given in [106, 108, 109]. The μ_t -dependence of the last term in (6.3) cancels to the considered order the μ_t -dependence of the leading term $X_0(x_t(\mu))$. The leftover μ_t -dependence in $X(x_t)$ is below 1%. The factor η_X summarizes the NLO corrections represented by the second term in (6.2). With $m_t \equiv \bar{m}_t(m_t)$ the QCD factor η_X is practically independent of m_t and $\Lambda_{\overline{\text{MS}}}$ and is very close to unity.

The expression corresponding to $X(x_t)$ in the charm sector is the function X_{NL}^l . It results from the NLO calculation [107] and is given explicitly in [109]. The inclusion of NLO corrections reduced considerably the large μ_c dependence (with $\mu_c = \mathcal{O}(m_c)$) present in the leading order expressions for the charm contribution [110]. Varying μ_c in the range $1 \text{ GeV} \leq \mu_c \leq 3 \text{ GeV}$ changes X_{NL} by roughly 24% after the inclusion of NLO corrections to be compared with 56% in the leading order. Further details can be found in [107, 2]. The impact of the μ_c uncertainties on the resulting branching ratio $Br(K^+ \rightarrow \pi^+ \nu \bar{\nu})$ is discussed below.

The numerical values for X_{NL}^l for $\mu = m_c$ and several values of $\Lambda_{\overline{\text{MS}}}^{(4)}$ and $m_c(m_c)$ can be found in [109]. The net effect of QCD corrections is to suppress the charm contribution by roughly 30%. For our purposes we need only

$$P_0(X) = \frac{1}{\lambda^4} \left[\frac{2}{3} X_{\text{NL}}^e + \frac{1}{3} X_{\text{NL}}^\tau \right] = 0.42 \pm 0.06 \quad (6.4)$$

where the error results from the variation of $\Lambda_{\overline{\text{MS}}}^{(4)}$ and $m_c(m_c)$.

6.2.2 Deriving the Branching Ratio

The relevant hadronic matrix element of the weak current $(\bar{s}d)_{V-A}$ in (6.1) can be extracted with the help of isospin symmetry from the leading decay $K^+ \rightarrow \pi^0 e^+ \nu$. Consequently the resulting theoretical expression for the branching fraction $Br(K^+ \rightarrow \pi^+ \nu \bar{\nu})$ can be related to the experimentally well known quantity $Br(K^+ \rightarrow \pi^0 e^+ \nu)$. Let us demonstrate this.

The effective Hamiltonian for the tree level decay $K^+ \rightarrow \pi^0 e^+ \nu$ is given by

$$\mathcal{H}_{\text{eff}}(K^+ \rightarrow \pi^0 e^+ \nu) = \frac{G_F}{\sqrt{2}} V_{us}^* (\bar{s}u)_{V-A} (\bar{\nu}_e e)_{V-A}. \quad (6.5)$$

Using isospin symmetry we have

$$\langle \pi^+ | (\bar{s}d)_{V-A} | K^+ \rangle = \sqrt{2} \langle \pi^0 | (\bar{s}u)_{V-A} | K^+ \rangle. \quad (6.6)$$

Consequently neglecting differences in the phase space of these two decays, due to $m_{\pi^+} \neq m_{\pi^0}$ and $m_e \neq 0$, we find

$$\frac{Br(K^+ \rightarrow \pi^+ \nu \bar{\nu})}{Br(K^+ \rightarrow \pi^0 e^+ \nu)} = \frac{\alpha^2}{|V_{us}|^2 2\pi^2 \sin^4 \Theta_W} \sum_{l=e,\mu,\tau} \left| V_{cs}^* V_{cd} X_{\text{NL}}^l + V_{ts}^* V_{td} X(x_t) \right|^2. \quad (6.7)$$

6.2.3 Basic Phenomenology

Using (6.7) and including isospin breaking corrections one finds

$$Br(K^+ \rightarrow \pi^+ \nu \bar{\nu}) = \kappa_+ \cdot \left[\left(\frac{\text{Im} \lambda_t}{\lambda^5} X(x_t) \right)^2 + \left(\frac{\text{Re} \lambda_c}{\lambda} P_0(X) + \frac{\text{Re} \lambda_t}{\lambda^5} X(x_t) \right)^2 \right], \quad (6.8)$$

$$\kappa_+ = r_{K^+} \frac{3\alpha^2 Br(K^+ \rightarrow \pi^0 e^+ \nu)}{2\pi^2 \sin^4 \Theta_W} \lambda^8 = 4.11 \cdot 10^{-11}, \quad (6.9)$$

where we have used

$$\alpha = \frac{1}{129}, \quad \sin^2 \Theta_W = 0.23, \quad Br(K^+ \rightarrow \pi^0 e^+ \nu) = 4.82 \cdot 10^{-2}. \quad (6.10)$$

Here $\lambda_i = V_{is}^* V_{id}$ with λ_c being real to a very high accuracy. $r_{K^+} = 0.901$ summarizes isospin breaking corrections in relating $K^+ \rightarrow \pi^+ \nu \bar{\nu}$ to $K^+ \rightarrow \pi^0 e^+ \nu$. These isospin breaking corrections are due to quark mass effects and electroweak radiative corrections and have been calculated in [111]. Finally $P_0(X)$ is given in (6.4).

Using the improved Wolfenstein parametrization and the approximate formulae (1.22) – (1.24) we can next put (6.8) into a more transparent form [10]:

$$Br(K^+ \rightarrow \pi^+ \nu \bar{\nu}) = 4.11 \cdot 10^{-11} A^4 X^2(x_t) \frac{1}{\sigma} \left[(\sigma \bar{\eta})^2 + (\varrho_0 - \bar{\varrho})^2 \right], \quad (6.11)$$

where

$$\sigma = \left(\frac{1}{1 - \frac{\lambda^2}{2}} \right)^2. \quad (6.12)$$

The measured value of $Br(K^+ \rightarrow \pi^+ \nu \bar{\nu})$ then determines an ellipse in the $(\bar{\varrho}, \bar{\eta})$ plane centered at $(\varrho_0, 0)$ with

$$\varrho_0 = 1 + \frac{P_0(X)}{A^2 X(x_t)} \quad (6.13)$$

and having the squared axes

$$\bar{\varrho}_1^2 = r_0^2, \quad \bar{\eta}_1^2 = \left(\frac{r_0}{\sigma}\right)^2 \quad (6.14)$$

where

$$r_0^2 = \frac{1}{A^4 X^2(x_t)} \left[\frac{\sigma \cdot Br(K^+ \rightarrow \pi^+ \nu \bar{\nu})}{4.11 \cdot 10^{-11}} \right]. \quad (6.15)$$

Note that r_0 depends only on the top contribution. The departure of ϱ_0 from unity measures the relative importance of the internal charm contributions.

The ellipse defined by r_0 , ϱ_0 and σ given above intersects with the circle (1.32). This allows to determine $\bar{\varrho}$ and $\bar{\eta}$ with

$$\bar{\varrho} = \frac{1}{1 - \sigma^2} \left(\varrho_0 - \sqrt{\sigma^2 \varrho_0^2 + (1 - \sigma^2)(r_0^2 - \sigma^2 R_b^2)} \right), \quad \bar{\eta} = \sqrt{R_b^2 - \bar{\varrho}^2} \quad (6.16)$$

and consequently

$$R_t^2 = 1 + R_b^2 - 2\bar{\varrho}, \quad (6.17)$$

where $\bar{\eta}$ is assumed to be positive. Given $\bar{\varrho}$ and $\bar{\eta}$ one can determine V_{td} :

$$V_{td} = A\lambda^3(1 - \bar{\varrho} - i\bar{\eta}), \quad |V_{td}| = A\lambda^3 R_t. \quad (6.18)$$

The determination of $|V_{td}|$ and of the unitarity triangle requires the knowledge of V_{cb} (or A) and of $|V_{ub}/V_{cb}|$. Both values are subject to theoretical uncertainties present in the existing analyses of tree level decays. Whereas the dependence on $|V_{ub}/V_{cb}|$ is rather weak, the very strong dependence of $Br(K^+ \rightarrow \pi^+ \nu \bar{\nu})$ on A or V_{cb} makes a precise prediction for this branching ratio difficult at present. We will return to this below. The dependence of $Br(K^+ \rightarrow \pi^+ \nu \bar{\nu})$ on m_t is also strong. However m_t is known already within $\pm 4\%$ and consequently the related uncertainty in $Br(K^+ \rightarrow \pi^+ \nu \bar{\nu})$ is substantially smaller than the corresponding uncertainty due to V_{cb} .

6.2.4 Numerical Analysis of $K^+ \rightarrow \pi^+ \nu \bar{\nu}$

The uncertainties in the prediction for $Br(K^+ \rightarrow \pi^+ \nu \bar{\nu})$ and in the determination of $|V_{td}|$ related to the choice of the renormalization scales μ_t and μ_c in the top part and the charm part, respectively have been investigated in [2]. To this end the scales μ_c and μ_t entering $m_c(\mu_c)$ and $m_t(\mu_t)$, respectively, have been varied in the ranges $1 \text{ GeV} \leq \mu_c \leq 3 \text{ GeV}$ and $100 \text{ GeV} \leq \mu_t \leq 300 \text{ GeV}$. It has been found that including the full next-to-leading corrections reduces the uncertainty in the determination of $|V_{td}|$ from $\pm 14\%$ (LO) to $\pm 4.6\%$ (NLO). The main

bulk of this theoretical error stems from the charm sector. In the case of $Br(K^+ \rightarrow \pi^+ \nu \bar{\nu})$, the theoretical uncertainty due to $\mu_{c,t}$ is reduced from $\pm 22\%$ (LO) to $\pm 7\%$ (NLO).

Scanning the input parameters of table 2 we find

$$Br(K^+ \rightarrow \pi^+ \nu \bar{\nu}) = (7.9 \pm 3.1) \cdot 10^{-11} \quad (6.19)$$

where the error comes dominantly from the uncertainties in the CKM parameters.

It is possible to derive an upper bound on $Br(K^+ \rightarrow \pi^+ \nu \bar{\nu})$ [109]:

$$Br(K^+ \rightarrow \pi^+ \nu \bar{\nu})_{\max} = \frac{\kappa_+}{\sigma} \left[P_0(X) + A^2 X(x_t) \frac{r_{sd}}{\lambda} \sqrt{\frac{\Delta M_d}{\Delta M_s}} \right]^2 \quad (6.20)$$

where $r_{ds} = \xi \sqrt{m_{B_s}/m_{B_d}}$. This equation translates a lower bound on ΔM_s into an upper bound on $Br(K^+ \rightarrow \pi^+ \nu \bar{\nu})$. This bound is very clean and does not involve theoretical hadronic uncertainties except for r_{sd} . Using

$$\sqrt{\frac{\Delta M_d}{\Delta M_s}} < 0.2, \quad A < 0.87, \quad P_0(X) < 0.48, \quad X(x_t) < 1.56, \quad r_{sd} < 1.2 \quad (6.21)$$

we find

$$Br(K^+ \rightarrow \pi^+ \nu \bar{\nu})_{\max} = 12.2 \cdot 10^{-11}. \quad (6.22)$$

This limit could be further strengthened with improved input. However, this bound is strong enough to indicate a clear conflict with the Standard Model if $Br(K^+ \rightarrow \pi^+ \nu \bar{\nu})$ should be measured at $2 \cdot 10^{-10}$.

6.2.5 $|V_{td}|$ from $K^+ \rightarrow \pi^+ \nu \bar{\nu}$

Once $Br(K^+ \rightarrow \pi^+ \nu \bar{\nu}) \equiv Br(K^+)$ is measured, $|V_{td}|$ can be extracted subject to various uncertainties:

$$\frac{\sigma(|V_{td}|)}{|V_{td}|} = \pm 0.04_{scale} \pm \frac{\sigma(|V_{cb}|)}{|V_{cb}|} \pm 0.7 \frac{\sigma(\bar{m}_c)}{\bar{m}_c} \pm 0.65 \frac{\sigma(Br(K^+))}{Br(K^+)}. \quad (6.23)$$

Taking $\sigma(|V_{cb}|) = 0.002$, $\sigma(\bar{m}_c) = 100 \text{ MeV}$ and $\sigma(Br(K^+)) = 10\%$ and adding the errors in quadrature we find that $|V_{td}|$ can be determined with an accuracy of $\pm 10\%$. This number is increased to $\pm 11\%$ once the uncertainties due to m_t , α_s and $|V_{ub}|/|V_{cb}|$ are taken into account. Clearly this determination can be improved although a determination of $|V_{td}|$ with an accuracy better than $\pm 5\%$ seems rather unrealistic.

6.2.6 Summary and Outlook

The accuracy of the Standard Model prediction for $Br(K^+ \rightarrow \pi^+ \nu \bar{\nu})$ has improved considerably during the last five years. This progress can be traced back to the improved values of

m_t and $|V_{cb}|$ and to the inclusion of NLO QCD corrections which considerably reduced the scale uncertainties in the charm sector.

Now, what about the experimental status of this decay ? One of the high-lights of 97 was the observation by BNL787 collaboration at Brookhaven [112] of one event consistent with the signature expected for this decay. The branching ratio:

$$Br(K^+ \rightarrow \pi^+ \nu \bar{\nu}) = (4.2_{-3.5}^{+9.7}) \cdot 10^{-10} \quad (6.24)$$

has the central value by a factor of 5 above the Standard Model expectation but in view of large errors the result is compatible with the Standard Model. The analysis of additional data on $K^+ \rightarrow \pi^+ \nu \bar{\nu}$ present on tape at BNL787 should narrow this range in the near future considerably. In view of the clean character of this decay a measurement of its branching ratio at the level of $2 \cdot 10^{-10}$ would signal the presence of physics beyond the Standard Model. The Standard Model sensitivity is expected to be reached at AGS around the year 2000 [113]. Also Fermilab with the Main Injector could measure this decay [114].

6.3 The Decay $K_L \rightarrow \pi^0 \nu \bar{\nu}$

6.3.1 The effective Hamiltonian

The effective Hamiltonian for $K_L \rightarrow \pi^0 \nu \bar{\nu}$ is given as follows:

$$\mathcal{H}_{\text{eff}} = \frac{G_F}{\sqrt{2}} \frac{\alpha}{2\pi \sin^2 \Theta_W} V_{ts}^* V_{td} X(x_t) (\bar{s}d)_{V-A} (\bar{\nu}\nu)_{V-A} + h.c., \quad (6.25)$$

where the function $X(x_t)$, present already in $K^+ \rightarrow \pi^+ \nu \bar{\nu}$, includes NLO corrections and is given in (6.2).

As we will demonstrate shortly, $K_L \rightarrow \pi^0 \nu \bar{\nu}$ proceeds in the Standard Model almost entirely through direct CP violation [115]. It is completely dominated by short-distance loop diagrams with top quark exchanges. The charm contribution can be fully neglected and the theoretical uncertainties present in $K^+ \rightarrow \pi^+ \nu \bar{\nu}$ due to m_c , μ_c and $\Lambda_{\overline{MS}}$ are absent here. Consequently the rare decay $K_L \rightarrow \pi^0 \nu \bar{\nu}$ is even cleaner than $K^+ \rightarrow \pi^+ \nu \bar{\nu}$ and is very well suited for the determination of the Wolfenstein parameter η and in particular $\text{Im}\lambda_t$.

It is usually stated in the literature that the decay $K_L \rightarrow \pi^0 \nu \bar{\nu}$ is dominated by *direct* CP violation. Now the standard definition of the direct CP violation requires the presence of strong phases which are completely negligible in $K_L \rightarrow \pi^0 \nu \bar{\nu}$. Consequently the violation of CP symmetry in $K_L \rightarrow \pi^0 \nu \bar{\nu}$ arises through the interference between $K^0 - \bar{K}^0$ mixing and the decay amplitude. This type of CP violation is often called *mixing-induced* CP violation. However, as already pointed out by Littenberg [115] and demonstrated explicitly in a moment, the contribution of CP violation to $K_L \rightarrow \pi^0 \nu \bar{\nu}$ via $K^0 - \bar{K}^0$ mixing alone is tiny. It gives

$Br(K_L \rightarrow \pi^0 \nu \bar{\nu}) \approx 2 \cdot 10^{-15}$. Consequently, in this sense, CP violation in $K_L \rightarrow \pi^0 \nu \bar{\nu}$ with $Br(K_L \rightarrow \pi^0 \nu \bar{\nu}) = \mathcal{O}(10^{-11})$ is a manifestation of CP violation in the decay and as such deserves the name of *direct* CP violation. In other words the difference in the magnitude of CP violation in $K_L \rightarrow \pi\pi$ (ε) and $K_L \rightarrow \pi^0 \nu \bar{\nu}$ is a signal of direct CP violation and measuring $K_L \rightarrow \pi^0 \nu \bar{\nu}$ at the expected level would be another signal of this phenomenon. More details on this issue can be found in [116, 117, 118].

6.3.2 Deriving the Branching Ratio

Let us derive the basic formula for $Br(K_L \rightarrow \pi^0 \nu \bar{\nu})$ in a manner analogous to the one for $Br(K^+ \rightarrow \pi^+ \nu \bar{\nu})$. To this end we consider one neutrino flavour and define the complex function:

$$F = \frac{G_F}{\sqrt{2}} \frac{\alpha}{2\pi \sin^2 \Theta_W} V_{ts}^* V_{td} X(x_t). \quad (6.26)$$

Then the effective Hamiltonian in (6.25) can be written as

$$\mathcal{H}_{\text{eff}} = F(\bar{s}d)_{V-A}(\bar{\nu}\nu)_{V-A} + F^*(\bar{d}s)_{V-A}(\bar{\nu}\nu)_{V-A}. \quad (6.27)$$

Now, from (3.8) we have

$$K_L = \frac{1}{\sqrt{2}}[(1 + \bar{\varepsilon})K^0 + (1 - \bar{\varepsilon})\bar{K}^0] \quad (6.28)$$

where we have neglected $|\bar{\varepsilon}|^2 \ll 1$. Thus the amplitude for $K_L \rightarrow \pi^0 \nu \bar{\nu}$ is given by

$$A(K_L \rightarrow \pi^0 \nu \bar{\nu}) = \frac{1}{\sqrt{2}} \left[F(1 + \bar{\varepsilon}) \langle \pi^0 | (\bar{s}d)_{V-A} | K^0 \rangle + F^*(1 - \bar{\varepsilon}) \langle \pi^0 | (\bar{d}s)_{V-A} | \bar{K}^0 \rangle \right] (\bar{\nu}\nu)_{V-A}. \quad (6.29)$$

Recalling

$$CP|K^0\rangle = -|\bar{K}^0\rangle, \quad C|\bar{K}^0\rangle = |K^0\rangle \quad (6.30)$$

we have

$$\langle \pi^0 | (\bar{d}s)_{V-A} | \bar{K}^0 \rangle = -\langle \pi^0 | (\bar{s}d)_{V-A} | K^0 \rangle, \quad (6.31)$$

where the minus sign is crucial for the subsequent steps.

Thus we can write

$$A(K_L \rightarrow \pi^0 \nu \bar{\nu}) = \frac{1}{\sqrt{2}} [F(1 + \bar{\varepsilon}) - F^*(1 - \bar{\varepsilon})] \langle \pi^0 | (\bar{s}d)_{V-A} | K^0 \rangle (\bar{\nu}\nu)_{V-A}. \quad (6.32)$$

Now the terms $\bar{\varepsilon}$ can be safely neglected in comparison with unity, which implies that the indirect CP violation (CP violation in the $K^0 - \bar{K}^0$ mixing) is negligible in this decay. We have then

$$F(1 + \bar{\varepsilon}) - F^*(1 - \bar{\varepsilon}) = \frac{G_F}{\sqrt{2}} \frac{\alpha}{\pi \sin^2 \Theta_W} \text{Im}(V_{ts}^* V_{td}) \cdot X(x_t). \quad (6.33)$$

Consequently using isospin relation

$$\langle \pi^0 | (\bar{d}s)_{V-A} | \bar{K}^0 \rangle = \langle \pi^0 | (\bar{s}u)_{V-A} | K^+ \rangle \quad (6.34)$$

together with (6.5) and taking into account the difference in the lifetimes of K_L and K^+ we have after summation over three neutrino flavours

$$\frac{Br(K_L \rightarrow \pi^0 \nu \bar{\nu})}{Br(K^+ \rightarrow \pi^0 e^+ \nu)} = 3 \frac{\tau(K_L)}{\tau(K^+)} \frac{\alpha^2}{|V_{us}|^2 2\pi^2 \sin^4 \Theta_W} [\text{Im} \lambda_t \cdot X(x_t)]^2 \quad (6.35)$$

where $\lambda_t = V_{ts}^* V_{td}$.

6.3.3 Master Formulae for $Br(K_L \rightarrow \pi^0 \nu \bar{\nu})$

Using (6.35) we can write $Br(K_L \rightarrow \pi^0 \nu \bar{\nu})$ simply as follows

$$Br(K_L \rightarrow \pi^0 \nu \bar{\nu}) = \kappa_L \cdot \left(\frac{\text{Im} \lambda_t}{\lambda^5} X(x_t) \right)^2 \quad (6.36)$$

$$\kappa_L = \frac{r_{K_L}}{r_{K^+}} \frac{\tau(K_L)}{\tau(K^+)} \kappa_+ = 1.80 \cdot 10^{-10} \quad (6.37)$$

with κ_+ given in (6.9) and $r_{K_L} = 0.944$ summarizing isospin breaking corrections in relating $K_L \rightarrow \pi^0 \nu \bar{\nu}$ to $K^+ \rightarrow \pi^0 e^+ \nu$ [111].

Using the Wolfenstein parametrization and (6.2) we can rewrite (6.36) as

$$Br(K_L \rightarrow \pi^0 \nu \bar{\nu}) = 3.0 \cdot 10^{-11} \left[\frac{\eta}{0.39} \right]^2 \left[\frac{\bar{m}_t(m_t)}{170 \text{ GeV}} \right]^{2.3} \left[\frac{|V_{cb}|}{0.040} \right]^4. \quad (6.38)$$

The determination of η using $Br(K_L \rightarrow \pi^0 \nu \bar{\nu})$ requires the knowledge of V_{cb} and m_t . The very strong dependence on V_{cb} or A makes a precise prediction for this branching ratio difficult at present.

On the other hand inverting (6.36) and using (6.2) one finds [118]:

$$\text{Im} \lambda_t = 1.36 \cdot 10^{-4} \left[\frac{170 \text{ GeV}}{\bar{m}_t(m_t)} \right]^{1.15} \left[\frac{Br(K_L \rightarrow \pi^0 \nu \bar{\nu})}{3 \cdot 10^{-11}} \right]^{1/2}. \quad (6.39)$$

without any uncertainty in $|V_{cb}|$. (6.39) offers the cleanest method to measure $\text{Im} \lambda_t$; even better than the CP asymmetries in B decays discussed briefly in section 8.

6.3.4 Numerical Analysis of $K_L \rightarrow \pi^0 \nu \bar{\nu}$

The μ_t -uncertainties present in the function $X(x_t)$ have already been discussed in connection with $K^+ \rightarrow \pi^+ \nu \bar{\nu}$. After the inclusion of NLO corrections they are so small that they can be neglected for all practical purposes. Scanning the input parameters of table 2 we find

$$Br(K_L \rightarrow \pi^0 \nu \bar{\nu}) = (2.8 \pm 1.1) \cdot 10^{-11} \quad (6.40)$$

where the error comes dominantly from the uncertainties in the CKM parameters.

6.3.5 Summary and Outlook

The accuracy of the Standard Model prediction for $Br(K_L \rightarrow \pi^0 \nu \bar{\nu})$ has improved considerably during the last five years. This progress can be traced back mainly to the improved values of m_t and $|V_{cb}|$ and to some extent to the inclusion of NLO QCD corrections.

The present upper bound on $Br(K_L \rightarrow \pi^0 \nu \bar{\nu})$ from FNAL experiment E799 [119] is

$$Br(K_L \rightarrow \pi^0 \nu \bar{\nu}) < 1.6 \cdot 10^{-6}. \quad (6.41)$$

This is about five orders of magnitude above the Standard Model expectation (6.40). Moreover this bound is substantially weaker than the *model independent* bound [116] from isospin symmetry:

$$Br(K_L \rightarrow \pi^0 \nu \bar{\nu}) < 4.4 \cdot Br(K^+ \rightarrow \pi^+ \nu \bar{\nu}) \quad (6.42)$$

which through (6.24) gives

$$Br(K_L \rightarrow \pi^0 \nu \bar{\nu}) < 6.1 \cdot 10^{-9} \quad (6.43)$$

Now FNAL-E799 expects to reach the accuracy $\mathcal{O}(10^{-8})$ and a very interesting new experiment at Brookhaven (BNL E926) [113] expects to reach the single event sensitivity $2 \cdot 10^{-12}$ allowing a 10% measurement of the expected branching ratio. There are furthermore plans to measure this gold-plated decay with comparable sensitivity at Fermilab [120] and KEK [121].

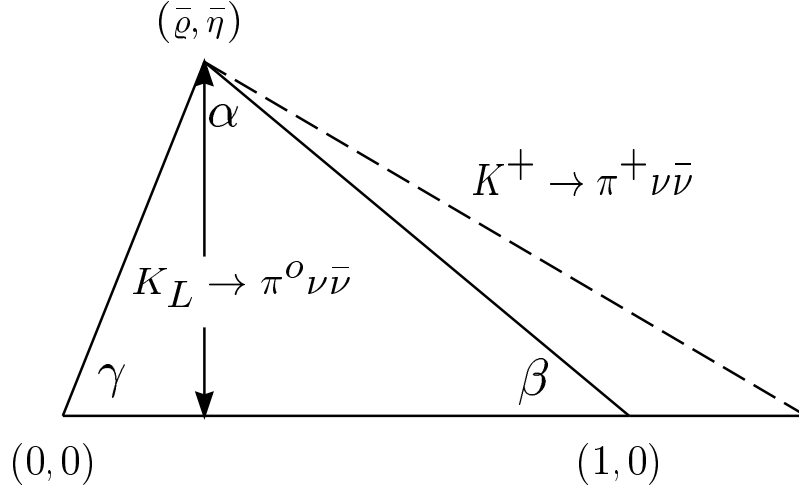


Figure 10: Unitarity triangle from $K \rightarrow \pi \nu \bar{\nu}$.

6.4 Unitarity Triangle and $\sin 2\beta$ from $K \rightarrow \pi\nu\bar{\nu}$

The measurement of $Br(K^+ \rightarrow \pi^+\nu\bar{\nu})$ and $Br(K_L \rightarrow \pi^0\nu\bar{\nu})$ can determine the unitarity triangle completely, (see fig. 10), provided m_t and V_{cb} are known [122]. Using these two branching ratios simultaneously allows to eliminate $|V_{ub}/V_{cb}|$ from the analysis which removes a considerable uncertainty. Indeed it is evident from (6.8) and (6.36) that, given $Br(K^+ \rightarrow \pi^+\nu\bar{\nu})$ and $Br(K_L \rightarrow \pi^0\nu\bar{\nu})$, one can extract both $\text{Im}\lambda_t$ and $\text{Re}\lambda_t$. One finds [122, 2]

$$\text{Im}\lambda_t = \lambda^5 \frac{\sqrt{B_2}}{X(x_t)} \quad \text{Re}\lambda_t = -\lambda^5 \frac{\frac{\text{Re}\lambda_c}{\lambda} P_0(X) + \sqrt{B_1 - B_2}}{X(x_t)}, \quad (6.44)$$

where we have defined the “reduced” branching ratios

$$B_1 = \frac{Br(K^+ \rightarrow \pi^+\nu\bar{\nu})}{4.11 \cdot 10^{-11}} \quad B_2 = \frac{Br(K_L \rightarrow \pi^0\nu\bar{\nu})}{1.80 \cdot 10^{-10}}. \quad (6.45)$$

Using next the expressions for $\text{Im}\lambda_t$, $\text{Re}\lambda_t$ and $\text{Re}\lambda_c$ given in (1.22)–(1.24) we find

$$\bar{\varrho} = 1 + \frac{P_0(X) - \sqrt{\sigma(B_1 - B_2)}}{A^2 X(x_t)}, \quad \bar{\eta} = \frac{\sqrt{B_2}}{\sqrt{\sigma} A^2 X(x_t)} \quad (6.46)$$

with σ defined in (6.12). An exact treatment of the CKM matrix shows that the formulae (6.46) are rather precise [122].

Using (6.46) one finds subsequently [122]

$$r_s = r_s(B_1, B_2) \equiv \frac{1 - \bar{\varrho}}{\bar{\eta}} = \cot \beta, \quad \sin 2\beta = \frac{2r_s}{1 + r_s^2} \quad (6.47)$$

with

$$r_s(B_1, B_2) = \sqrt{\sigma} \frac{\sqrt{\sigma(B_1 - B_2)} - P_0(X)}{\sqrt{B_2}}. \quad (6.48)$$

Thus within the approximation of (6.46) $\sin 2\beta$ is independent of V_{cb} (or A) and m_t .

It should be stressed that $\sin 2\beta$ determined this way depends only on two measurable branching ratios and on the function $P_0(X)$ which is completely calculable in perturbation theory. Consequently this determination is free from any hadronic uncertainties and its accuracy can be estimated with a high degree of confidence.

An extensive numerical analysis of the formulae above has been presented in [122, 118]. Assuming that the branching ratios are known to within $\pm 10\%$ and m_t within ± 3 GeV one finds the results in table 9 [118]. We observe that respectable determinations of all considered quantities except for $\bar{\varrho}$ can be obtained. Of particular interest are the accurate determinations of $\sin 2\beta$ and of $\text{Im}\lambda_t$. The latter quantity as seen in (6.39) can be obtained from $K_L \rightarrow \pi^0\nu\bar{\nu}$ alone and does not require knowledge of V_{cb} . The importance of measuring accurately $\text{Im}\lambda_t$ is evident. It plays a central role in the phenomenology of CP violation in K decays and is furthermore equivalent to the Jarlskog parameter J_{CP} [12], the invariant measure of CP violation in the Standard Model, $J_{\text{CP}} = \lambda(1 - \lambda^2/2)\text{Im}\lambda_t$.

Table 9: Illustrative example of the determination of CKM parameters from $K \rightarrow \pi\nu\bar{\nu}$.

	$\sigma(V_{cb}) = \pm 0.002$	$\sigma(V_{cb}) = \pm 0.001$
$\sigma(V_{td})$	$\pm 10\%$	$\pm 9\%$
$\sigma(\bar{\varrho})$	± 0.16	± 0.12
$\sigma(\bar{\eta})$	± 0.04	± 0.03
$\sigma(\sin 2\beta)$	± 0.05	± 0.05
$\sigma(\text{Im}\lambda_t)$	$\pm 5\%$	$\pm 5\%$

The accuracy to which $\sin 2\beta$ can be obtained from $K \rightarrow \pi\nu\bar{\nu}$ is, in the example discussed above, comparable to the one expected in determining $\sin 2\beta$ from CP asymmetries in B decays prior to LHC experiments. In this case $\sin 2\beta$ is determined best by measuring CP violation in $B_d \rightarrow J/\psi K_S$. Using the formula for the corresponding time-integrated CP asymmetry one finds an interesting connection between rare K decays and B physics [122]

$$\frac{2r_s(B_1, B_2)}{1 + r_s^2(B_1, B_2)} = -a_{\text{CP}}(B_d \rightarrow J/\psi K_S) \frac{1 + x_d^2}{x_d} \quad (6.49)$$

which must be satisfied in the Standard Model. Here x_d is a $B_d^0 - \bar{B}_d^0$ parameter. We stress that except for $P_0(X)$ all quantities in (6.49) can be directly measured in experiment and that this relationship is essentially independent of m_t and V_{cb} . Due to very small theoretical uncertainties in (6.49), this relation is particularly suited for tests of CP violation in the Standard Model and offers a powerful tool to probe the physics beyond it.

7 Express Review of Rare K and B Decays

7.1 The Decays $B \rightarrow X_{s,d}\nu\bar{\nu}$

The decays $B \rightarrow X_{s,d}\nu\bar{\nu}$ are the theoretically cleanest decays in the field of rare B -decays. They are dominated by the same Z^0 -penguin and box diagrams involving top quark exchanges which we encountered already in the case of $K^+ \rightarrow \pi^+\nu\bar{\nu}$ and $K_L \rightarrow \pi^0\nu\bar{\nu}$ except for the appropriate change of the external quark flavours. Since the change of external quark flavours has no impact on the m_t dependence, the latter is fully described by the function $X(x_t)$ in (6.2) which includes the NLO corrections. The charm contribution is fully negligible here and the resulting effective Hamiltonian is very similar to the one for $K_L \rightarrow \pi^0\nu\bar{\nu}$ given in (6.25). For the decay $B \rightarrow X_{s,d}\nu\bar{\nu}$ it reads

$$\mathcal{H}_{\text{eff}} = \frac{G_F}{\sqrt{2}} \frac{\alpha}{2\pi \sin^2 \Theta_W} V_{tb}^* V_{ts} X(x_t) (\bar{b}s)_{V-A} (\bar{\nu}\nu)_{V-A} + h.c. \quad (7.1)$$

with s replaced by d in the case of $B \rightarrow X_d \nu \bar{\nu}$.

The theoretical uncertainties related to the renormalization scale dependence are as in $K_L \rightarrow \pi^0 \nu \bar{\nu}$ and can be essentially neglected. The same applies to long distance contributions considered in [123]. The calculation of the branching fractions for $B \rightarrow X_{s,d} \nu \bar{\nu}$ can be done in the spectator model corrected for short distance QCD effects. Normalizing to $Br(B \rightarrow X_c e \bar{\nu})$ and summing over three neutrino flavours one finds

$$\frac{Br(B \rightarrow X_s \nu \bar{\nu})}{Br(B \rightarrow X_c e \bar{\nu})} = \frac{3\alpha^2}{4\pi^2 \sin^4 \Theta_W} \frac{|V_{ts}|^2}{|V_{cb}|^2} \frac{X^2(x_t)}{f(z)} \frac{\kappa(0)}{\kappa(z)}. \quad (7.2)$$

Here $f(z)$ is the phase-space factor for $B \rightarrow X_c e \bar{\nu}$ with $z = m_c^2/m_b^2$ and $\kappa(z) = 0.88$ [124, 125] is the corresponding QCD correction. The factor $\kappa(0) = 0.83$ represents the QCD correction to the matrix element of the $b \rightarrow s \nu \bar{\nu}$ transition due to virtual and bremsstrahlung contributions. In the case of $B \rightarrow X_d \nu \bar{\nu}$ one has to replace V_{ts} by V_{td} which results in a decrease of the branching ratio by roughly an order of magnitude.

Setting $Br(B \rightarrow X_c e \bar{\nu}) = 10.4\%$, $f(z) = 0.54$, $\kappa(z) = 0.88$ and using the values in (6.10) we have

$$Br(B \rightarrow X_s \nu \bar{\nu}) = 3.7 \cdot 10^{-5} \frac{|V_{ts}|^2}{|V_{cb}|^2} \left[\frac{\overline{m}_t(m_t)}{170 \text{ GeV}} \right]^{2.30}. \quad (7.3)$$

Taking next, $f(z) = 0.54 \pm 0.04$ and $Br(B \rightarrow X_c e \bar{\nu}) = (10.4 \pm 0.4)\%$ and scanning the input parameters of table 2 we find

$$Br(B \rightarrow X_s \nu \bar{\nu}) = (3.5 \pm 0.7) \cdot 10^{-5} \quad (7.4)$$

to be compared with the experimental upper bound:

$$Br(B \rightarrow X_s \nu \bar{\nu}) < 7.7 \cdot 10^{-4} \quad (90\% \text{ C.L.}) \quad (7.5)$$

obtained for the first time by ALEPH [126]. This is only a factor of 20 above the Standard Model expectation. Even if the actual measurement of this decay is extremely difficult, all efforts should be made to measure it. One should also make attempts to measure $Br(B \rightarrow X_d \nu \bar{\nu})$. Indeed

$$\frac{Br(B \rightarrow X_d \nu \bar{\nu})}{Br(B \rightarrow X_s \nu \bar{\nu})} = \frac{|V_{td}|^2}{|V_{ts}|^2} \quad (7.6)$$

offers the cleanest direct determination of $|V_{td}|/|V_{ts}|$ as all uncertainties related to m_t , $f(z)$ and $Br(B \rightarrow X_c e \bar{\nu})$ cancel out.

7.2 The Decays $B_{s,d} \rightarrow l^+ l^-$

The decays $B_{s,d} \rightarrow l^+ l^-$ are after $B \rightarrow X_{s,d} \nu \bar{\nu}$ the theoretically cleanest decays in the field of rare B -decays. They are dominated by the Z^0 -penguin and box diagrams involving top

quark exchanges which we encountered already in the case of $B \rightarrow X_{s,d}\nu\bar{\nu}$ except that due to charged leptons in the final state the charge flow in the internal lepton line present in the box diagram is reversed. This results in a different m_t dependence summarized by the function $Y(x_t)$, the NLO generalization [106, 108, 109] of the function $Y_0(x_t)$ given in (2.15). The charm contributions are fully negligible here and the resulting effective Hamiltonian is given for $B_s \rightarrow l^+l^-$ as follows:

$$\mathcal{H}_{\text{eff}} = -\frac{G_F}{\sqrt{2}} \frac{\alpha}{2\pi \sin^2 \Theta_W} V_{tb}^* V_{ts} Y(x_t) (\bar{b}s)_{V-A} (\bar{l}l)_{V-A} + h.c. \quad (7.7)$$

with s replaced by d in the case of $B_d \rightarrow l^+l^-$.

The function $Y(x)$ is given by

$$Y(x_t) = Y_0(x_t) + \frac{\alpha_s}{4\pi} Y_1(x_t) \equiv \eta_Y Y_0(x_t), \quad \eta_Y = 1.012 \quad (7.8)$$

where $Y_1(x_t)$ can be found in [106, 108, 109]. The leftover μ_t -dependence in $Y(x_t)$ is tiny and amounts to an uncertainty of $\pm 1\%$ at the level of the branching ratio. With $m_t \equiv \bar{m}_t(m_t)$ the QCD factor η_Y depends only very weakly on m_t . The dependence on $\Lambda_{\overline{MS}}$ can be neglected.

The branching ratio for $B_s \rightarrow l^+l^-$ is given by [106]

$$Br(B_s \rightarrow l^+l^-) = \tau(B_s) \frac{G_F^2}{\pi} \left(\frac{\alpha}{4\pi \sin^2 \Theta_W} \right)^2 F_{B_s}^2 m_l^2 m_{B_s} \sqrt{1 - 4 \frac{m_l^2}{m_{B_s}^2}} |V_{tb}^* V_{ts}|^2 Y^2(x_t) \quad (7.9)$$

where B_s denotes the flavour eigenstate $(\bar{b}s)$ and F_{B_s} is the corresponding decay constant. Using (6.10) and (7.8) we find in the case of $B_s \rightarrow \mu^+\mu^-$

$$Br(B_s \rightarrow \mu^+\mu^-) = 3.5 \cdot 10^{-9} \left[\frac{\tau(B_s)}{1.6\text{ps}} \right] \left[\frac{F_{B_s}}{210\text{MeV}} \right]^2 \left[\frac{|V_{ts}|}{0.040} \right]^2 \left[\frac{\bar{m}_t(m_t)}{170\text{GeV}} \right]^{3.12}. \quad (7.10)$$

The main uncertainty in this branching ratio results from the uncertainty in F_{B_s} . Scanning the input parameters of table 2 together with $\tau(B_s) = 1.6\text{ ps}$ and $F_{B_s} = (210 \pm 30)\text{ MeV}$ we find

$$Br(B_s \rightarrow \mu^+\mu^-) = (3.2 \pm 1.5) \cdot 10^{-9}. \quad (7.11)$$

For $B_d \rightarrow \mu^+\mu^-$ a similar formula holds with obvious replacements of labels ($s \rightarrow d$). Provided the decay constants F_{B_s} and F_{B_d} will have been calculated reliably by non-perturbative methods or measured in leading leptonic decays one day, the rare processes $B_s \rightarrow \mu^+\mu^-$ and $B_d \rightarrow \mu^+\mu^-$ should offer clean determinations of $|V_{ts}|$ and $|V_{td}|$. In particular the ratio

$$\frac{Br(B_d \rightarrow \mu^+\mu^-)}{Br(B_s \rightarrow \mu^+\mu^-)} = \frac{\tau(B_d)}{\tau(B_s)} \frac{m_{B_d}}{m_{B_s}} \frac{F_{B_d}^2}{F_{B_s}^2} \frac{|V_{td}|^2}{|V_{ts}|^2} \quad (7.12)$$

having smaller theoretical uncertainties than the separate branching ratios should offer a useful measurement of $|V_{td}|/|V_{ts}|$. Since $Br(B_d \rightarrow \mu^+\mu^-) = \mathcal{O}(10^{-10})$ this is, however, a very

difficult task. For $B_s \rightarrow \tau^+\tau^-$ and $B_s \rightarrow e^+e^-$ one expects branching ratios $\mathcal{O}(10^{-6})$ and $\mathcal{O}(10^{-13})$, respectively, with the corresponding branching ratios for B_d -decays by one order of magnitude smaller.

The bounds on $B_{s,d} \rightarrow l\bar{l}$ are still many orders of magnitude away from Standard Model expectations. The best bounds come from CDF [127]. One has:

$$Br(B_s \rightarrow \mu^+\mu^-) \leq 2.6 \cdot 10^{-6} \quad (95\%C.L.) \quad (7.13)$$

and $Br(B_d \rightarrow \mu^+\mu^-) \leq 8.6 \cdot 10^{-7}$. CDF should reach in Run II the sensitivity of $1 \cdot 10^{-8}$ and $4 \cdot 10^{-8}$ for $B_d \rightarrow \mu\bar{\mu}$ and $B_s \rightarrow \mu\bar{\mu}$, respectively. It is hoped that these decays will be observed at LHC-B. The experimental status of $B \rightarrow \tau^+\tau^-$ and its usefulness in tests of the physics beyond the Standard Model is discussed in [128].

7.3 $B \rightarrow X_s\gamma$ and $B \rightarrow X_sl^+l^-$

In view of space limitations I will be very brief on these two decays.

A lot of efforts have been put into predicting the branching ratio for the inclusive radiative decay $B \rightarrow X_s\gamma$ including NLO QCD corrections and higher order electroweak corrections. The relevant references can be found in [1, 21], where also theoretical details are given. The final result of these efforts can be summarized by

$$Br(B \rightarrow X_s\gamma)_{\text{th}} = (3.30 \pm 0.15(\text{scale}) \pm 0.26(\text{par})) \cdot 10^{-4} \quad (7.14)$$

where the first error represents residual scale dependences and the second error is due to uncertainties in input parameters. The main achievement is the reduction of the scale dependence through NLO calculations, in particular those given in [129] and [130]. In the leading order the corresponding error would be roughly ± 0.6 .

The theoretical result in (7.14) should be compared with experimental data:

$$Br(B \rightarrow X_s\gamma)_{\text{exp}} = \begin{cases} (3.15 \pm 0.35 \pm 0.41) \cdot 10^{-4}, & \text{CLEO} \\ (3.11 \pm 0.80 \pm 0.72) \cdot 10^{-4}, & \text{ALEPH,} \end{cases} \quad (7.15)$$

which implies the combined branching ratio:

$$Br(B \rightarrow X_s\gamma)_{\text{exp}} = (3.14 \pm 0.48) \cdot 10^{-4}. \quad (7.16)$$

Clearly, the Standard Model result agrees well with the data. In order to see whether any new physics can be seen in this decay, the theoretical and in particular experimental errors should be reduced. This is certainly a very difficult task.

The rare decays $B \rightarrow X_{s,d}l^+l^-$ have been the subject of many theoretical studies. It is clear that once these decays have been observed, they will offer useful tests of the Standard Model and of its extensions. Most recent reviews can be found in [131, 132].

7.4 $K_L \rightarrow \pi^0 e^+ e^-$

There are three contributions to this decay: CP conserving, indirectly CP violating and directly CP violating. Unfortunately out of these three contributions only the directly CP violating can be calculated reliably. Including NLO corrections [133] and scanning the input parameters of table 2 we find

$$Br(K_L \rightarrow \pi^0 e^+ e^-)_{\text{dir}} = (4.6 \pm 1.8) \cdot 10^{-12}, \quad (7.17)$$

where the errors come dominantly from the uncertainties in the CKM parameters. The remaining two contributions to this decay are plagued by theoretical uncertainties [134]. They are expected to be $\mathcal{O}(10^{-12})$ but generally smaller than $Br(K_L \rightarrow \pi^0 e^+ e^-)_{\text{dir}}$. This implies that within the Standard Model $Br(K_L \rightarrow \pi^0 e^+ e^-)$ is expected to be at most 10^{-11} .

Experimentally we have the bound [135]

$$Br(K_L \rightarrow \pi^0 e^+ e^-) < 4.3 \cdot 10^{-9}. \quad (7.18)$$

and considerable improvements are expected in the coming years.

7.5 $K_L \rightarrow \mu^+ \mu^-$

The $K_L \rightarrow \mu^+ \mu^-$ branching ratio can be decomposed generally as follows:

$$Br(K_L \rightarrow \mu^+ \mu^-) = |\text{Re}A|^2 + |\text{Im}A|^2, \quad (7.19)$$

where $\text{Re}A$ denotes the dispersive contribution and $\text{Im}A$ the absorptive one. The latter contribution can be determined in a model independent way from the $K_L \rightarrow \gamma\gamma$ branching ratio. The resulting $|\text{Im}A|^2$ is very close to the experimental branching ratio $Br(K_L \rightarrow \mu^+ \mu^-) = (7.2 \pm 0.5) \cdot 10^{-9}$ [136] so that $|\text{Re}A|^2$ is substantially smaller and extracted to be [136]

$$|\text{Re}A_{\text{exp}}|^2 < 5.6 \cdot 10^{-10} \quad (90\% \text{ C.L.}). \quad (7.20)$$

Now $\text{Re}A$ can be decomposed as

$$\text{Re}A = \text{Re}A_{\text{LD}} + \text{Re}A_{\text{SD}}, \quad (7.21)$$

with

$$|\text{Re}A_{\text{SD}}|^2 \equiv Br(K_L \rightarrow \mu^+ \mu^-)_{\text{SD}} \quad (7.22)$$

representing the short-distance contribution which can be calculated reliably. An improved estimate of the long-distance contribution $\text{Re}A_{\text{LD}}$ has been recently presented in [137]

$$|\text{Re}A_{\text{LD}}| < 2.9 \cdot 10^{-5} \quad (90\% \text{ C.L.}). \quad (7.23)$$

Together with (7.20) this gives

$$Br(K_L \rightarrow \mu^+ \mu^-)_{SD} < 2.8 \cdot 10^{-9}. \quad (7.24)$$

This result is very close to the one presented by Gomez Dumm and Pich [138]. More pesimistic view on the extraction of the short distance part from $Br(K_L \rightarrow \mu^+ \mu^-)$ can be found in [139].

The bound in (7.24) should be compared with the short distance contribution within the Standard Model for which we find

$$Br(K_L \rightarrow \mu^+ \mu^-)_{SD} = (8.7 \pm 3.6) \cdot 10^{-10}. \quad (7.25)$$

This implies that there is a considerable room for new physics contributions. We will return to this point in section 9. Reviews of rare K decays are listed in [140].

8 Express Review of CP Violation in B Decays

8.1 CP-Asymmetries in B-Decays: General Picture

CP violation in B-decays is certainly one of the most important targets of B-factories and of dedicated B-experiments at hadron facilities. It is well known that CP violating effects are expected to occur in a large number of channels at a level attainable at forthcoming experiments. Moreover there exist channels which offer the determination of CKM phases essentially without any hadronic uncertainties. Since extensive reviews on CP violation in B decays can be found in the literature [141, 142, 3] and I am running out of space, let me concentrate only on a few points beginning with a quick review of classic methods for the determination of the angles α , β and γ in the unitarity triangle.

The classic determination of α by means of the time dependent CP asymmetry in the decay $B_d^0 \rightarrow \pi^+ \pi^-$ is affected by the "QCD penguin pollution" which has to be taken care of in order to extract α . The recent CLEO results for penguin dominated decays indicate that this pollution could be substantial as stressed in particular in [143]. The most popular strategy to deal with this "penguin problem" is the isospin analysis of Gronau and London [144]. It requires however the measurement of $Br(B^0 \rightarrow \pi^0 \pi^0)$ which is expected to be below 10^{-6} : a very difficult experimental task. For this reason several, rather involved, strategies [145] have been proposed which avoid the use of $B_d \rightarrow \pi^0 \pi^0$ in conjunction with $a_{CP}(\pi^+ \pi^-, t)$. They are reviewed in [3]. It is to be seen which of these methods will eventually allow us to measure α with a respectable precision. It is however clear that the determination of this angle is a real challenge for both theorists and experimentalists.

The CP-asymmetry in the decay $B_d \rightarrow \psi K_S$ allows in the Standard Model a direct measurement of the angle β in the unitarity triangle without any theoretical uncertainties

[146]. Of considerable interest [142, 147] is also the pure penguin decay $B_d \rightarrow \phi K_S$, which is expected to be sensitive to physics beyond the Standard Model. Comparison of β extracted from $B_d \rightarrow \phi K_S$ with the one from $B_d \rightarrow \psi K_S$ should be important in this respect. An analogue of $B_d \rightarrow \psi K_S$ in B_s -decays is $B_s \rightarrow \psi \phi$. The CP asymmetry measures here η [148] in the Wolfenstein parametrization. It is very small, however, and this fact makes it a good place to look for the physics beyond the Standard Model. In particular the CP violation in $B_s^0 - \bar{B}_s^0$ mixing from new sources beyond the Standard Model should be probed in this decay.

The two theoretically cleanest methods for the determination of γ are: i) the full time dependent analysis of $B_s \rightarrow D_s^+ K^-$ and $\bar{B}_s \rightarrow D_s^- K^+$ [149] and ii) the well known triangle construction due to Gronau and Wyler [150] which uses six decay rates $B^\pm \rightarrow D_{CP}^0 K^\pm$, $B^+ \rightarrow D^0 K^+$, $\bar{D}^0 K^+$ and $B^- \rightarrow D^0 K^-$, $\bar{D}^0 K^-$. Both methods are unaffected by penguin contributions. The first method is experimentally very challenging because of the expected large $B_s^0 - \bar{B}_s^0$ mixing. The second method is problematic because of the small branching ratios of the colour suppressed channel $B^+ \rightarrow D^0 K^+$ and its charge conjugate, giving a rather squashed triangle and thereby making the extraction of γ very difficult. Variants of the latter method which could be more promising have been proposed in [151, 152]. It appears that these methods will give useful results at later stages of CP-B investigations. In particular the first method will be feasible only at LHC-B. Other recent strategies for γ will be mentioned below.

8.2 B^0 -Decays to CP Eigenstates

Let us demonstrate some of the statements made above explicitly.

A time dependent asymmetry in the decay $B^0 \rightarrow f$ with f being a CP eigenstate is given by

$$a_{CP}(t, f) = \mathcal{A}_{CP}^{dir}(B \rightarrow f) \cos(\Delta M t) + \mathcal{A}_{CP}^{mix-ind}(B \rightarrow f) \sin(\Delta M t) \quad (8.1)$$

where we have separated the *direct* CP-violating contributions from those describing *mixing-induced* CP violation:

$$\mathcal{A}_{CP}^{dir}(B \rightarrow f) \equiv \frac{1 - |\xi_f|^2}{1 + |\xi_f|^2}, \quad \mathcal{A}_{CP}^{mix-ind}(B \rightarrow f) \equiv \frac{2\text{Im}\xi_f}{1 + |\xi_f|^2}. \quad (8.2)$$

In (8.1), ΔM denotes the mass splitting of the physical $B^0 - \bar{B}^0$ -mixing eigenstates. The quantity ξ_f containing essentially all the information needed to evaluate the asymmetries (8.2) is given by

$$\xi_f = \exp(i2\phi_M) \frac{A(\bar{B} \rightarrow f)}{A(B \rightarrow f)} \quad (8.3)$$

with ϕ_M denoting the weak phase in the $B - \bar{B}$ mixing and $A(B \rightarrow f)$ the decay amplitude.

Generally several decay mechanisms with different weak and strong phases can contribute to $A(B \rightarrow f)$. These are tree diagram (current-current) contributions, QCD penguin contributions and electroweak penguin contributions. If they contribute with similar strength to a given decay amplitude the resulting CP asymmetries suffer from hadronic uncertainties related to matrix elements of the relevant operators Q_i .

An interesting case arises when a single mechanism dominates the decay amplitude or the contributing mechanisms have the same weak phases. Then

$$\xi_f = \exp(i2\phi_M) \exp(-i2\phi_D), \quad |\xi_f|^2 = 1 \quad (8.4)$$

where ϕ_D is the weak phase in the decay amplitude. In this particular case the hadronic matrix elements drop out, the direct CP violating contribution vanishes and the mixing-induced CP asymmetry is given entirely in terms of the weak phases ϕ_M and ϕ_D . In particular the time integrated asymmetry is given by

$$a_{CP}(f) = \pm \sin(2\phi_D - 2\phi_M) \frac{x_{d,s}}{1 + x_{d,s}^2} \quad (8.5)$$

where \pm refers to f being a $CP = \pm$ eigenstate and $x_{d,s}$ are the $B_{d,s}^0 - \bar{B}_{d,s}^0$ mixing parameters.

If a single tree diagram dominates, the factor $\sin(2\phi_D - 2\phi_M)$ can be calculated by using

$$\phi_D = \begin{cases} \gamma & b \rightarrow u \\ 0 & b \rightarrow c \end{cases} \quad \phi_M = \begin{cases} -\beta & B_d^0 \\ 0 & B_s^0 \end{cases} \quad (8.6)$$

where we have indicated the basic transition of the b-quark into a lighter quark. On the other hand if the penguin diagram with internal top exchange dominates one has

$$\phi_D = \begin{cases} -\beta & b \rightarrow d \\ 0 & b \rightarrow s \end{cases} \quad \phi_M = \begin{cases} -\beta & B_d^0 \\ 0 & B_s^0 \end{cases} \quad (8.7)$$

These rules have been obtained using Wolfenstein parametrization in the leading order. Let us practice these formulae. Assuming that $B_d \rightarrow \psi K_S$ and $B_d \rightarrow \pi^+ \pi^-$ are dominated by tree diagrams with $b \rightarrow c$ and $b \rightarrow u$ transitions respectively we readily find

$$a_{CP}(\psi K_S) = -\sin(2\beta) \frac{x_d}{1 + x_d^2}, \quad (8.8)$$

$$a_{CP}(\pi^+ \pi^-) = -\sin(2\alpha) \frac{x_d}{1 + x_d^2}. \quad (8.9)$$

Now in the case of $B_d \rightarrow \psi K_S$ the penguin diagrams have to a very good approximation the same phase ($\phi_D = 0$) as the tree contribution and moreover are Zweig suppressed. Consequently (8.8) is very accurate. This is not the case for $B_d \rightarrow \pi^+ \pi^-$ where the penguin

contribution could be substantial. Heaving weak phase $\phi_D = -\beta$, which differs from the tree phase $\phi_D = \gamma$, this penguin contribution changes effectively (8.9) to

$$a_{CP}(\pi^+\pi^-) = -\sin(2\alpha + \theta_P) \frac{x_d}{1 + x_d^2} \quad (8.10)$$

where θ_P is a function of β and hadronic parameters. The isospin analysis [144] mentioned before is supposed to determine θ_P so that α can be extracted from $a_{CP}(\pi^+\pi^-)$.

Similarly the pure penguin dominated decay $B_d \rightarrow \phi K_S$ is governed by the $b \rightarrow s$ penguin with internal top exchange which implies that in this decay the angle β is measured. The accuracy of this measurement is a bit lower than using $B_d \rightarrow \psi K_S$ as penguins with internal u and c exchanges may introduce a small pollution.

Finally we can consider the asymmetry in $B_s \rightarrow \psi\phi$, an analog of $B_d \rightarrow \psi K_s$. In the leading order of the Wolfenstein parametrization the asymmetry $a_{CP}(\psi\phi)$ vanishes. Including higher order terms in λ one finds [148]

$$a_{CP}(\psi\phi) = 2\lambda^2 \eta \frac{x_s}{1 + x_s^2} \quad (8.11)$$

where λ and η are the Wolfenstein parameters.

8.3 Recent Developments

All this has been known already for some time and is well documented in the literature. The most recent developments are related to the extraction of the angle γ from the decays $B \rightarrow PP$ (P =pseudoscalar) and their charge conjugates [153]–[156]. Some of these modes have been observed by the CLEO collaboration [157]. In the future they should allow us to obtain direct information on γ at B -factories (BaBar, BELLE, CLEO III) (for interesting feasibility studies, see [154, 155, 131]). At present, there are only experimental results available for the combined branching ratios of these modes, i.e. averaged over decay and its charge conjugate, suffering from large hadronic uncertainties.

There has been large activity in this field during the last two years. The main issues here are the final state interactions, SU(3) symmetry breaking effects and the importance of electroweak penguin contributions. Several interesting ideas have been put forward to extract the angle γ in spite of large hadronic uncertainties in $B \rightarrow \pi K$ decays [153, 154]. Also other $B \rightarrow PP$ decays have been investigated. As this field became rather technical, I decided not to include it in these lectures. A subset of relevant papers is listed in [153, 154, 156, 158, 159, 160], where further references can be found. In particular in [156, 159] general parametrizations for the study of the final state interactions, SU(3) symmetry breaking effects and the importance of electroweak penguin contributions have been presented. Moreover, upper bounds on the latter contributions following from SU(3) symmetry have been derived

[160]. Recent reviews can be found in [161] and [162]. New strategies for γ which include $B_s \rightarrow \psi K_S$ and $B_s \rightarrow K^+ K^-$ have been suggested very recently in [163].

There is no doubt that these new ideas will be helpful in the future. They are, however, rather demanding for experimentalist as often several branching ratios have to be studied simultaneously and each has to be measured precisely in order to obtain an acceptable measurement of γ . On the other hand various suggested bounds on γ may either exclude the region around 90° [153] or give an improved lower bound on it [160, 162, 164] which would remove a large portion of the allowed range from the analysis of the unitarity triangle. In this context it has been pointed out in [165] (see also [164]) that generally charmless hadronic B decay results from CLEO seem to prefer negative values of $\cos \gamma$ which is not the case in the standard analysis of section 4.

Finally I would like to mention a recent interesting paper of Lenz, Nierste and Ostermaier [166], where inclusive direct CP-asymmetries in charmless B^\pm -decays including QCD effects have been studied. These asymmetries should offer additional useful means to constrain the unitarity triangle.

8.4 CP-Asymmetries in B -Decays versus $K \rightarrow \pi \nu \bar{\nu}$

Let us next compare the potentials of the CP asymmetries in determining the parameters of the Standard Model with those of the cleanest rare K -decays: $K_L \rightarrow \pi^0 \nu \bar{\nu}$ and $K^+ \rightarrow \pi^+ \nu \bar{\nu}$.

Measuring $\sin 2\alpha$ and $\sin 2\beta$ from CP asymmetries in B decays allows, in principle, to fix the parameters $\bar{\eta}$ and $\bar{\varrho}$, which can be expressed as [167]

$$\bar{\eta} = \frac{r_-(\sin 2\alpha) + r_+(\sin 2\beta)}{1 + r_+^2(\sin 2\beta)}, \quad \bar{\varrho} = 1 - \bar{\eta} r_+(\sin 2\beta), \quad (8.12)$$

where $r_\pm(z) = (1 \pm \sqrt{1 - z^2})/z$. In general the calculation of $\bar{\varrho}$ and $\bar{\eta}$ from $\sin 2\alpha$ and $\sin 2\beta$ involves discrete ambiguities. As described in [167] they can be resolved by using further information, e.g. bounds on $|V_{ub}/V_{cb}|$, so that eventually the solution (8.12) is singled out.

Let us then consider two scenarios of the measurements of CP asymmetries in $B_d \rightarrow \pi^+ \pi^-$ and $B_d \rightarrow J/\psi K_S$, expressed in terms of $\sin 2\alpha$ and $\sin 2\beta$:

$$\sin 2\alpha = 0.40 \pm 0.10, \quad \sin 2\beta = 0.70 \pm 0.06 \quad (\text{scenario I}) \quad (8.13)$$

$$\sin 2\alpha = 0.40 \pm 0.04, \quad \sin 2\beta = 0.70 \pm 0.02 \quad (\text{scenario II}). \quad (8.14)$$

Scenario I corresponds to the accuracy being aimed for at B -factories and HERA-B prior to the LHC era. An improved precision can be anticipated from LHC experiments, which we illustrate with the scenario II. We assume that the problems with the determination of α will be solved somehow.

Table 10: Illustrative example of the determination of CKM parameters from $K \rightarrow \pi\nu\bar{\nu}$ and B-decays. We use $\sigma(|V_{cb}|) = \pm 0.002(0.001)$.

	$K \rightarrow \pi\nu\bar{\nu}$	Scenario I	Scenario II
$\sigma(V_{td})$	$\pm 10\%(9\%)$	$\pm 5.5\%(3.5\%)$	$\pm 5.0\%(2.5\%)$
$\sigma(\bar{\varrho})$	$\pm 0.16(0.12)$	± 0.03	± 0.01
$\sigma(\bar{\eta})$	$\pm 0.04(0.03)$	± 0.04	± 0.01
$\sigma(\sin 2\beta)$	± 0.05	± 0.06	± 0.02
$\sigma(\text{Im}\lambda_t)$	$\pm 5\%$	$\pm 14\%(11\%)$	$\pm 10\%(6\%)$

In table 10 this way of the determination of the Standard Model parameters is compared [118] with the analogous analysis using $K_L \rightarrow \pi^0\nu\bar{\nu}$ and $K^+ \rightarrow \pi^+\nu\bar{\nu}$ which has been presented in section 6. As can be seen in table 10, the CKM determination using $K \rightarrow \pi\nu\bar{\nu}$ is competitive with the one based on CP violation in B decays in scenario I, except for $\bar{\varrho}$ which is less constrained by the rare kaon processes. On the other hand as advertised previously $\text{Im}\lambda_t$ is better determined in $K \rightarrow \pi\nu\bar{\nu}$ even if scenario II is considered. The virtue of the comparison of the determinations of various parameters using CP-B asymmetries with the determinations in very clean decays $K \rightarrow \pi\nu\bar{\nu}$ is that any substantial deviations from these two determinations would signal new physics beyond the Standard Model. Formula (6.49) is an example of such a comparison. There are other strategies for determination of the unitarity triangle using combinations of CP asymmetries and rare decays. They are reviewed in [1].

9 A Brief Look Beyond the Standard Model

9.1 General Remarks

We begin the discussion of the Physics beyond the Standard Model with a few general remarks. As the new particles in the extensions of the Standard Model are generally substantially heavier than W^\pm , the impact of new physics on charged current tree level decays should be marginal. On the other hand these new contributions could have in principle an important impact on loop induced decays. From these two observations we conclude:

- New physics should have only marginal impact on the determination of $|V_{us}|$, $|V_{cb}|$ and $|V_{ub}|$.

- There is no impact on the calculations of the low energy non-perturbative parameters B_i except that new physics can bring new local operators implying new parameters B_i .
- New physics could have substantial impact on rare and CP violating decays and consequently on the determination of the unitarity triangle.

9.2 Classification of New Physics

Let us then group the extensions of the Standard Model in three classes.

Class A

- There are no new complex phases and quark mixing is described by the CKM matrix.
- There are new contributions to rare and CP violating decays through diagrams involving new internal particles.

These new contributions will have impact on the determination of α , β , γ , $|V_{td}|$ and λ_t and will be signaled by

- Inconsistencies in the determination of $(\bar{\varrho}, \bar{\eta})$ through ε , $B_{s,d}^0 - \bar{B}_{s,d}^0$ mixing and rare decays.
- Disagreement of $(\bar{\varrho}, \bar{\eta})$ extracted from loop induced decays with $(\bar{\varrho}, \bar{\eta})$ extracted using CP asymmetries.

Examples are two Higgs doublet model II and the constrained MSSM.

Class B

- Quark mixing is described by the CKM matrix.
- There are new phases in the new contributions to rare and CP violating decays.

This kind of new physics will also be signaled by inconsistencies in the $(\bar{\varrho}, \bar{\eta})$ plane. However, new complication arises. Because of new phases CP violating asymmetries measure generally different quantities than α , β and γ . For instance the CP asymmetry in $B \rightarrow \psi K_S$ will no longer measure β but $\beta + \theta_{NP}$ where θ_{NP} is a new phase. Strategies for dealing with such situation have been developed. See for instance [116, 168] and references therein.

Examples are multi-Higgs models with complex phases in the Higgs sector, general SUSY models, models with spontaneous CP violation and left-right symmetric models.

Class C

- The unitarity of the three generation CKM matrix does not hold.

Examples are four generation models and models with tree level FCNC transitions. If this type of physics is present, the unitarity triangle will not close or some inconsistencies in the $(\bar{\varrho}, \bar{\eta})$ plane take place.

Clearly in order to sort out which type of new physics is responsible for deviations from the Standard Model expectations one has to study many loop induced decays and many CP asymmetries. Some ideas in this direction can be found in [168, 116].

9.3 Upper Bounds on $K \rightarrow \pi \nu \bar{\nu}$ and $K_L \rightarrow \pi^0 e^+ e^-$ from ε'/ε and $K_L \rightarrow \mu^+ \mu^-$

We have seen in previous sections that the rare kaon decays $K_L \rightarrow \pi^0 \nu \bar{\nu}$, $K^+ \rightarrow \pi^+ \nu \bar{\nu}$ and $K_L \rightarrow \pi^0 e^+ e^-$ are governed by Z -penguin diagrams. Within the Standard Model the branching ratios for these decays have been found to be

$$Br(K_L \rightarrow \pi^0 \nu \bar{\nu}) = (2.8 \pm 1.1) \cdot 10^{-11}, \quad (9.1)$$

$$Br(K^+ \rightarrow \pi^+ \nu \bar{\nu}) = (7.9 \pm 3.1) \cdot 10^{-11}, \quad (9.2)$$

$$Br(K_L \rightarrow \pi^0 e^+ e^-)_{\text{dir}} = (4.6 \pm 1.8) \cdot 10^{-12}, \quad (9.3)$$

where the errors come dominantly from the uncertainties in the CKM parameters. The branching ratio in (9.3) represents the so-called direct CP-violating contribution to $K_L \rightarrow \pi^0 e^+ e^-$. The remaining two contributions to this decay, the CP-conserving one and the indirect CP-violating one are plagued by theoretical uncertainties [134]. They are expected to be $\mathcal{O}(10^{-12})$ but generally smaller than $Br(K_L \rightarrow \pi^0 e^+ e^-)_{\text{dir}}$. This implies that within the Standard Model $Br(K_L \rightarrow \pi^0 e^+ e^-)$ is expected to be at most 10^{-11} .

In this context a very interesting claim has been made by Colangelo and Isidori [169], who analyzing rare kaon decays in supersymmetric theories pointed out a possible large enhancement of the effective $\bar{s}dZ$ vertex leading to an enhancement of $Br(K^+ \rightarrow \pi^+ \nu \bar{\nu})$ by one order of magnitude and of $Br(K_L \rightarrow \pi^0 \nu \bar{\nu})$ and $Br(K_L \rightarrow \pi^0 e^+ e^-)$ by two orders of magnitude relative to the Standard Model expectations. Not surprisingly these results brought a lot of excitement among experimentalists.

Whether substantial enhancements of the branching ratios in question are indeed possible in supersymmetric theories is being investigated at present. On the other hand it can be shown [170] that in models in which the dominant new effect is an enhanced $\bar{s}dZ$ vertex, enhancements of $Br(K_L \rightarrow \pi^0 \nu \bar{\nu})$ and $Br(K_L \rightarrow \pi^0 e^+ e^-)$ as large as claimed in [169] are already excluded by the existing data on ε'/ε in spite of large theoretical uncertainties. Similarly the large enhancement of $Br(K^+ \rightarrow \pi^+ \nu \bar{\nu})$ can be excluded by the data on ε'/ε and in particular by the present information on the short distance contribution to $K_L \rightarrow \mu^+ \mu^-$. The latter can be bounded by analysing the data on $Br(K_L \rightarrow \mu^+ \mu^-)$ in conjunction with improved estimates of long distance dispersive contributions [137, 138]. In [169] only

constraints from $K_L \rightarrow \mu^+ \mu^-$, the $K_L - K_S$ mass difference ΔM_K and ε have been taken into account. As ε'/ε depends sensitively on the size of Z -penguin contributions and generally on the size of the effective $\bar{s}dZ$ vertex it is clear that the inclusion of the constraints from ε'/ε should have an important impact on the bounds for the rare decays in question. I will only describe the basic idea of [170] and give numerical results. The relevant expressions can be found in this paper. Here we go.

In the Standard Model Z -penguins are represented by the function C_0 which enters the functions X_0 , Y_0 and Z_0 . In order to study the effect of an enhanced $\bar{s}dZ$ vertex one simply makes the following replacement in the formulae for ε'/ε , $K_L \rightarrow \mu^+ \mu^-$ and rare decays in question:

$$\lambda_t C_0(x_t) \implies Z_{ds} \quad (9.4)$$

where Z_{ds} denotes an effective $\bar{s}dZ$ vertex. The remaining contributions to ε'/ε , $K_L \rightarrow \mu^+ \mu^-$ and rare K decays are evaluated in the Standard model as we assume that they are only marginally affected by new physics. We will, however, consider three scenarios for λ_t , which enters these remaining contributions.

Indeed there is the possibility that the value of λ_t is modified by new contributions to ε and $B_{d,s}^0 - \bar{B}_{d,s}^0$ mixings. We consider therefore three scenarios:

- **Scenario A:** λ_t is taken from the standard analysis of the unitarity triangle
- **Scenario B:** $\text{Im}\lambda_t = 0$ and $\text{Re}\lambda_t$ is varied in the full range consistent with the unitarity of the CKM matrix. In this scenario CP violation comes entirely from new physics contributions.
- **Scenario C:** λ_t is varied in the full range consistent with the unitarity of the CKM matrix. This means in particular that $\text{Im}\lambda_t$ can be negative.

Table 11: Upper bounds for the rare decays $K_L \rightarrow \pi^0 \nu \bar{\nu}$, $K_L \rightarrow \pi^0 e^+ e^-$ and $K^+ \rightarrow \pi^+ \nu \bar{\nu}$, obtained in various scenarios by imposing $\varepsilon'/\varepsilon \geq 2.5 \cdot 10^{-3}$, in the case $\text{Im}Z_{ds} > 0$.

Scenario	A	B	C	SM
$Br(K_L \rightarrow \pi^0 \nu \bar{\nu})[10^{-10}]$	0.5	—	0.7	0.4
$Br(K_L \rightarrow \pi^0 e^+ e^-)[10^{-11}]$	0.8	—	1.0	0.7
$Br(K^+ \rightarrow \pi^+ \nu \bar{\nu})[10^{-10}]$	1.8	—	2.2	1.1

Now Z_{ds} is a complex number. $\text{Im}Z_{ds}$ can be best bounded by ε'/ε . This implies bounds for $Br(K_L \rightarrow \pi^0 \nu \bar{\nu})$ and $Br(K_L \rightarrow \pi^0 e^+ e^-)$ which are sensitive functions of $\text{Im}Z_{ds}$. $\text{Re}Z_{ds}$

Table 12: Upper bounds for the rare decays $K_L \rightarrow \pi^0 \nu \bar{\nu}$, $K_L \rightarrow \pi^0 e^+ e^-$ and $K^+ \rightarrow \pi^+ \nu \bar{\nu}$, obtained in various scenarios by imposing $\varepsilon'/\varepsilon \geq 1.5 \cdot 10^{-3}$, in the case $\text{Im}Z_{ds} > 0$.

Scenario	A	B	C	SM
$Br(K_L \rightarrow \pi^0 \nu \bar{\nu})[10^{-10}]$	1.1	—	1.2	0.4
$Br(K_L \rightarrow \pi^0 e^+ e^-)[10^{-11}]$	1.5	—	1.8	0.7
$Br(K^+ \rightarrow \pi^+ \nu \bar{\nu})[10^{-10}]$	1.9	—	2.3	1.1

can be bounded by the present information on the short distance contribution to $K_L \rightarrow \mu^+ \mu^-$. This bound implies a bound on $Br(K^+ \rightarrow \pi^+ \nu \bar{\nu})$. Since $Br(K^+ \rightarrow \pi^+ \nu \bar{\nu})$ depends on both $\text{Re}Z_{ds}$ and $\text{Im}Z_{ds}$ also the bound on $\text{Im}Z_{ds}$ from ε'/ε matters in cases where $\text{Im}Z_{ds}$ is very enhanced over the Standard Model value.

The branching ratios $Br(K_L \rightarrow \pi^0 \nu \bar{\nu})$ and $Br(K_L \rightarrow \pi^0 e^+ e^-)$ are dominated by $(\text{Im}Z_{sd})^2$. Yet, the outcome of this analysis depends sensitively on the sign of $\text{Im}Z_{sd}$. Indeed, $\text{Im}Z_{sd} > 0$ results in the suppression of ε'/ε and as in the Standard Model the value for ε'/ε is generally below the data substantial enhancements of $\text{Im}Z_{sd}$ with $\text{Im}Z_{sd} > 0$ are not possible. The situation changes if new physics reverses the sign of $\text{Im}Z_{sd}$ so that it becomes negative. Then the upper bound on $\text{Im}Z_{sd}$ is governed by the upper bound on ε'/ε and with suitable choice of hadronic parameters and $\text{Im}\lambda_t$ (in particular in scenario C) large enhancements of $-\text{Im}Z_{sd}$ and of rare decay branching ratios are possible. The largest branching ratios are found when the neutral meson mixing is dominated by new physics contributions which force $\text{Im}\lambda_t$ to be as negative as possible within the unitarity of the CKM matrix. This possibility is quite remote. However, if this situation could be realized in some exotic model, then the branching ratios in question could be very high.

In table 11 we show the upper bounds on rare decays for $\text{Im}Z_{sd} > 0$ for three scenarios in question and $\varepsilon'/\varepsilon \geq 2.5 \cdot 10^{-3}$. In table 12 the corresponding bounds for $\varepsilon'/\varepsilon \geq 1.5 \cdot 10^{-3}$ are given. To this end all parameters relevant for ε'/ε have been scanned in the ranges used in section 5. In tables 13 and 14 the case $\text{Im}Z_{sd} < 0$ for $\varepsilon'/\varepsilon \leq 2.0 \cdot 10^{-3}$ and $\varepsilon'/\varepsilon \leq 3.0 \cdot 10^{-3}$ is considered respectively. In the last column we always give the upper bounds obtained in the Standard Model. Evidently for positive $\text{Im}Z_{sd}$ the enhancement of branching ratios are moderate but they can be very large when $\text{Im}Z_{sd} < 0$.

Other recent extensive analyses of supersymmetry effects in $K \rightarrow \pi \nu \bar{\nu}$ have been presented in [116, 171, 172] where further references can be found. Model independent studies of these decays can be found in [116, 172]. The corresponding analyses in various no-supersymmetric extensions of the Standard Model are listed in [173]. In particular, enhancement of $Br(K_L \rightarrow$

Table 13: Upper bounds for the rare decays $K_L \rightarrow \pi^0 \nu \bar{\nu}$, $K_L \rightarrow \pi^0 e^+ e^-$ and $K^+ \rightarrow \pi^+ \nu \bar{\nu}$, obtained in various scenarios by imposing $\varepsilon'/\varepsilon \leq 2.0 \cdot 10^{-3}$, in the case $\text{Im}Z_{ds} < 0$.

Scenario	A	B	C	SM
$BR(K_L \rightarrow \pi^0 \nu \bar{\nu})[10^{-10}]$	1.3	2.9	11.2	0.4
$BR(K_L \rightarrow \pi^0 e^+ e^-)[10^{-11}]$	2.9	5.1	18.2	0.7
$BR(K^+ \rightarrow \pi^+ \nu \bar{\nu})[10^{-10}]$	2.0	2.7	4.6	1.1

Table 14: Upper bounds for the rare decays $K_L \rightarrow \pi^0 \nu \bar{\nu}$, $K_L \rightarrow \pi^0 e^+ e^-$ and $K^+ \rightarrow \pi^+ \nu \bar{\nu}$, obtained in various scenarios by imposing $\varepsilon'/\varepsilon \leq 3.0 \cdot 10^{-3}$, in the case $\text{Im}Z_{ds} < 0$.

Scenario	A	B	C	SM
$BR(K_L \rightarrow \pi^0 \nu \bar{\nu})[10^{-10}]$	3.9	6.5	17.6	0.4
$BR(K_L \rightarrow \pi^0 e^+ e^-)[10^{-11}]$	7.9	11.5	28.0	0.7
$BR(K^+ \rightarrow \pi^+ \nu \bar{\nu})[10^{-10}]$	2.6	3.5	6.1	1.1

$\pi^0 \nu \bar{\nu}$) by 1–2 orders of magnitude above the Standard Model expectations is according to [174] still possible in four-generation models.

10 Summary and Outlook

I hope that I have convinced the students that the field of CP violation and rare decays plays an important role in the deeper understanding of the Standard Model and particle physics in general. Indeed the field of weak decays and of CP violation is one of the least understood sectors of the Standard Model. Even if the Standard Model is still consistent with the existing data for weak decay processes, the near future could change this picture dramatically through the advances in experiment and theory. In particular the experimental work done in the next ten years at BNL, CERN, CORNELL, DAΦNE, DESY, FNAL, KEK, SLAC and eventually LHC will certainly have considerable impact on this field.

Let us then make a list of things we could expect in the next ten years. This list is certainly very biased by my own interests but could be useful anyway. Here we go:

- The error on the CKM elements $|V_{cb}|$ and $|V_{ub}/V_{cb}|$ could be decreased below 0.002 and 0.01, respectively. This progress should come mainly from Cornell, B -factories and new theoretical efforts. It would have considerable impact on the unitarity triangle

and would improve theoretical predictions for rare and CP-violating decays sensitive to these elements.

- The error on m_t should be decreased down to ± 3 GeV at Tevatron in the Main Injector era and to ± 1 GeV at LHC.
- The measurement of non-vanishing ratio of ε'/ε by NA31 and KTeV, excluding confidently the superweak models, has been an important achievement. The improved measurements of ε'/ε with the accuracy of $\pm(1-2) \cdot 10^{-4}$ from NA48, KTeV and KLOE should give some insight into the physics of direct CP violation inspite of large theoretical uncertainties. In this respect measurements of CP-violating asymmetries in charged B decays will also play an outstanding role. These experiments can be performed e.g. at CLEO since no time-dependences are needed. The situation concerning hadronic uncertainties is quite similar to ε'/ε . Therefore one should hope that some definite progress in calculating relevant hadronic matrix elements will also be made.
- More events for $K^+ \rightarrow \pi^+ \nu \bar{\nu}$ could in principle be reported from BNL already this year. In view of the theoretical cleanliness of this decay an observation of events at the $2 \cdot 10^{-10}$ level would signal physics beyond the Standard Model. A detailed study of this very important decay requires, however, new experimental ideas and new efforts. The new efforts [113, 114] in this direction allow to hope that a measurement of $Br(K^+ \rightarrow \pi^+ \nu \bar{\nu})$ with an accuracy of $\pm 10\%$ should be possible before 2005. This would have a very important impact on the unitarity triangle and would constitute an important test of the Standard Model.
- The future improved inclusive $B \rightarrow X_{s,d} \gamma$ measurements confronted with improved Standard Model predictions could give the first signals of new physics. It appears that the errors on the input parameters could be lowered further and the theoretical error on $Br(B \rightarrow X_s \gamma)$ could be decreased confidently down to $\pm 8\%$ in the next years. The same accuracy in the experimental branching ratio will hopefully come from Cornell and later from KEK and SLAC. This may, however, be insufficient to disentangle new physics contributions although such an accuracy should put important constraints on the physics beyond the Standard Model. It would also be desirable to look for $B \rightarrow X_d \gamma$, but this is clearly a much harder task.
- Similar comments apply to transitions $B \rightarrow X_s l^+ l^-$ which appear to be even more sensitive to new physics contributions than $B \rightarrow X_{s,d} \gamma$. An observation of $B \rightarrow X_s \mu \bar{\mu}$ is expected from D0 and B -physics dedicated experiments at the beginning of the next

decade. The distributions of various kind when measured should be very useful in the tests of the Standard Model and its extensions.

- The theoretical status of $K_L \rightarrow \pi^0 e^+ e^-$ and of $K_L \rightarrow \mu \bar{\mu}$, should be improved to confront future data. Experiments at DAΦNE should be very helpful in this respect. The first events of $K_L \rightarrow \pi^0 e^+ e^-$ should come in the first years of the next decade from KAMI at FNAL. The experimental status of $K_L \rightarrow \mu \bar{\mu}$, with the experimental error of $\pm 7\%$ to be decreased soon down to $\pm 1\%$, is truly impressive.
- The newly approved experiment at BNL to measure $Br(K_L \rightarrow \pi^0 \nu \bar{\nu})$ at the $\pm 10\%$ level before 2005 may make a decisive impact on the field of CP violation. In particular $K_L \rightarrow \pi^0 \nu \bar{\nu}$ seems to allow the cleanest determination of $\text{Im}\lambda_t$. Taken together with $K^+ \rightarrow \pi^+ \nu \bar{\nu}$ a very clean determination of $\sin 2\beta$ can be obtained.
- The measurement of the $B_s^0 - \bar{B}_s^0$ mixing and in particular of $B \rightarrow X_{s,d} \nu \bar{\nu}$ and $B_{s,d} \rightarrow \mu \bar{\mu}$ will take most probably longer time but as stressed in these lectures all efforts should be made to measure these transitions. Considerable progress on $B_s^0 - \bar{B}_s^0$ mixing should be expected from HERA-B, SLAC and TEVATRON in the first years of the next decade. LHC-B should measure it to a high precision. With the improved calculations of ξ in (4.58) this will have important impact on the determination of $|V_{td}|$ and on the unitarity triangle.
- Clearly future precise studies of CP violation at SLAC-B, KEK-B, HERA-B, CORNELL, FNAL and LHC-B providing first direct measurements of α , β and γ may totally revolutionize our field. In particular the first signals of new physics could be found in the $(\bar{\varrho}, \bar{\eta})$ plane. During the recent years several, in some cases quite sophisticated and involved, strategies have been developed to extract these angles with small or even no hadronic uncertainties. Certainly the future will bring additional methods to determine α , β and γ . Obviously it is very desirable to have as many such strategies as possible available in order to overconstrain the unitarity triangle and to resolve certain discrete ambiguities which are a characteristic feature of these methods.
- The forbidden or strongly suppressed transitions such as $D^0 - \bar{D}^0$ mixing and $K_L \rightarrow \mu e$ are also very important in this respect. Considerable progress in this area should come from the experiments at BNL, FNAL and KEK.
- On the theoretical side, one should hope that the non-perturbative methods will be considerably improved so that various B_i parameters will be calculated with sufficient precision. It is very important that simultaneously with advances in lattice QCD,

further efforts are being made in finding efficient analytical tools for calculating QCD effects in the long distance regime. This is, in particular very important in the field of non-leptonic decays, where one should not expect too much from our lattice friends in the coming ten years unless somebody will get a brilliant idea which will revolutionize lattice calculations. The accumulation of data for non-leptonic B and D decays at Cornell, SLAC, KEK and FNAL should teach us more about the role of non-factorizable contributions and in particular about the final state interactions. In this context, in the case of K-decays, important lessons will come from DAΦNE which is an excellent machine for testing chiral perturbation theory and other non-perturbative methods.

In any case the field of weak decays and in particular of the FCNC transitions and of CP violation have a great future and one should expect that they could dominate particle physics in the first part of the next decade. Clearly the next ten years should be very exciting in this field.

Acknowledgements

I would like to thank Bruce Campbell, Faqir Khanna and Manuella Vincter for inviting me to such a wonderful Winter Institute and a great hospitality. I would also like to thank M. Gorbahn and L. Silvestrini for comments on the manuscript and the authors of [35] for a most enjoyable collaboration.

References

- [1] A.J. Buras, hep-ph/9806471, to appear in *Probing the Standard Model of Particle Interactions*, eds. R. Gupta, A. Morel, E. de Rafael and F. David (Elsevier Science B.V., Amsterdam, 1998).
- [2] G. Buchalla, A.J. Buras and M. Lautenbacher, *Rev. Mod. Phys.* **68** (1996) 1125.
- [3] A.J. Buras and R. Fleischer, hep-ph/9704376, in *Heavy Flavours II*, eds. A.J. Buras and M. Lindner, (World Scientific, 1998) page 65.
- [4] N. Cabibbo, *Phys. Rev. Lett.* **10** (1963) 531.
- [5] M. Kobayashi and K. Maskawa, *Prog. Theor. Phys.* **49** (1973) 652.
- [6] S.L. Glashow, J. Iliopoulos and L. Maiani *Phys. Rev. D* **2** (1970) 1285.
- [7] L.L. Chau and W.-Y. Keung, *Phys. Rev. Lett.* **53** (1984) 1802.
- [8] Particle Data Group, *Euro. Phys. J. C* **3** (1998) 1.

- [9] L. Wolfenstein, Phys. Rev. Lett. **51** (1983) 1945.
- [10] A.J. Buras, M.E. Lautenbacher and G. Ostermaier, Phys. Rev. **D 50** (1994) 3433.
- [11] M. Schmidtler and K.R. Schubert, Z. Phys. **C 53** (1992) 347.
- [12] C. Jarlskog, Phys. Rev. Lett. **55**, (1985) 1039; Z. Phys. **C29** (1985) 491.
- [13] C. Jarlskog and R. Stora, Phys. Lett. **B 208** (1988) 268.
- [14] A. Ali and D. London, hep-ph/9903535; F. Parodi, P. Roudeau, and A. Stocchi, hep-ex/9903063.
- [15] A. Stocchi, hep-ex/9902004.
- [16] K.G. Wilson, Phys. Rev. **179** (1969) 1499; K.G. Wilson and W. Zimmermann, Comm. Math. Phys. **24** (1972) 87.
- [17] W. Zimmermann, in Proc. 1970 Brandeis Summer Institute in Theor. Phys, (eds. S. Deser, M. Grisaru and H. Pendleton), MIT Press, 1971, p.396; Ann. Phys. **77** (1973) 570.
- [18] E.C.G. Sudarshan and R.E. Marshak, Proc. Padua-Venice Conf. on Mesons and Recently Discovered Particles (1957).
- [19] R.P. Feynman and M. Gell-Mann, Phys. Rev. **109** (1958) 193.
- [20] J. Chay, H. Georgi and B. Grinstein, Phys. Lett. **B 247** (1990) 399; I.I. Bigi, N.G. Uraltsev and A.I. Vainshtein, Phys. Lett. **B 293** (1992) 430 [E: **B 297** (1993) 477]; I.I. Bigi, M.A. Shifman, N.G. Uraltsev and A.I. Vainshtein, Phys. Rev. Lett. **71** (1993) 496; B. Blok, L. Koyrakh, M.A. Shifman and A.I. Vainshtein, Phys. Rev. **D 49** (1994) 3356 [E: **D 50** (1994) 3572]; A.V. Manohar and M.B. Wise, Phys. Rev. **D 49** (1994) 1310.
- [21] A.J. Buras, hep-ph/9901409.
- [22] T. Inami and C.S. Lim, Progr. Theor. Phys. **65** (1981) 297.
- [23] G. Buchalla, A.J. Buras and M.K. Harlander, Nucl. Phys. **B 349** (1991) 1.
- [24] M.K. Gaillard and B.W. Lee, Phys. Rev. **D10** (1974) 897.
- [25] H. Albrecht et al. (ARGUS), Phys. Lett. **B192** (1987) 245; M. Artuso et al. (CLEO), Phys. Rev. Lett. **62** (1989) 2233.

- [26] J.H. Christenson, J.W. Cronin, V.L. Fitch and R. Turlay, Phys. Rev. Lett. **13** (1964) 128.
- [27] L.L. Chau, Physics Reports, **95** (1983) 1.
- [28] A.J. Buras, W. Slominski and H. Steger, Nucl. Phys. **B245** (1984) 369.
- [29] Y. Nir, SLAC-PUB-5874 (1992).
- [30] J. Bijnens, J.-M. Gérard and G. Klein, Phys. Lett. **B257** (1991) 191.
- [31] S. Herrlich and U. Nierste, Nucl. Phys. **B419** (1994) 292.
- [32] A.J. Buras, M. Jamin, and P.H. Weisz, Nucl. Phys. **B347** (1990) 491;
J. Urban, F. Krauss, U. Jentschura and G. Soff, Nucl. Phys. **B523** (1998) 40.
- [33] S. Herrlich and U. Nierste, Phys. Rev. **D52** (1995) 6505; Nucl. Phys. **B476** (1996) 27.
- [34] R. Gupta, hep-ph/9801412.
- [35] S. Bosch, A.J. Buras, M. Gorbahn, S. Jäger, M. Jamin, M.E. Lautenbacher and L. Silvestrini, hep-ph/9904408.
- [36] S. Bertolini, J.O. Eeg, M. Fabbrichesi and E.I. Lashin, Nucl. Phys. **B514** (1998) 63.
- [37] L. Conti, A. Donini, V. Gimenez, G. Martinelli, M. Talevi and A. Vladikas, Phys. Lett. **B421** (1998) 273.
- [38] S. Aoki et al., JLQCD collaboration, Phys. Rev. Lett. **80** (1998) 5271; hep-lat/9901018.
- [39] G. Kilcup, R. Gupta and S.R. Sharpe, Phys. Rev. **D57** (1998) 1654.
- [40] L. Lellouch, talk given at Recontres de Moriond, March 1999.
- [41] W.A. Bardeen, A.J. Buras and J.-M. Gérard, Phys. Lett. **B211** (1988) 343; J.-M. Gérard, Acta Physica Polonica **B21** (1990) 257.
- [42] J. Bijnens and J. Prades, Nucl. Phys. **B444** (1995) 523; hep-ph/9811472.
- [43] T. Hambye, G.O. Köhler and P.H. Soldan, hep-ph/9902334.
- [44] N. Bilic, C.A. Dominguez and B. Guberina, Z. Phys. **C39** (1988) 351. R. Decker, Nucl. Phys. Proc. Suppl. **7A** (1989) 180; S. Narison, Phys. Lett. **B351** (1995) 369.
- [45] C. Bruno, Phys. Lett. **B320** (1994) 135.

- [46] A. Pich and E. de Rafael, Phys. Lett. **B158** (1985) 477; J. Prades et al, Z. Phys. **C51** (1991) 287.
- [47] J.F. Donoghue, E. Golowich and B.R. Holstein, Phys. Lett. **B119** (1982) 412.
- [48] T. Draper, hep-lat/9810065; S. Sharpe, hep-lat/9811006; C. Bernard et al., Phys. Rev. Lett. **81** (1998) 4812.
- [49] E. Bagan, P. Ball, V.M. Braun and H.G. Dosch, Phys. Lett. **B278** (1992) 457; M. Neubert, Phys. Rev. **D45** (1992) 2451 and references therein.
- [50] F. Abe et al. (CDF Collaboration), Phys. Rev. Lett. **82** (1999) 271; B. Abbott et al. (D0 Collaboration), hep-ex/9808029.
- [51] The LEP B Oscillation Working Group, LEPBOSC 98/3.
- [52] S. Narison, Phys. Lett. **B322** (1994) 247.
- [53] M. Gorbahn, unpublished.
- [54] CDF Collaboration, CDF/PUB/BOTTOM/CDF/4855,1999.
- [55] Y. Grossman, Y. Nir, S. Plaszczynski and M. Schune, Nucl. Phys. **B511** (1998) 69.
- [56] P. Paganini, F. Parodi, P. Roudeau and A. Stocchi, Phys. Scripta **58** (1998) 556, hep-ph/9711261; F. Parodi, P. Roudeau and A. Stocchi, hep-ph/9802289.
- [57] L. Wolfenstein, Phys. Rev. Lett. **13** (1964) 562.
- [58] G. D. Barr et al., Phys. Lett. **B317** (1993) 233.
- [59] L. K. Gibbons et al., Phys. Rev. Lett. **70** (1993) 1203.
- [60] Seminar presented by P. Shawhan for KTeV collaboration, Fermilab, Feb. 24 1999; <http://fnphyx-www.fnal.gov/experiments/ktev/epsprime/epsprime.html>.
- [61] J. Ellis, M.K. Gaillard and D.V. Nanopoulos, Nucl. Phys. **B109** (1976) 213.
- [62] F.J. Gilman and M.B. Wise, Phys. Lett. **B83** (1979) 83; B. Guberina and R.D. Peccei, Nucl. Phys. **B163** (1980) 289.
- [63] F.J. Gilman and J.S. Hagelin, Phys. Lett. **B126** (1983) 111; A.J. Buras, W. Slominski and H. Steger, Nucl. Phys. **B238** (1984) 529; A.J. Buras and J.-M. Gérard, Phys. Lett. **B203** (1988) 272.

- [64] J. Bijnens and M.B. Wise, Phys. Lett. **B137** (1984) 245.
- [65] J.F. Donoghue, E. Golowich, B.R. Holstein and J. Trampetic, Phys. Lett. **B179** (1986) 361.
- [66] A. J. Buras and J.-M. Gérard, Phys. Lett. **B192** (1987) 156.
- [67] H.-Y. Cheng, Phys. Lett. **B201** (1988) 155; M. Lusignoli, Nucl. Phys. **B325** (1989) 33.
- [68] W. A. Bardeen, A. J. Buras and J.-M. Gérard, Phys. Lett. **B180** (1986) 133; Nucl. Phys. **B293** (1987) 787; Phys. Lett. **B192** (1987) 138.
- [69] J. M. Flynn and L. Randall, Phys. Lett. **B224** (1989) 221; erratum ibid. Phys. Lett. **B235** (1990) 412.
- [70] G. Buchalla, A. J. Buras, and M. K. Harlander, Nucl. Phys. **B337** (1990) 313.
- [71] E.A. Paschos and Y.L. Wu, Mod. Phys. Lett. **A6** (1991) 93; M. Lusignoli, L. Maiani, G. Martinelli and L. Reina, Nucl. Phys. **B369** (1992) 139.
- [72] A.J. Buras, M. Jamin, M.E. Lautenbacher and P.H. Weisz, Nucl. Phys. **B 370** (1992) 69; Nucl. Phys. **B 400** (1993) 37.
- [73] A.J. Buras, M. Jamin and M.E. Lautenbacher, Nucl. Phys. **B 400** (1993) 75.
- [74] A.J. Buras, M. Jamin and M.E. Lautenbacher, Nucl. Phys. **B 408** (1993) 209.
- [75] M. Ciuchini, E. Franco, G. Martinelli and L. Reina, Phys. Lett. **B 301** (1993) 263.
- [76] M. Ciuchini, E. Franco, G. Martinelli and L. Reina, Nucl. Phys. **B 415** (1994) 403.
- [77] M. Ciuchini, E. Franco, G. Martinelli, L. Reina and L. Silvestrini, Z. Phys. **C68** (1995) 239.
- [78] A. J. Buras, M. Jamin, and M. E. Lautenbacher, Phys. Lett. **B389** (1996) 749.
- [79] M. Ciuchini, Nucl. Phys. B. Proc. Suppl. **59** (1997) 149.
- [80] J. Heinrich, E.A. Paschos, J.-M. Schwarz, and Y.L. Wu, Phys. Lett. **B279** (1992) 140; E.A. Paschos, review presented at the 27th Lepton-Photon Symposium, Beijing, China (August 1995).
- [81] S. Bertolini, M. Fabbrichesi and J.O. Eeg, hep-ph/9802405.

- [82] B. Winstein and L. Wolfenstein, *Rev. Mod. Phys.* **65** (1993) 1113.
- [83] A.A. Belkov, G. Bohm, A.V. Lanyov and A.A. Moshkin, hep-ph/9704354.
- [84] A. J. Buras and M. E. Lautenbacher, *Phys. Lett.* **B318** (1993) 212.
- [85] R.D. Kenway, Plenary talk at LATTICE 98, hep-ph/9810054.
- [86] M. Jamin and M. Münz, *Z. Phys.* **C66** (1995) 633; S. Narison, *Phys. Lett.* **B358** (1995) 113; K. G. Chetyrkin, D. Pirjol, and K. Schilcher, *Phys. Lett.* **B404** (1997) 337; P. Colangelo, F. De Fazio, G. Nardulli, and N. Paver, *Phys. Lett.* **B408** (1997) 340; M. Jamin, *Nucl. Phys. B. Proc. Suppl.* **64** (1998) 250.
- [87] L. Lellouch, E. de Rafael, and J. Taron, *Phys. Lett.* **B414** (1997) 195; F.J. Yndurain, *Nucl. Phys. B* **517** (1998) 324. H.G. Dosch and S. Narison, *Phys. Lett.* **B417** (1998) 173.
- [88] J. Prades and A. Pich, hep-ph/9811263, proceedings of QCD 98, Montpellier.
- [89] ALEPH collaboration, CERN-EP/99-026, hep-ex/9903015.
- [90] S. Narison, hep-ph/9905264.
- [91] R. Gupta, T. Bhattacharaya, and S.R. Sharpe, *Phys. Rev.* **D55** (1997) 4036.
- [92] T. Hambye, G.O. Köhler, E.A. Paschos, P.H. Soldan and W.A. Bardeen, *Phys. Rev.* **D58** (1998) 014017.
- [93] G. W. Kilcup, *Nucl. Phys. (Proc. Suppl.)* **B20** (1991) 417.
- [94] S. R. Sharpe, *Nucl. Phys. (Proc. Suppl.)* **B20** (1991) 429.
- [95] D. Pekurovsky and G. Kilcup, hep-lat/9709146.
- [96] D. Pekurovsky and G. Kilcup, hep-lat/9812019.
- [97] S. Bethke, hep-ex/9812026.
- [98] Y.-Y. Keum, U. Nierste and A.I. Sanda, hep-ph/9903230.
- [99] L.F. Abbot, P. Sikivie and M.B. Wise, *Phys. Rev.* **D21** (1980) 1393.
- [100] E. Gabrielli and G.F. Giudice, *Nucl. Phys.* **B433** (1995) 3.
- [101] E. Gabrielli, A. Masiero and L. Silvestrini, *Phys. Lett.* **B374** (1996) 80; F. Gabbiani, E. Gabrielli, A. Masiero and L. Silvestrini, *Nucl. Phys. B* **477** (1996) 321.

- [102] A. Masiero and H. Murayama, hep-ph/9903363.
- [103] D. Rein and L.M. Sehgal, Phys. Rev. **D39** (1989) 3325; J.S. Hagelin and L.S. Littenberg, Prog. Part. Nucl. Phys. **23** (1989) 1; M. Lu and M.B. Wise, Phys. Lett. **B324** (1994) 461; S. Fajfer, [hep-ph/9602322]; C.Q. Geng, I.J. Hsu and Y.C. Lin, Phys. Rev. **D54** (1996) 877.
- [104] G. Buchalla and G. Isidori, Phys. Lett. **B440** (1998) 170.
- [105] G. Buchalla and A.J. Buras, Nucl. Phys. **B 398** (1993) 285.
- [106] G. Buchalla and A.J. Buras, Nucl. Phys. **B 400** (1993) 225.
- [107] G. Buchalla and A.J. Buras, Nucl. Phys. **B 412** (1994) 106.
- [108] M. Misiak and J. Urban, Phys. Lett. **B541** (1999) 161.
- [109] G. Buchalla and A.J. Buras, hep-ph/9901288.
- [110] V.A. Novikov, A.I. Vainshtein, V.I. Zakharov and M.A. Shifman, Phys. Rev. **D16**, (1977) 223; J. Ellis and J.S. Hagelin, Nucl. Phys. **B217** (1983) 189; C.O. Dib, I. Dunietz and F.J. Gilman, Mod. Phys. Lett. **A6** (1991) 3573.
- [111] W. Marciano and Z. Parsa, Phys. Rev. **D53**, R1 (1996).
- [112] S. Adler et al., Phys. Rev. Lett. **79**, (1997) 2204.
- [113] L. Littenberg and J. Sandweiss, eds., AGS2000, Experiments for the 21st Century, BNL 52512.
- [114] P. Cooper, M. Crisler, B. Tschirhart and J. Ritchie (CKM collaboration), EOI for measuring $Br(K^+ \rightarrow \pi^+ \nu \bar{\nu})$ at the Main Injector, Fermilab EOI 14, 1996.
- [115] L. Littenberg, Phys. Rev. **D39** (1989) 3322.
- [116] Y. Grossman, Y. Nir and R. Rattazzi, hep-ph/9701231, in Heavy Flavours II, eds. A.J. Buras and M. Lindner, (World Scientific, 1998) page 755. Y. Nir, hep-ph/9904271.
- [117] G. Buchalla, hep-ph/9612307.
- [118] G. Buchalla and A.J. Buras, Phys. Rev. **D54** (1996) 6782.
- [119] J. Adams et al., Phys. Lett. **B447** (1999) 240.
- [120] K. Arisaka et al., KAMI conceptual design report, FNAL, June 1991.

- [121] T. Inagaki, T. Sato and T. Shinkawa, Experiment to search for the decay $K_L \rightarrow \pi^0 \nu \bar{\nu}$ at KEK 12 GeV proton synchrotron, 30 Nov. 1991.
- [122] G. Buchalla and A.J. Buras, *Phys. Lett.* **B333** (1994) 221.
- [123] G. Buchalla, G. Isidori and S.-J. Rey, *Nucl. Phys.* **B511** (1998) 594.
- [124] N. Cabibbo and L. Maiani, *Phys. Lett.* **B79** (1978) 109.
- [125] C.S. Kim and A.D. Martin, *Phys. Lett.* **B225** (1989) 186.
- [126] ALEPH Collaboration, Contribution (PA10-019) to the 28th International Conference on High Energy Physics, July 1996, Warsaw, Poland.
- [127] F. Abe et al. (CDF), *Phys. Rev.* **D57** (1998) R3811.
- [128] Y. Grossman, Z. Ligeti and E. Nardi, *Phys. Rev.* **D55** (1997) 2768.
- [129] C. Greub, T. Hurth and D. Wyler, *Phys. Lett.* **B380** (1996) 385; *Phys. Rev.* **D 54** (1996) 3350;
- [130] K.G. Chetyrkin, M. Misiak and M. Münz, *Phys. Lett.* **B400** (1997) 206; Erratum-ibid. **B425** (1998) 414.
- [131] The BaBar Physics Book, preprint SLAC-R-504.
- [132] A. Ali and G. Hiller, hep-ph/9812267.
- [133] A. J. Buras, M. E. Lautenbacher, M. Misiak and M. Münz, *Nucl. Phys.* **B423** (1994) 349.
- [134] G. Ecker, A. Pich, and E. de Rafael, *Nucl. Phys.* **B291** (1987) 692, *Nucl. Phys.* **B303** (1988) 665; A. G. Cohen, G. Ecker, and A. Pich, *Phys. Lett.* **B304** (1993) 347; P. Heiliger and L. Seghal, *Phys. Rev.* **D47** (1993) 4920; C. Bruno and J. Prades, *Z. Phys.* **C57** (1993) 585; J. F. Donoghue and F. Gabbiani, *Phys. Rev.* **D51** (1995) 2187; A. Pich, hep-ph/9610243.
- [135] D.A. Harris et al., *Phys. Rev. Lett.* **71** (1993) 3918.
- [136] A.P. Heinson et al., *Phys. Rev.* **D 51** (1995) 985; T. Akagi et al., *Phys. Rev.* **D 51** (1995) 2061.
- [137] G. D'Ambrosio, G. Isidori and J Portolés, *Phys. Lett.* **B423** (1998) 385.
- [138] D. Gomez Dumm and A. Pich, hep-ph/9810523.

- [139] G. Valencia, hep-ph/9711377.
- [140] L. Littenberg and G. Valencia, *Ann. Rev. Nucl. Part. Sci.* **43** (1993) 729; J.L. Ritchie and S.G. Wojcicki, *Rev. Mod. Phys.* **65** (1993) 1149; A. Pich, hep-ph/9610243; G. D'Ambrosio and G. Isidori, hep-ph/9611284.
- [141] Y. Nir and H.R. Quinn *Ann. Rev. Nucl. Part. Sci.* **42** (1992) 211 and in " B Decays ", ed S. Stone (World Scientific, 1994), p. 520; I. Dunietz, *ibid* p.550 and refs. therein.
- [142] R. Fleischer, *Int. J. of Mod. Phys.* **A12** (1997) 2459.
- [143] M. Ciuchini, E. Franco, G. Martinelli, and L. Silvestrini, *Nucl. Phys.* **B501** (1997) 271; M. Ciuchini, R. Contino, E. Franco, G. Martinelli, and L. Silvestrini, *Nucl. Phys.* **B512** (1998) 3.
- [144] M. Gronau and D. London, *Phys. Rev. Lett.* **65** (1990) 3381.
- [145] A. Snyder and H.R. Quinn, *Phys. Rev.* **D48** (1993) 2139; A.J. Buras and R. Fleischer, *Phys. Lett.* **B360** (1995) 138; J.P. Silva and L. Wolfenstein, *Phys. Rev.* **D49** (1995) R1151; A.S. Dighe, M. Gronau and J. Rosner, *Phys. Rev.* **D54** (1996) 3309; R. Fleischer and T. Mannel, *Phys. Lett.* **B397** (1997) 269; C.S. Kim, D. London and T. Yoshikawa, *Phys. Rev.* **D57** (1998) 4010.
- [146] I.I.Y. Bigi and A.I. Sanda, *Nucl. Phys.* **B193** (1981) 85.
- [147] D. London and A. Soni, *Phys. Lett.* **B407** (1997) 61; Y. Grossman and M.P. Worah, *Phys. Lett.* **B395** (1997) 241; M. Ciuchini et al., *Phys. Rev. Lett.* **79** (1997) 978; R. Barbieri and A. Strumia, *Nucl. Phys.* **B508** (1997) 3.
- [148] A.J. Buras, *Nucl. Instr. Meth.* **A368** (1995) 1.
- [149] R. Aleksan, I. Dunietz and B. Kayser, *Z.Phys.* **C54** (1992) 653; R. Fleischer and I. Dunietz, *Phys. Lett.* **B387** (1996) 361.
- [150] M. Gronau and D. Wyler, *Phys. Lett.* **B265** (1991) 172.
- [151] M. Gronau and D. London, *Phys. Lett.* **B253** (1991) 483. I. Dunietz, *Phys. Lett.* **B270** (1991) 75.
- [152] D. Atwood, I. Dunietz and A. Soni, *Phys. Rev. Lett.* **B78** (1997) 3257.
- [153] R. Fleischer, *Phys. Lett.* **B365** (1996) 399; R. Fleischer and T. Mannel, *Phys. Rev.* **D57** (1998) 2752;

- [154] M. Gronau and J.L. Rosner, Phys. Rev. **D57** (1998) 6843;
- [155] F. Würthwein and P. Gaidarev, hep-ph/9712531.
- [156] R. Fleischer, Eur. Phys. J. **C6** (1999) 451; A.J. Buras and R. Fleischer, hep-ph/9810260.
- [157] R. Godang et al., Phys. Rev. Lett. **80** (1998) 3456; B.H. Behrens et al., Phys. Rev. Lett. **80** (1998) 3710; D.M. Asner et al., Phys. Rev. **D53** (1996) 1039;
- [158] L. Wolfenstein, Phys. Rev. **D52** (1995) 537; J. Donoghue, E. Golowich, A. Petrov and J. Soares, Phys. Rev. Lett. **77** (1996) 2178; B. Blok and I. Halperin, Phys. Lett. **B385** (1996) 324; B. Blok, M. Gronau and J.L. Rosner, Phys. Rev. Lett. **78** (1997) 3999; A.J. Buras, R. Fleischer and T. Mannel, Nucl. Phys. **B533** (1998) 3; J.-M. Gérard and J. Weyers, hep-ph/9711469; M. Neubert, Phys. Lett. **B424** (1998) 152; A.F. Falk, A.L. Kagan, Y. Nir and A.A. Petrov, Phys. Rev. **D57** (1998) 4290; D. Atwood and A. Soni (1997), Phys. Rev. **D58** (1998) 036005; R. Fleischer, Phys. Lett. **B435** (1998) 221; M. Gronau and J.L. Rosner, Phys. Rev. **D58** (1998) 113005;
- [159] M. Neubert, JHEP 9902 (1998) 014.
- [160] M. Neubert and J.L. Rosner, Phys. Lett. **B441** (1998) 403; Phys. Rev. Lett. **81** (1998) 5076;
- [161] R. Fleischer, hep-ph/9904313.
- [162] M. Neubert, hep-ph/9904321.
- [163] R. Fleischer, hep-ph/9903455, hep-ph/9903456.
- [164] Y. Gao and F. Würthwein, hep-ex/9904008.
- [165] X-G. He, W-S. Hou and K-Ch. Yang, hep-ph/9902256.
- [166] A. Lenz, U. Nierste and G. Ostermaier, Phys. Rev. **D59** (1999) 034008; U. Nierste, hep-ph/9805388.
- [167] A.J. Buras, Phys. Lett. **B333** (1994) 476.
- [168] M. Gronau and D. London, Phys. Rev. **D55** (1997) 2845; Y. Grossman, Y. Nir and M.P. Worah, Phys. Lett. **B407** (1997) 307.
- [169] G. Colangelo and G. Isidori, JHEP 09 (1998) 009.
- [170] A.J. Buras and L. Silvestrini, Nucl. Phys. **B 546** (1999) 299.

- [171] Y. Nir and M.P. Worah, Phys. Lett. **B423** (1998) 319.
- [172] A.J. Buras, A. Romanino and L. Silvestrini, Nucl. Phys. **B520** (1998) 3.
- [173] Y. Grossman and Y. Nir, Phys. Lett. **B398** (1997) 163; C.E. Carlson, G.D. Dorada and M. Sher, Phys. Rev. **D54** (1996) 4393; G. Burdman, Phys. Lett. **B409** (1997) 443; A. Berera, T.W. Kephart and M. Sher, Phys. Rev. **D56** (1997) 7457; Gi-Chol Cho, hep-ph/9804327.
- [174] T. Hattori, T. Hasuike and S. Wakaizumi, hep-ph/9804412.